Design and Development of Metamaterial Inspired Fractal Antenna for Modern Wireless Applications

A Thesis submitted to Gujarat Technological University

For the Award of

Doctor of Philosophy

in

Electronics And Communication Engineering

by

Dalsania Piyushkumar Chandulal

Enrollment No.: **209999915019**

Under Supervision of

Prof. (Dr.) Jagdish M Rathod



GUJARAT TECHNOLOGICAL UNIVERSITY

AHMEDABAD

MAY – 2026

Design and Development of Metamaterial Inspired Fractal Antenna for Modern Wireless Applications

A Thesis submitted to Gujarat Technological University

For the Award of

Doctor of Philosophy

in

Electronics And Communication Engineering

by

Dalsania Piyushkumar Chandulal

Enrollment No.: **209999915019**

Under Supervision of

Prof. (Dr.) Jagdish M Rathod



GUJARAT TECHNOLOGICAL UNIVERSITY

AHMEDABAD

MAY – 2026

© Dalsania Piyushkumar Chandulal

DECLARATION

I declare that the thesis entitled **Design and Development of Metamaterial Inspired Fractal Antenna for Modern Wireless Applications** submitted by me for the degree of Doctor of Philosophy is the record of research work carried out by me during the period from **July - 2021 to May - 2026** under the supervision of **Prof. (Dr.) Jagdish M Rathod** and this has not formed the basis for the award of any degree, diploma, associateship, fellowship, titles in this or any other University or other institution of higher learning.

I further declare that the material obtained from other sources has been duly acknowledged in the thesis. I shall be solely responsible for any plagiarism or other irregularities, if noticed in the thesis.



Signature of the Research Scholar: Date: 16/05/2026

Name of Research Scholar: **Dalsania Piyushkumar Chandulal**

Place: **Ahmedabad, Gujarat**

CERTIFICATE

I certify that the work incorporated in the thesis **Design and Development of Metamaterial Inspired Fractal Antenna for Modern Wireless Applications** submitted by **Mr. Dalsania Piyushkumar Chandulal** was carried out by the candidate under my supervision/guidance. To the best of my knowledge: (i) the candidate has not submitted the same research work to any other institution for any degree/diploma, Associateship, Fellowship or other similar titles (ii) the thesis submitted is a record of original research work done by the Research Scholar during the period of study under my supervision, and (iii) the thesis represents independent research work on the part of the Research Scholar.

Signature of the Research Supervisor:  Date:16/05/2026

Name of Supervisor: **Prof. (Dr.) Jagdish M Rathod**

Place: **Ahmedabad, Gujarat**

COURSE-WORK COMPLETION CERTIFICATE

This is to certify that **Mr. Dalsania Piyushkumar Chandulal,** enrolment no. **209999915019** is enrolled for a PhD program in the faculty of **Electronics and Communication Engineering** of Gujarat Technological University, Ahmedabad.

(Please tick the relevant option(s))

☐ He/she has been exempted from the course-work (successfully completed during M.Phil. Course

☐ He/ Course She has been exempted from Research Methodology Course only (successfully completed during M.Phil.)

☑ He/she has successfully completed the PhD course work for the partial requirement for the award of PhD Degree. His/ Her performance in the course work is as follows-

Grade Obtained in Research Methodology (PHD2001)	Grade Obtained in Research and Publication Ethics (PHD2002)	Grade Obtained in Self-Study Course (PHD2003)
AA	**AB**	**AA**

Signature of the Research Supervisor:  Date: 16/05/2026

Name of Supervisor: **Prof. (Dr.) Jagdish M Rathod**

Place: **Ahmedabad, Gujarat**

ORIGINALITY REPORT CERTIFICATE

It is certified that the PhD Thesis titled **Design and Development of Metamaterial Inspired Fractal Antenna for Modern Wireless Applications** by **Dalsania Piyushkumar Chandulal** has been examined by us. We undertake the following:

a. Thesis has significant new work / knowledge as compared already published or are under consideration to be published elsewhere. No sentence, equation, diagram, table, paragraph or section has been copied verbatim from previous work unless it is placed under quotation marks and duly referenced.

b. The work presented is original and the author's own work (i.e. there is no plagiarism). No ideas, processes, results or words of others have been presented as Author own work.

c. There is no fabrication of data or results which have been compiled / analysed.

d. There is no falsification by manipulating research materials, equipment or processes, or changing or omitting data or results such that the research is not accurately represented in the research record.

e. The thesis has been checked using **Turnitin** (copy of originality report attached) and found within limits as per GTU Plagiarism Policy and instructions issued from time to time (i.e. permitted similarity index <=10%).



Signature of the Research Scholar: Date: 16/05/2026

Name of the Research Scholar: **Dalsania Piyushkumar Chandulal**



Signature of the Research Supervisor: Date: 16/05/2026

Name of the Research Supervisor: **Prof. (Dr.) Jagdish M Rathod**

Place: **Ahmedabad, Gujarat**

Dr. Jagdishkumar M Rathod

Thesis

Review Paper

PhD_GTU

Gujarat Technological University

Document Details

Submission ID
trn:oid:::1:3484719708

Submission Date
Feb 18, 2026, 4:46 PM GMT+5:30

Download Date
Feb 18, 2026, 4:53 PM GMT+5:30

File Name
Piyush_final_Draft_thesis_to_TURNITIN_17-02-2026.pdf

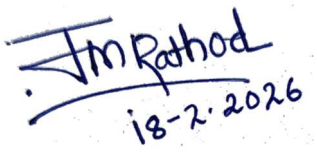
File Size
3.3 MB

105 Pages

28,513 Words

170,787 Characters

turnitin Page 1 of 111 - Cover Page Submission ID trn:oid:::1:3484719708



6% Overall Similarity

The combined total of all matches, including overlapping sources, for each database.

Filtered from the Report

- Bibliography
- Quoted Text
- Cited Text
- Small Matches (less than 10 words)

Match Groups

101 Not Cited or Quoted 6%
Matches with neither in-text citation nor quotation marks

0 Missing Quotations 0%
Matches that are still very similar to source material

0 Missing Citation 0%
Matches that have quotation marks, but no in-text citation

0 Cited and Quoted 0%
Matches with in-text citation present, but no quotation marks

Top Sources

2% Internet sources
5% Publications
1% Submitted works (Student Papers)

Integrity Flags

0 Integrity Flags for Review

No suspicious text manipulations found.

Our system's algorithms look deeply at a document for any inconsistencies that would set it apart from a normal submission. If we notice something strange, we flag it for you to review.

A Flag is not necessarily an indicator of a problem. However, we'd recommend you focus your attention there for further review.

JM Rathod
18-2-2026

turnitin Page 2 of 111 - Integrity Overview Submission ID trn:oid:::1:3484719708

Match Groups

- **101** Not Cited or Quoted 6%
  Matches with neither in-text citation nor quotation marks
- **0** Missing Quotations 0%
  Matches that are still very similar to source material
- **0** Missing Citation 0%
  Matches that have quotation marks, but no in-text citation
- **0** Cited and Quoted 0%
  Matches with in-text citation present, but no quotation marks

Top Sources

- 2% Internet sources
- 5% Publications
- 1% Submitted works (Student Papers)

Top Sources

The sources with the highest number of matches within the submission. Overlapping sources will not be displayed.

1	Publication	Piyush Dalsania, Jagdish M. Rathod. "Design and analysis of an asymmetrical star... 3%
2	Internet	ebin.pub <1%
3	Publication	Mohammad Ameen, Raghvendra Chaudhary. "Metamaterial Circularly Polarized ... <1%
4	Internet	www.researchgate.net <1%
5	Publication	A. K. Singh, Reneez Ahamad Kabeer, Z. Ali, D. Gurjar. "Performance analysis of co... <1%
6	Publication	Ravindra, Asari Gauravkumar. "Metamaterial Based Bandpass Filter for 5G Applic... <1%
7	Internet	nozdr.ru <1%
8	Internet	www.mdpi.com <1%
9	Publication	Springer Series in Optical Sciences, 2014. <1%
10	Publication	Biswas, Samarjith. "Development of Thermoacoustic Metastructures.", Oklahoma... <1%

turnitin Page 3 of 111 - Integrity Overview Submission ID trn:oid:::1:3484719708

JM Rathod
18-2-2026

PH. D. THESIS NON-EXCLUSIVE LICENSE TO GTU

GUJARAT TECHNOLOGICAL UNIVERSITY

In consideration of being a Research Scholar at Gujarat Technological University, and in the interests of the facilitation of research at the University and elsewhere, I, **Dalsania Piyushkumar Chandulal,** having Enrolment No. **209999915019,** hereby grant a non-exclusive, royalty free and perpetual license to the University on the following terms:

a. The University is permitted to archive, reproduce, and distribute my thesis, in whole or in part, and/or my abstract, in whole or in part (referred to collectively as the "Work") anywhere in the world, for non-commercial purposes, in all forms of media;
b. The University is permitted to authorize, sub-lease, sub-contract, or procure any of the acts mentioned in paragraph (a);
c. The University is authorized to submit the Work at any National / International Library, under the authority of their "Thesis Non-Exclusive License";
d. The Universal Copyright Notice (©) shall appear on all copies made under the authority of this license;
e. I undertake to submit my thesis, through my university, to any Library and Archives. Any abstract submitted with the thesis will be considered to form part of the thesis.
f. I represent that my thesis is my original work, does not infringe any rights of others, including privacy rights, and that I have the right to make the grant conferred by this non-exclusive license.
g. If third party copyrighted material was included in my thesis for which, under the terms of the Copyright Act, written permission from the copyright owners is required, I have obtained such permission from the copyright owners to do the acts mentioned in paragraph (a) above for the full term of copyright protection.
h. I understand that the responsibility for the matter as mentioned in the paragraph (g) rests with the authors / me solely. In no case shall GTU have any liability for any acts / omissions / errors / copyright infringement from the publication of the said thesis or otherwise.
i. I retain copyright ownership and moral rights in my thesis, and may deal with the copyright in my thesis, in any way consistent with rights granted by me to my university in this non-exclusive license.

j. GTU logo shall not be used /printed in the book (in any manner whatsoever) being published or any promotional or marketing materials or any such similar documents.

k. The following statement shall be included appropriately and displayed prominently in the book or any material being published anywhere: "The content of the published work is part of the thesis submitted in partial fulfilment for the award of the degree of Ph.D. in **Electronics and Communication Engineering** of the Gujarat Technological University".

l. I further promise to inform any person to whom I may hereafter assign or license my copyright in my thesis of the rights granted by me to my university in this nonexclusive license. I shall keep GTU indemnified from any and all claims from the Publisher(s) or any third parties at all times resulting or arising from the publishing, use, or intended use of the book / such similar document or its contents.

m. I am aware of and agree to accept the conditions and regulations of Ph.D., including all policy matters related to authorship and plagiarism.

Date: 16/05/2026

Place: **Ahmedabad, Gujarat**

Signature of the Research Scholar: 

Recommendation of the Research Supervisor: **Recommended for the award of the Ph.D. degree**

Signature of the Research Supervisor:  Date: 16/05/2026

THESIS APPROVAL FORM

The viva-voce of the PhD Thesis submitted by Shri **Dalsania Piyushkumar Chandulal** (Enrolment No. **209999915019)** entitled **Design and Development of Metamaterial Inspired Fractal Antenna for Modern Wireless Applications** was conducted on ……16-05-2026 (day and date) at Gujarat Technological University.

(Please tick any one of the following options)

☑ The performance of the candidate was satisfactory. We recommend that he be awarded the PhD degree.

☐ Any further modifications in research work recommended by the panel after 3 months from the date of first viva-voce upon request of the Supervisor or request of Independent Research Scholar after which viva-voce can be re-conducted by the same panel again.

(Briefly specify the modifications suggested by the panel)

☐ The performance of the candidate was unsatisfactory. We recommend that he should not be awarded the PhD degree.

(The panel must give justifications for rejecting the research work)

1) (External Examiner 1) Name and Signature

16/05/2026

Dr. Dinesh Yadav

2) (External Examiner 2) Name and Signature

Dr. Shilpi Gupta

JM Rathod

Prof. (Dr.) Jagdish M Rathod

16.05.2026

Name and Signature of Supervisor with Seal

ABSTRACT

The usage of Fractal and Metamaterial based antennas has become a very viable solution for the future of wireless communication and the Internet of Things (IoT) applications that require compact size, multi-band operation, higher bandwidth, enhanced radiation efficiency, and reliable connectivity. These antennas utilize the unique properties of fractal geometries and engineered metasurfaces based on metamaterials to allow them to surpass the limits of traditional antenna designs. Fractal structures possess the properties of self-similarity and space filling, allowing them to be very efficient in the miniaturization of antennas and providing them with the capability of supporting multi-band or wideband resonant behaviour inherently. The addition of metamaterial elements to the antenna design will enable the antenna's overall performance to be improved significantly from both an operational as well as a design perspective, particularly in situations where space is limited and the electromagnetic environment is complex. The incorporation of fractal geometries into antenna design (star patterns, Sierpinski triangles, etc.) creates multiple current paths of different electrical lengths that produce resonant behaviour within multiple frequency bands while retaining the ability to have a small physical profile for the antenna. The use of metamaterial components, such as split-ring resonators, metasurface superstrates, and engineered ground planes are very important in enhancing the control of the propagation behaviour of electromagnetic waves. These components provide surface wave suppression, increase electromagnetic coupling, improve impedance matching, and enhance gain and directivity to provide enhanced radiation characteristics and increase bandwidth. The effectiveness of this composite approach is demonstrated via practical implementations in the development of antennas such as an asymmetrical notch fractal antenna with a well-designed and positioned metasurface layer that provides a stable impedance match with a return loss below -10 dB and peak resonance at 5.2 GHz with increased directivity and radiation efficiency. Combining the fractal and metamaterial concepts offers significant advantages for mid-band wireless applications. Further performance enhancements were also accomplished by incorporating a double-fractal configuration comprising a symmetrical star fractal radiating patch, a fractal-defective ground structure and a rectangular split-ring resonator (RSRR) array metasurface superstructure. This advanced combined design provides an impedance bandwidth of about 10.24%, operates effectively in the C-band from 5.22 to 5.78 GHz, has significantly higher gain and directivity compared to conventional

antenna designs. The above symmetrical and asymmetrical fractal designs made with metasurfaces have been fabricated and tested, yielding good correlation between the electromagnetic simulations in Ansys HFSS and the experimental results from a vector network analyzer (VNA) performed with an anechoic chamber. These results demonstrate that these designs are trustworthy, robust, and practical. Overall, there is a lot of potential for using metamaterial based fractal antennas to produce a compact, efficient and high performing antenna structure suitable for many applications such as: multi-standard IoT systems; wearable and flexible devices; energy harvesting systems; and for the development of dense wireless networks. Due to their versatility and performance advantages, they represent one of the most promising enabling technologies for future wireless communications systems.

***Keywords**:* Fractal Antenna, Metamaterial, Metasurface, Multi-band Operation, Miniaturization, Radiation Efficiency, Fractal Defective Ground Structure (FDGS), Rectangular Split-Ring Resonator (RSRR), Wireless Communication, Internet of Things (IoT)

ACKNOWLEDGEMENT

First and foremost, I bow to **Shri Radhe Krishna** for the divine blessings, strength, and guidance that have sustained me throughout my PhD journey.

I express my deepest gratitude to my research supervisor, **Prof. (Dr.) Jagdish M. Rathod**, for his invaluable guidance, constant encouragement, and insightful suggestions, which have shaped the quality and direction of this thesis. I am sincerely thankful to the Doctoral Progress Committee (DPC) members, **Dr. Trushit Upadhyaya and Dr. Tushar Dave**, for their constructive feedback, critical comments, and continuous support throughout the various stages of my research.

I extend my heartfelt thanks to **Gujarat Technological University (GTU)** for providing the academic platform and support for my doctoral studies, and to all the members of **the EC Department and PhD Section** for their cooperation and encouragement.

I gratefully acknowledge the research facilities and technical support provided by the **ELARC Lab, Electronics Department, B. V. M. Engineering College, VV Nagar,** which were instrumental in conducting the experimental and measurement work reported in this thesis.

I am especially thrilled to express my heartfelt gratitude to my vibrant peer research group and dear friends – **Dr. Shahid Modasiya, Dr. Vishal Polara, Dr. Nitin Bathani, Dr. Rasmin Tanna, and Ms. Devyani Varadiya** – whose inspiring discussions, constant encouragement, and unwavering moral support infused every phase of this journey with energy. Their companionship has turned this demanding academic journey into an enriching and truly memorable experience.

I also extend my sincere thanks to my enthusiastic students, the supportive **staff of the EC Department, and the respected HOD and Principal of A. V. Parekh Technical Institute, Rajkot,** for their continued encouragement, cooperation, and confidence in my work, which greatly motivated me to complete this thesis. Lastly, I thank all my well-wishers who have encouraged and supported me, directly or indirectly, throughout my research.

Dalsania Piyushkumar Chandulal

DEDICATION

This thesis is dedicated with deepest love and gratitude to my beloved wife, **Susmita,** whose unwavering support, patience, and understanding have been my constant strength. It is also dedicated to our cherished children, **Shreeya and Devam**, whose smiles, innocence, and joy have been a source of inspiration and motivation throughout this journey.

I also lovingly dedicate this work to my parents, **Kantaben and Chandubhai**, whose sacrifices, values, and blessings have shaped who I am and made this achievement possible.

This work is a testament to the strength of our family bond. I am profoundly grateful for the love and stability you brought into my life. Thank you for being my pillars of support and for sharing the joys and sacrifices that come with academic pursuits. This achievement is as much yours as it is mine.

With all my love,

Dalsania Piyushkumar Chandulal

Table of Contents

DECLARATION ..... **I**
CERTIFICATE ..... **II**
COURSE-WORK COMPLETION CERTIFICATE ..... **III**
ORIGINALITY REPORT CERTIFICATE ..... **IV**
PH. D. THESIS NON-EXCLUSIVE LICENSE TO GTU ..... **VIII**
THESIS APPROVAL FORM ..... **X**
ABSTRACT ..... **XI**
ACKNOWLEDGEMENT ..... **XIII**
DEDICATION ..... **XIV**
LIST OF FIGURES ..... **XVIII**
LIST OF TABLES ..... **XX**
LIST OF ABBREVIATIONS ..... **XXI**
CHAPTER 1 ..... **1**
INTRODUCTION **1**
1.1. Introduction 1
1.2. Overview of Next-Generation Antennas & Classification by Application 3
1.3. Key Performance Requirements of Next-Generation Antennas 8
1.4. Fractals and Metamaterials for Antenna Design 11
1.5. Significance of the study 26
1.6. Contributions of the study 26
1.7. Organization of Thesis 27
CHAPTER 2 ..... **29**
LITERATURE REVIEW **29**
2.1. Introduction 29
2.2. Fractal Based Antennas: Concepts and Applications 30
2.3. Metamaterials and Metasurfaces for Antenna Performance Enhancement 34
2.4. Hybrid Fractal-Metamaterial Antennas 39
2.5. Research Gaps 43
2.6. Motivation 44
2.7. Research Objectives 45

CHAPTER 3 46

DESIGN-1 METHODOLOGY AND RESULT AND DISCUSSION: AN ASYMMETRICAL NOTCH FRACTAL ANTENNA WITH METASURFACE 46

3.1. Introduction 46

3.2. Method 47

3.3. Antenna design Specifications 49

3.3.1. Fractal Antenna Design 51

3.3.2. Notch Characteristics 51

3.3.3. Metasurface integration 51

3.4. Anechoic Chamber Testing of the Fractal Antenna 52

3.4.1. Ground Plane Configurations 54

3.4.2. Performance Optimization 54

3.5. Results and Discussion 55

3.5.1. Return Loss and Bandwidth 55

3.5.2. Voltage standing wave ratio analysis 57

3.5.3. Gain and Directivity 57

3.5.4. Radiation Patterns and Axial Ratio 58

3.5.5. S-Parameter and Impedance 60

3.5.6. Efficiency and Radiation Intensity 61

3.5.7. Power Handling and Ground Effects 62

DESIGN-2 METHODOLOGY AND RESULT AND DISCUSSION: PERFORMANCE ENHANCED STAR FRACTAL ANTENNA WITH FRACTAL DGS AND METASURFACE INTEGRATION 67

4.1. Introduction 67

4.2. Fractal Geometry-Based Design and Its Impact on Antenna Performance 68

4.2.1. Design Architecture 70

4.2.2. Mathematical Modeling of Fractal Geometry 72

4.2.3. Procedure for Designing the R-SRR Metasurface 73

4.3. Results and Discussions 77

4.3.1. Experimental Setup 77

4.3.2. Detailed Analysis of Return Loss Measurements 78

4.3.3. Analysis of Voltage Standing Wave Ratio (VSWR) 80

4.3.4. Interpretation of the Impedance plot 80

4.3.5. Analysis of Gain and Directivity Characteristics 81

4.3.6. Analysis of Radiation Efficiency 83
4.3.7. Analysis of Radiation Efficiency 84
4.3.8. Comprehensive Discussion of Experimental Results 85
CHAPTER 5 90
CONCLUSION AND FUTURE WORK 90
5.1. Conclusion 90
5.2. Future Work 91
REFERENCES 92
List of Publications 103
Patent Published 103

LIST OF FIGURES

Figure 1.1. Fern 12
Figure 1.3. Example of a space-filling (SF) fractal illustrating the iterative construction of the Hilbert curve: (a) third-order iteration, (b) fourth-order iteration, and (c) fifth-order iteration. 13
Figure 1.4. Iterations of Koch Curve Fractal 15
Figure 1.5. Sierpinski gasket 16
Figure 1.6. Minkowski curve: a) First iteration, b) Second iteration, c) Third iteration 17
Figure 1.7. Metamaterial classification based on permittivity (ε) and permeability (μ) 19
Figure 1.8. Square structure SRR & CSRR 21
Figure 1.9. Frequency dependence of effective permittivity for a SRR 21
Figure 2.1. Key features and performance advantages of fractal and metamaterial-inspired antennas 39
Figure 3.1. Design flow of the proposed fractal antenna integrated with a metasurface 47
Figure 3.2. Triangular fractal ground plan……...48
Figure 3.3. Multi-layered configuration R-SRR Metasurface, Fractal Patch-Feedline, Fractal Ground & Detail view of Asymmetrical Notch Patch 49
Figure 3.4. Fabricated proposed asymmetrical star-shaped fractal antenna incorporating a metasurface and fractal ground 50
Figure 3.5. Experimental setup of the fractal antenna inside the anechoic chamber 53
Figure 3.6. Simulated S-parameter (S11) plot across 2.0–7.0 GHz 56
Figure 3.7. Measured reflection loss (S11) of the fabricated antenna: (a) higher-frequency resonance and (b) lower-frequency resonance 56
Figure 3.8. VSWR plot across a wide frequency range for the proposed fractal antenna... 57
Figure 3.9. Gain and directivity plots with maximum and minimum values across various angles 58
Figure 3.10. Polar radiation characteristics of the proposed antenna at f = 5.2075 GHz: (a) gain plot 2 for Φ=0◦ and Φ=90◦ and(b)gain plot 3 for Θ = 0◦ and Θ = 90◦ 59
Figure 3.11. Axial ratio variations at 5.2075 GHz for Φ = 0◦, Φ = 90◦, and Φ = 180◦ orientations 59
Figure 3.12. S-parameter chart showing reflection characteristics at 5.2075 GHz 60
Figure 3.13. Antenna gain and directivity over the frequency range of 5.00–6.00 GHz 61

Figure 3.14. Antenna performance between 5.00–6.00 GHz: (a) radiation efficiency and (b) radiation intensity with peaks at 5.2075 GHz 62
Figure 3.15. Antenna performance showing power handling capability..... 63
Figure 3.16. Antenna performance showing return loss for different ground configurations. 63
Figure 4.1. (a) Star-shaped fractal Patch with symmetric Notch (b) Sierpinski triangle fractal antenna with recursive design as defective ground structure. 68
Figure 4.2. 3 × 4 Rectangular Split Ring Resonator (R-SRR) Metasurface as super substrate 69
Figure 4.3. Star-shaped fractal antenna with fractal DGS and metasurface..... 70
Figure 4.4. Design Flow for Fractal Antenna with Meta Material Inspired metasurface.... 71
Figure 4.5. Figure Super-subtract Based Arrangement 73
Figure 4.6. Fabry–Perot cavity-based arrangement in Proposed Antenna 74
Figure 4.7. Fabricated star-shaped fractal patch with asymmetric notch and a metasurface. 75
Figure 4.8 Bottom Group Layer of a fractal DGS with a Sierpinski triangle design 76
Figure 4.9. Proposed Star Fractal antenna with Metasurface in an anechoic chamber for measurement 78
Figure 4.10. Return Loss Plot demonstrating impedance matching with full ground and with Fractal DGS and MS. 79
Figure 4.11. VSWR vs frequency plot. 80
Figure 4.12. Impedance plot at the resonant frequency showing near-ideal antenna impedance with minimal reactive component and optimal resistive matching. 81
Figure 4.13. Simulated and measured radiation plots. 82
Figure 4.14. 3D directive plot indicating the fractal antenna's ability to focus energy, highlighting its peak and minimum directivity values across different angles. 82
Figure 4.15 Radiation efficiency plot showing the proportion of input power effectively radiated across the frequency range..... 83
Figure 4.16. Radiation intensity plot showing the peak emission across the operational frequency range, highlighting the antenna's optimal operating frequency. 84
Figure 4.17. Return loss plots of simulated and measured in VNA 86
Figure 4.18. Simulated and measured gain plots with and without a metasurface..... 86

LIST OF TABLES

Table 3.1. Design parameters of the proposed asymmetrical star-shaped fractal antenna .. 50
Table 3.2: Summary of Antenna Performance Metrics across Various Measurements 64
Table 3.3. Comparison of the proposed antenna with recent state-of-the-art designs..... 65
Table 4.1. Antenna component dimensions. 76
Table 4.2. Experimental assessment of antenna performance parameters. 85
Table 4.3. Performance comparison of the proposed metamaterial-inspired fractal antenna with existing literature. 88

LIST OF ABBREVIATIONS

4G	Fourth Generation Wireless Communication
5G	Fifth Generation Wireless Communication
6G	Sixth Generation Wireless Communication
AMC	Artificial Magnetic Conductor
AMC-MS	Artificial Magnetic Conductor Metasurface
BER	Bit Error Rate
C-Band	C Frequency Band
CMOS	Complementary Metal Oxide Semiconductor
CP	Circular Polarization
CPW	Coplanar Waveguide
CSRR	Complementary Split Ring Resonator
FDGS	Fractal Defective Ground Structure
DNG	Double Negative
DPS	Double Positive
EBG	Electromagnetic Band-Gap
eMBB	Enhanced Mobile Broadband
eMTC	Enhanced Machine-Type Communication
ENG	Epsilon Negative
ENG-TL	Epsilon Negative Transmission Line
FBR	Front-to-Back Ratio
FCC	Federal Communications Commission
FR4	Flame Retardant-4 Substrate
FSS	Frequency Selective Surface
GHz	Gigahertz
HFSS	High-Frequency Structure Simulator
IFS	Iterative Function System
IoT	Internet of Things
ISM	Industrial, Scientific and Medical Band
Ka-Band	Ka Frequency Band
Ku-Band	Ku Frequency Band
LEO	Low Earth Orbit

LDR	Light Dependent Resistor
MIMO	Multiple Input Multiple Output
mmWave	Millimeter Wave
MNG	Mu Negative
MRIS	Metamaterial Reactive Impedance Substrate
MS	Metasurface
NZRI	Near-Zero Refractive Index
PEC	Perfect Electric Conductor
PMC	Perfect Magnetic Conductor
RF	Radio Frequency
RCS	Radar Cross Section
RSRR	Rectangular Split Ring Resonator
SAR	Specific Absorption Rate
SF	Space Filling
SNG	Single Negative
SRR	Split Ring Resonator
SSR	Single Split Ring Resonator
SSRR	Symmetric Split Ring Resonator
SWB	Super Wideband
THz	Terahertz
UHF	Ultra High Frequency
UWB	Ultra-Wideband
URLLC	Ultra-Reliable Low-Latency Communication
V2X	Vehicle-to-Everything
VNA	Vector Network Analyzer
VSWR	Voltage Standing Wave Ratio
WBASN	Wireless Body Area Sensor Network
WLAN	Wireless Local Area Network
WiMAX	Worldwide Interoperability for Microwave Access

CHAPTER 1

INTRODUCTION

1.1. Introduction

Modern society relies heavily on wireless communication systems for various purposes, connecting with one another over distance in both personal and professional arena, entertainment of all types and acquiring information that we take for granted today. The last few decades have seen an unprecedented change in the speed at which wireless technologies have developed and their ability to change how information is sent and received, the 4th Generation (4G) wireless communications system has been the primary means of mobile communications over the past ten years or longer, but it is fast nearing its theoretical capacity to carry information due to limitations on data capacity, latency and spectral efficiency [1][2]. The explosion of connected devices such as smartphones, IoT enabled devices, wearables and M2M communications is putting enormous pressure on the wireless infrastructure [3].

The GSMA Mobile Economy Report states that more than 1 billion 5G connections will exist worldwide and that their numbers will keep increasing because many people around the world will gain 5G network access [4]. The fifth generation (5G) system provides data transmission speeds that reach 100 Gbps while maintaining ultra low latency of 1 ms, which enables the operation of augmented reality (AR), virtual reality (VR), self driving vehicles, industrial automation, and extensive Internet of Things (IoT) systems. Through its implementation of variable subcarrier spacing together with adaptive time frequency resource allocation 5G achieves operational flexibility that enables it to provide service support for three different categories, enhanced Mobile Broadband (eMBB) and enhanced Machine Type Communications (eMTC) and Ultra-Reliable Low Latency Communications (URLLC) [5][6].

Antennas are at the core of all wireless communication systems acting as an essential component that connects guided electromagnetic waves with free space radiation. Due to advances in wireless systems and the increase in data rates, having access to multiple frequency bands, and denser network deployment, the design and performance requirements

of antennas are much more complex than ever before. Today, modern wireless and IoT devices require antennas that are compact, lightweight, energy efficient, and that can operate across many frequency bands while maintaining high levels of radiation efficiency and stable radiation characteristics [7][8].

Currently, one of the largest challenges in antenna design is miniaturization. The trend toward miniaturizing electronic components (including integrated circuits) has made antennas the bottleneck for producing fully compact wireless devices. Antennas differ from electronic components in that their size is determined by the physical properties of electromagnetism, specifically wavelength-based criteria. Reducing an antenna to a smaller than average size results in undesirable degradation of critical performance parameters such as bandwidth, gain, radiation efficiency, and polarization [9]. Thus, minimizing the size of antennas necessitates careful balancing of size reduction versus acceptable levels of radiation performance and commonly requires creative geometry or material based design alternatives [10]. Modern wireless devices need two essential requirements which are miniaturization and multiband operation. Contemporary communication systems need to work across multiple frequency bands because they must support different standards and services. The implementation of multiple antennas provides an easy solution but its deployment faces restrictions because of expenses and spatial requirements and difficulties in system integration. The design of multiband antennas which enable simultaneous operation at multiple frequency bands has become a research focus. The research community has studied various techniques which include parasitic elements and slot loading and advanced feeding mechanisms and fractal geometries to achieve multiband and wideband functionality without increasing antenna dimensions [11] [12].

Attaining high radiation efficiency and high gain from small antennas for mobile and IoT systems, with their critical need for low power consumption, is a long standing challenge. Smaller antenna designs typically experience poor radiating efficiency and incur greater losses which require the development of new design methodologies to improve the electrical performance of antennas while still keeping them small [13]. As part of these efforts, there has been the introduction of new concepts such as fractals and metamaterials which are expected to provide better performance from antennas than previously available, allowing the antennas to perform effectively in future wireless and IoT communication systems.

1.2. Overview of Next-Generation Antennas & Classification by Application

Advanced antenna architecture is required for next generation wireless communication systems to support a wide variety of applications across multiple frequency bands with high performance standards. The increased deployment of 5G, IoT, satellite, and emerging terahertz systems has resulted in the creation of unique antenna technologies designed to meet unique requirements for their environments. Therefore, this section will begin with a classification of next generation antennas based on application and operating frequency, then discuss key attributes necessary to achieve modern antenna design.

Modern wireless communication system technology is rapidly changing, which means that there are a lot of different types of antennas required for the many different types of applications and frequency ranges. As new technologies like 5G and IoT move forward, so the ways in which antennas are designed to meet their challenges (including size, efficiency, gain, reliability, bandwidth, etc.) [14][15][16]. Because of this, next generation antennas will be organized by the application for which they will be used and the frequency range of that application in order to make it easier to analyze the design criteria, trade offs and the use of advanced technology (such as metamaterials or fractal geometry) when designing and producing new antennas to support wireless communication in the future.

5G Antennas

5G networks offer major improvements in wireless communications with incredibly fast data speeds, close to no delay and dependable connections to huge quantities of devices. 5G technology has been designed to support real time and data intensive applications such as autonomous vehicles, industrial automation, augmented reality and large scale IoT installations. Antenna technology is key to achieving these functions. The two frequency bands for 5G are below 6 GHz (sub-6) and in the mmWave range (above 24 GHz). Sub-6 antennas have a wide coverage area and work well through obstacles. However, mmWave antennas operate at much higher speeds but employ special techniques such as beamforming and high gain concentrations in order to compensate for extreme signal loss. To comply with demanding metrics such as multiple gigabits per second, near real time latency, high levels of reliability, and enabling large numbers of connected devices, specific antenna configurations have been developed for use with 5G networks including massive MIMO.

To meet user safety requirements, antennas need to be small, efficient, precise in their ability to steer a beam, and provide wide bandwidths. Furthermore, the speed with which 5G will be deployed around the world also creates pressure for low energy antennas and low carbon solutions now that we are building densified networks of small radio cells [18]. One way to achieve many of these characteristics is through the use of novel antenna designs based on metamaterials or fractal geometries since they facilitate the miniaturization of an antenna, allow for operations in multiple frequency bands, and improve the radiation properties of the antenna, thereby playing an essential role in the success of future wireless communication systems.

IoT and Wi-Fi Antennas

In response to the fast moving world of modern technology featuring increasing amounts of connected devices, the need for the further development of small, low power, and cost effective IoT and Wi-Fi antennas capable of supporting this new generation of products has arisen. Battery powered (or energy harvesting) devices design require that the ability to operate using low power be a primary performance criterion. Therefore, antennas used in the IoT and Wi-Fi ecosystems must deliver high radiation efficiency while featuring small form factor dimensions and low profile so that they are capable of being incorporated into small form factor devices [19].

Another major requirement for antennas designed for IoT and Wi-Fi applications is the capability to operate in multiband frequency ranges, i.e., the antennas must be designed to provide coverage in the 2.4GHz, 5GHz, and the emerging sub-GHz bands used to provide long range and low data rate communications. Achieving effective impedance matching and stable radiation patterns in each of these frequency ranges is critical to providing reliable performance in high density environments with interference [20]. Finally, the use of low cost planar and printed circuit antenna technology is needed to produce antennas at a low cost to facilitate mass deployment of IoT networks. Because of this, antenna designers developing antennas for the IoT and Wi-Fi spaces are concentrating on providing an optimal balance between being small, low power, multiband capable, and low cost to manufacture.

On-Chip Antennas

On-chip antennas function as direct silicon platform antennas which operate at frequencies above 30 GHz for millimeter wave and terahertz wireless systems by enabling direct connection to RF and mixed signal circuits. Their primary advantage is the elimination

of drawbacks, which off chip antennas create because they require multiple connections, and they occupy large space and they need extra power and their packaging process becomes difficult when operating at high frequencies. The integration enables development of compact low power system on chip transceivers which support high speed wireless communication. On- chip antenna design presents difficulties because designers must achieve extreme miniaturization while semiconductor substrates, particularly silicon, create losses that decrease both radiation efficiency and gain. Antenna structures from the early period exhibited low performance which restricted their practical applications. Substrate isolation and multilayer configurations and suspended radiating elements represent three techniques which have been developed to overcome these restrictions [21].

Recent developments have made progress with metamaterials and metasurfaces and substrate-integrated waveguides which enhance radiation performance through their ability to curb surface waves and control electromagnetic fields while remaining compatible with CMOS technology. The development of on-chip antennas has become essential technology for upcoming wireless systems because it provides compact design and production compatibility and better radiation performance [22] [23].

Satellite Communication Antennas

Global communications, positioning, earth observation and television broadcasts all require satellite communication antennas operating in C, X, Ku, and Ka frequency bands within the upper microwave region of the electromagnetic spectrum. The antennas in these bands support the long distance link between an earth station and a satellite, the transfer of large volumes of information via high data rates, and wide area coverage of the earth's surface, making them very common in today's satellite systems. Antennas in C, X, Ku and Ka bands must provide high gain, high directivity and high radiation efficiency to meet the demands of increasing bandwidth and capacity resulting from the rapid growth in satellite communications. The higher frequencies of operation provide narrow angle antennas with high directivity, thus improving reliability of the link and reducing interference for both space to ground and inter satellite communications. At the same time, operating at higher frequency bands also presents challenges that include atmospheric attenuation, such as rain fade at Ku and Ka bands, and greater sensitivity to manufacturing tolerances [24]. Therefore, satellite communication antennas must be designed to ensure the stable and reliable performance of the antenna in a wide variety of environmental conditions over the expected life of the antenna.

Satellite technology has advanced toward high throughput satellites and low earth orbit (LEO) constellations and mobile terminals that creates demand for antennas that are compact and lightweight yet provide high gain performance. The latest advancements in antenna technology show adoption of reflect arrays and phased arrays and metamaterial based designs as methods to achieve beam steering and polarization diversity and multi band functionality [25]. The new technologies drive development of satellite communication systems which exceed current microwave band systems.

Navigation and Defense Antennas

The design of navigation and defense antennas allows their operation in environments which require both dependable performance and accurate results and strong resistance to all forms of testing. The system provides significant support to global navigation satellite systems and radar and surveillance and electronic warfare and military communications through its ability to transmit accurate signals in changing environments that contain multiple sources of interference. The antennas provide operational capabilities that span L and S bands through to X and Ku bands based on the needs of their specific operational systems.

The platform needs wideband and multiband capabilities to accommodate multiple navigation signals together with radar modes and communication standards. The system requires strong protection against electromagnetic interference and jamming as well as multipath effects to maintain signal integrity throughout operational missions [26]. To achieve optimal performance requirements, the system needs to maintain constant polarization while delivering strong radiation output and maintaining minimal side lobe levels which will enhance detection capabilities while reducing risks from enemy signal detection. The navigation and defense antennas need to maintain their operational capabilities under both mechanical and environmental challenges which occur during deployment on aircraft and ships and ground vehicles and unmanned systems that need durable conformal designs [27]. The combination of phased arrays with adaptive beamforming and metamaterials enhances system performance by increasing beam agility while improving interference management and overall system reliability. The research demonstrates that modern antenna design directly affects navigation systems and defense systems through its impact on their operational effectiveness.

Terahertz (THz) Antennas:

Terahertz (THz) antennas represent a new technological field, which enables wireless communication and sensing, and imaging applications to function across a frequency range that spans from 0.1 to 10 THz between microwave and optical systems. The THz spectrum provides a vast bandwidth capacity that makes THZ antennas suitable for upcoming 5G systems and future 6G networks that need higher data transfer rates than millimeter wave technology can provide. The implementation of THZ antennas encounters significant challenges that prevent their operational use. The production of antennas that operate at these frequencies needs specialized micro and nano manufacturing techniques because their dimensions become extremely tiny. The use of conventional metals leads to severe propagation losses, atmospheric absorption, material dispersion, and conductor losses which cause decreased radiation efficiency and shorter transmission distances. The research currently focuses on developing new materials while using advanced design methods that include plasmonic structures and graphene based antennas, metamaterials, and metasurfaces to achieve better electromagnetic confinement and radiation performance at THz frequencies. The research investigates how to connect with on-chip and system on chip platforms in order to decrease interconnect losses while creating small yet fast transceivers. The field of THZ antenna development remains vital because researchers strive to solve fabrication problems and propagation issues while using THZ spectrum bandwidth capabilities [28][29].

This classification will give a clear overview of the different types of antennas for next generation wireless networks by their intended use (or application) and the range of frequencies they operate on. Antennas for sub-6 GHz 5G, mmWave 5G, and the emerging terahertz systems pose unique performance challenges, still they all demonstrate an increasing demand for compact, high performance antenna solutions that are tailored exclusively to a specific application. Although the categorization of antennas helps us understand how to design antennas for specific wireless applications and specific frequency bands; it is important to also identify common fundamental performance requirements among all of the different types of antenna systems. Therefore, in this section we will discuss the primary characteristics that modern antennas must possess in order to properly provide for next generation wireless technologies.

1.3. Key Performance Requirements of Next-Generation Antennas

Modern antenna designs need to meet a number of crucial performance requirements to successfully accommodate a range of different next generation wireless system applications. As a result of the increasing size reduction of devices, limited spectrum resources, and the many varied types of applications which require wireless devices, the requirements that are imposed on antenna solutions are strict, conflicting and sometimes overlapping. This leads to the development of numerous antennas that will enable reliable, efficient, and flexible operation on various wireless technologies and frequency bands.

Miniaturization and Low-Profile Antenna Architecture:

Among modern antenna engineering challenges, miniaturization and low profile design are extremely important. As demand for small, portable and the multifunctional wireless devices continues to grow, so has the need for small form factor antennas with high levels of integration within rapidly evolving communication systems. For this reason, antennas must take up as little physical volume as possible while still providing suitable electrical (impedance bandwidth) and radiation performance. This will create room for many different applications, such as smartphones, wearables, IoT devices, biomedical implants, and on-chip wireless systems where available space is limited and available options for optimum antenna placement are few. In short, antennas must work effectively in very small physical locations. From an electromagnetic standpoint, the antenna's dimensions are also determined by the wavelength of the transmitted and received signal, when antennas are miniaturized to a great extent, their electrical performance is degraded (i.e. impedance bandwidth shrinks, gain and radiation efficiency decreases, fabrication tolerances become critical). Therefore, antenna miniaturization must involve careful consideration of the tradeoff between antenna performance parameters and physical size of the antenna. Low profile antenna configurations (i.e. antennas with low vertical aspects and which utilize planar geometries) make it easy to integrate with printed circuit boards and inside of final product packaging while also improving the overall appearance and structural integrity of the antennas.

To address the limitations imposed by size reduction, several advanced design approaches have been explored, including the use of fractal geometries, metamaterial inspired structures, defected ground planes, and high permittivity substrates. The techniques enable antennas to achieve lower frequency resonance through electrical length expansion

which takes place within restricted physical dimensions. Low-profile designs increase user safety through their two main benefits which include decreased electromagnetic exposure and better compatibility with conformal and wearable platforms [31]. As a result, attaining compact and low profile antenna architectures without sacrificing performance remains a central objective in the design of next generation wireless communication systems.

Multiband and Reconfigurable Operation

Antenna design has become an increasingly important part of wireless technology development, antennas are now required to operate in multiple frequency bands (multiband antennas) and to be more flexible (reconfigurable antennas). By using a single radiating element, a multiband antenna can provide radio frequency coverage in several different frequency bands. For example, mobile terminals or satellites must include antennas that can support multiple services, therefore an antenna designed for multiple services reduces the amount of space, weight, and cost necessary to support multiple antennas. While reducing the number of radiating elements will lead to compact system architectures and simplified hardware integration, designing a compact antenna that can achieve good multiband performance is a major challenge. In general, traditional multiband antenna topologies may suffer from degraded performance as a result of electrically complex current distributions, higher losses, and limitations on the ability to allocate frequency to the antenna. Several techniques have been proposed to achieve multiband performance including the use of different electrical length slots, parasitic elements, pyramidal configurations, and RF multiplexing. While these techniques have been helpful in creating multiple resonance frequencies, they may also introduce additional losses and lower the overall radiation efficiency of the antenna especially when the size of the antenna is constrained [32].

The need for adaptive communication and dynamic spectrum utilization has created demand for reconfigurable antennas which can change their operating frequency and radiation pattern and polarization during operation. The ability to reconfigure an antenna system enables it to adapt for different channel conditions and communication requirements which leads to better spectral efficiency and system adaptability [33]. Advanced mobile communication and multimedia transmission and satellite systems increasingly require such capabilities because they need to use their limited spectral resources efficiently. The development of multiband reconfigurable antenna designs enables wireless communication systems to achieve their requirements for versatility and compactness and high performance capabilities.

Ultra-Wideband (UWB) Performance

UWB offers a solution for transmitting high speed, low latency data wirelessly. UWB antennas use a very broad frequency range, enabling the transmission of short pulses with low average power, which supports high speed data transmission for accurate location tracking, sensing and positioning for short range applications. UWB is defined by the Federal Communications Commission (FCC) as having a fractional bandwidth of greater than 20% or a total bandwidth greater than 500 MHz, with the majority of the bandwidth occurring in the 3.1 to 10.6 GHz frequency range. Due to their low transmit power, UWB can only be used for short distances (approximately 10 meters) where there is no interference with other narrow-band communication systems [34].

UWB technology can be used for many applications including high speed personal area networks (PAN), wireless sensor networks, indoor positioning systems, radar systems, medical imaging systems, and advanced vehicle safety systems. The ultra-wide bandwidth of UWB allows for increased temporal resolution which is crucial for precise range measurements and accurate detections in sensing applications. Newer UWB antenna designs are now using techniques such as fractal geometry and band notch structures to improve the amount of frequency spectrum that can be covered and to operate efficiently. Band notching is particularly important to prevent UWB transmissions from interfering with existing narrow-band operations such as WiMAX, WLAN, and IEEE 802.11a, all of which share segments of the UWB frequency spectrum. Consequently, UWB antennas must deliver broad impedance bandwidth, stable radiation characteristics, and effective interference suppression. By providing wideband, low latency performance with precise spatial resolution, UWB antennas play a critical role in enabling next-generation wireless communication and sensing applications.

Enhanced Radiation Characteristics

For reliable signal transmission in next generation wireless communication systems that utilize dense deployment, are subject to high interference levels, and contain multipath reflections, there is a need for enhanced radiation characteristics. In particular, high antenna gain provides effective directional focusing of electromagnetic (EM) energy resulting in improved signal to noise ratio and extended coverage area at the same transmit power. Radiation efficiency provides for the conversion of the majority of the input power into useful radiated energy which is particularly important in the case of battery powered or energy constrained devices. Polarization control is another important characteristic that aids

in mitigating the effects of multipath since it ensures a consistent electric field orientation at the receiving antenna, reduces fading and provides for a more reliable link in metropolitan and indoor environments. Advanced design techniques such as metamaterials, metasurfaces, and fractal geometries have been developed and widely used to obtain these improvements without requiring an increase in antenna size [36] [37]. In summary, antennas with enhanced radiation characteristics that include high gain, efficient power conversion, and accurate polarization control are a necessity for current wireless communications applications including 5G, IoT, satellite communications, and terahertz systems. These characteristics, along with miniaturization, multiband reconfigurable operation, and ultra-wideband performance represent the fundamental design principles of future generations of antennas.

1.4. Fractals and Metamaterials for Antenna Design

The design of next generation antennas requires advanced fractal and metamaterial design methods which allow antennas to achieve better performance within smaller devices. The techniques use self-similar geometric patterns together with created electromagnetic traits to achieve four goals which include system size reduction and multiple frequency bands and increased bandwidth and better radiation performance for contemporary wireless technologies.

Fractal Antenna

Fractals are based on mathematical principles and were created by using a wide variety of fractal shapes and sizes in their designs. The word "fractal" was first used by Mandelbrot to describe this new branch of mathematics, which takes its name from the Latin prefix "fractus," which means "broken" or "broken too small." The defining features of fractals are that they consist of a complex pattern that repeats over time; they have many unique properties; and they tend to have a very high level of division between their constituent elements. After Cohen published his first paper showing how to build antenna elements from fractals in 1988, it was Werner who, in 1994, published the first work to use the term "fractal antenna" to refer to antennas made from these designs. In general, a fractal can be understood as a way to classify a geometric structure's properties that create both an infinite number of ways in which to duplicate it and an infinite number of ways to fill up space. Essentially, a fractal is a structure in which there is a clearly identifiable relationship between the parts and the whole. The geometrical characteristics of fractals lend themselves well to modeling many different kinds of break-up patterns in nature, such as the breakdown

of costliness, the breakdown of mountains, and so forth; therefore, if one takes this type of structure and applies it to the design of antennas, one will have a compact structure that has an extended electrical length and will naturally provide multiple frequency responses that are inherently broadband and multiband.

- **Self-similarity property**

Self-similar properties represent a type of structural characteristic where the overall geometry of a complex cluster consists of smaller sub clusters, each with similar geometry. At every level of the structure one can find representations of the same pattern only scaled, thus, there is no fixed or defined size to them. An example of a self-similar fractal can be seen in a fern leaf (shown in Figure 1.1) and will have either the same scaling factor in both orthogonal directions or different scaling factors; geometries with different scaling factors are known as self-affine fractals. Because this repeated form of scaling behaviour occurs, there has been considerable interest in conducting research into the self-similar property of fractals since they can be beneficial in designing and understanding multiband and wideband antennas.



Figure 1.1. Fern

- **Space-Filling Properties**

The space-filling property describes the ability of a fractal curve, when iterated a large number of times, to occupy a two dimensional region while its effective curve length approaches infinity. Fractal geometries possess fundamental complexity which enhances

radiation performance when used in antenna elements and antenna arrays. Fractals enable antennas to achieve much smaller physical sizes because their operational frequency relies less on the total size of the antenna design. Antenna gain and bandwidth improvement, which covers a wide frequency range, can be achieved through the multilevel space-filling nature of fractal geometries, which enables antenna miniaturization. The space-filling curve serves as a sample space-filling fractal, which demonstrates its compact fractal structure through the diagram in Figure 1.2. The copper traces in these structures represent only a tiny portion of the operating wavelength. The typical appearance of iterated Hilbert curve fractal antennas is shown in Figure 1.3.



Figure 1.2. Space filling curve fractal antenna

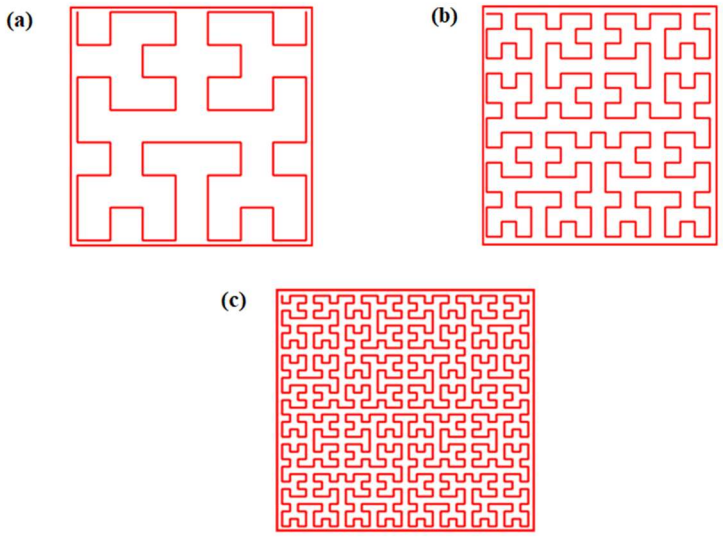


Figure 1.3. Example of a space-filling (SF) fractal illustrating the iterative construction of the Hilbert curve: (a) third-order iteration, (b) fourth-order iteration, and (c) fifth-order iteration.

- **Iterative Function System**

The Iterative Function System (IFS) serves as a mathematical method which use to create fractal geometries. The system delivers a structured method which enables users to display and store and manage fractal designs through their use of successive transformations. The IFS system operates through a series of interconnected shape changes which users apply through repeated cycles. Fractal generation using IFS typically starts with a basic geometric shape referred to as the initiator. A Euclidean triangle functions as the initiator which creates the Sierpinski gasket and the Koch snowflake while a square serves as the initiator for the Minkowski Island fractal. The fractal design process begins with an initiator which the system uses to apply a series of transformation rules known as the generator. The fractal patterns develop into more intricate designs through the process of applying the initiator together with the generator in an alternating pattern.

An important parameter related with fractal structures is the self-similarity dimension ($\boldsymbol{D_s}$), which characterizes the scaling behavior of the geometry and is defined as

$$\boldsymbol{D_s} = \frac{\log(\boldsymbol{N})}{\log(\boldsymbol{1/s})} \tag{1.1}$$

Where, $\boldsymbol{N}$ represents the total number of self-similar copies produced at each iteration, and s denotes the scaling factor. The self-similarity dimension is not necessarily an integer, reflecting the inherent complexity of fractal geometries.

The unified framework provided by IFS enables users to create and manage fractal patterns, which makes it an ideal tool for constructing fractal geometric designs. The approach uses transformation patterns which repeat until the resulting basic units become identical, as those units only differ by their size when compared to the original initiator [40].

- **Common Fractal Geometries Used in Antenna Design**

The Koch, Sierpinski, and Minkowski fractals are the three most well researched fractal geometries for use as antennas because they have mathematical structure that is well defined and electromagnetic performance advantages that are established. The Koch fractal geometry is based on the classical Koch curve and is generated by recursively replacing a straight line segment with a scaled bent version of itself. As you move up in level of recursion, there is an increase in the overall length of the Koch curve while the amount of area occupied remains almost constant. It is this type of behaviour, which is known as space-

filling, that increases the electrical length of the antenna and keeps the physical size of the antenna very small. Therefore, antennas based on the Koch fractal are useful for miniaturizing antennas and increasing their bandwidth capabilities, making them particularly good candidates for small wireless devices that will operate at lower frequencies. Figure 1.4 illustrates a number of different iterations of the Koch curve fractal geometry.

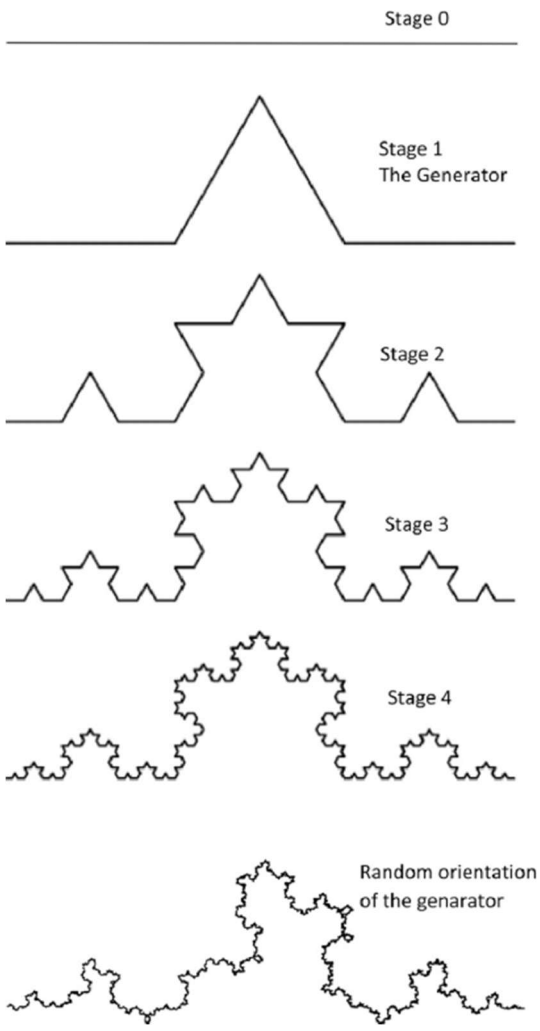


Figure 1.4. Iterations of Koch Curve Fractal

The geometry of the Sierpinski Gasket (a Sierpinski structure) is a result of removing self-similar forms from an initial triangular or square shape (as shown in Figure 1.5). The Sierpinski fractal is very self-similar and therefore it produces a multitude of

resonant modes when applied to antenna designs. Each iteration of removal produces many new resonant paths within the frequency range and adds higher frequency and shorter length resonances to the overall structure, creating a truly multi-band antenna. Because of this, Sierpinski antennas are widely used for applications that require an antenna capable of supporting multiple communications standards simultaneously.

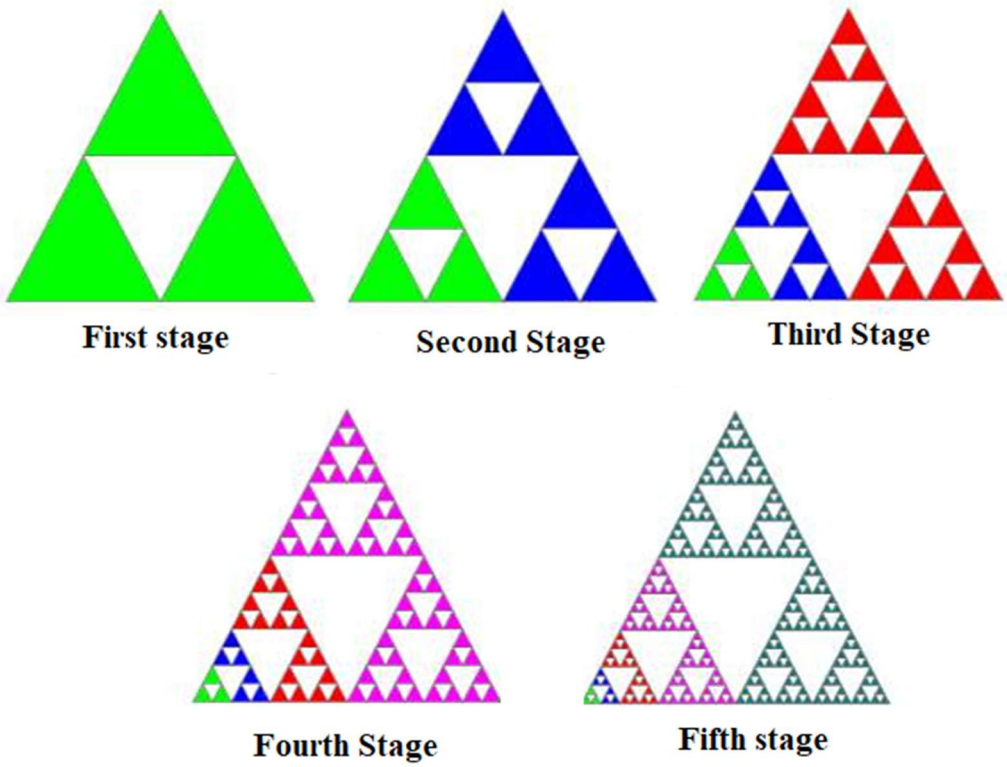


Figure 1.5. Sierpinski gasket

The Minkowski Island exists as a Minkowski geometry which begins from a square shape that develops through its edges being repeatedly indented according to a specified generator pattern throughout Figure 1.6. The method creates an extremely complex boundary which expands the electrical perimeter but maintains a small physical size. The design of Minkowski fractal antennas provides engineers with a solution that enables them to reduce equipment dimensions while achieving sufficient impedance bandwidth and radiation performance. Engineers use these antennas in patch and planar antenna designs which require space efficient solutions.

The three fractal geometries of Koch Sierpinski and Minkowski provide different design benefits which work together to improve antenna performance. Koch geometries enable

devices to use less space while achieving better bandwidth performance Sierpinski structures enable multiband operation through their self-similar design and Minkowski islands deliver both compact size and effective radiation ability. Fractal geometries provide designers with an advanced design method that improves wireless systems for present and future communication networks.

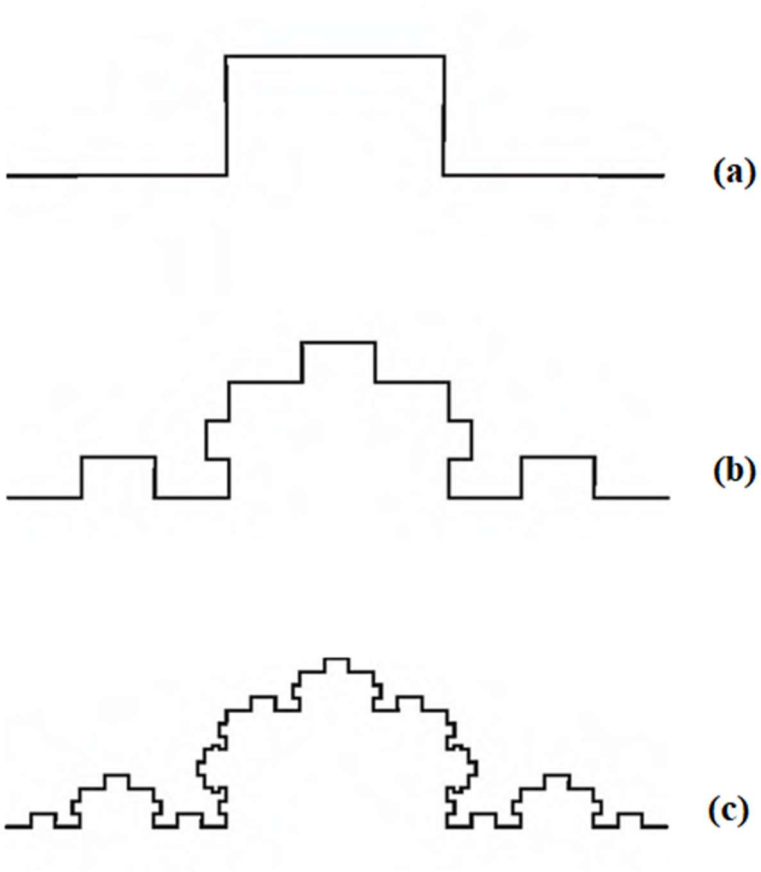


Figure 1.6. Minkowski curve: a) First iteration, b) Second iteration, c) Third iteration

Fractal antennas provide multiple unique benefits which make them ideal for use in current wireless communication systems. Fractal geometries display self-similar and space-filling properties which allow engineers to create compact antennas that maintain their original performance through increased effective electrical length. The self-similar nature of the design allows the antenna to operate at multiple frequency bands through its various resonant points. The introduction of fractal iterations creates additional perimeter and current path elements which result in better impedance matching and increased bandwidth

performance. The combination of these properties leads to the development of compact antennas which maintain high efficiency and adaptability while fulfilling demanding size and performance requirements.

Fractal antennas have become essential components for various wireless systems because of their small size and ability to operate on multiple frequency bands. Fractal antennas provide mobile devices which include smartphones and tablets and wearable electronics with their ability to support multiple communication standards while using minimal space. The technology suits Internet of Things applications because it provides both small device sizes and multiple frequency band support which is necessary for handling numerous sensors in tight spaces. Fractal antennas establish their use in wideband and multiband wireless systems which include WLAN, 4G/5G transceivers, satellite communication, and cognitive radio systems because they need adaptable systems which can maintain dependable performance across various frequency ranges. Fractal antennas exploit self-similarity, space-filling properties, and IFS-based geometries to realize compact, multiband, and wideband antenna designs suitable for modern wireless systems [42]. Their capacity to create extended electrical routes in compact areas makes them ideal for applications that need to transmit multiple communication standards from restricted spaces. The next section presents metamaterial based antennas which use geometric optimization techniques as their foundation to achieve better antenna performance through specially designed electromagnetic characteristics and innovative material integration methods which enhance gain, bandwidth, miniaturization, and radiation control capabilities.

Metamaterials

The discovery of metamaterials, which people call negative index materials, has created a new category of artificial electromagnetic materials because these materials behave differently from traditional wave interaction patterns. Metamaterials function as artificial materials which scientists design by arranging subwavelength resonant elements at specific intervals to create electromagnetic properties that nature does not produce. The design of metamaterials with specific effective permittivity values (ε) and permeability values (μ) allows engineers to achieve precise control over electromagnetic wave movement, which enables the development of new compact antenna systems that function multiple tasks while delivering high performance [43].

The refractive index (n) of a material is fundamentally governed by its effective permittivity and permeability and is expressed as

$$\boldsymbol{n = \sqrt{\varepsilon_r \mu_r}} \tag{1.2}$$

Where, $\boldsymbol{\varepsilon_r}$ and $\boldsymbol{\mu_r}$ signify the relative permittivity and relative permeability of the medium, respectively. The relative permittivity is defined as the ratio of the material permittivity to the free space permittivity, given by

$$\boldsymbol{\varepsilon_r = \frac{\varepsilon}{\varepsilon_0}} \tag{1.3}$$

Similarly, the relative permeability is expressed as

$$\boldsymbol{\mu_r = \frac{\mu}{\mu_0}} \tag{1.4}$$

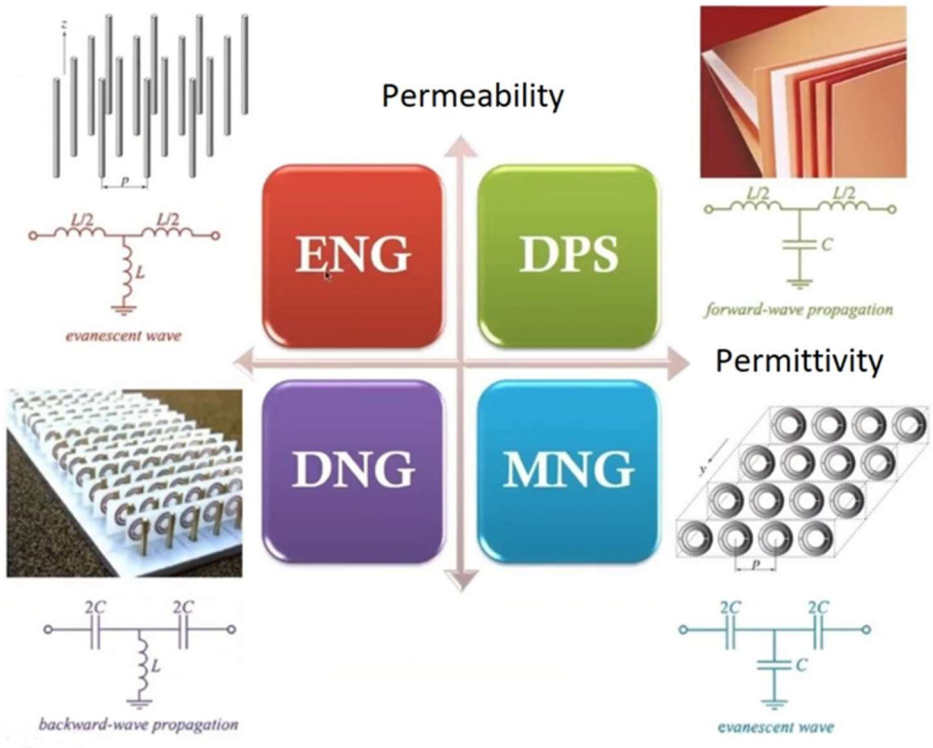


Figure 1.7. Metamaterial classification based on permittivity (ε) and permeability (μ)

Electromagnetic materials can be divided into four different groups which depend on the values of ε and μ. Materials that have positive permittivity and permeability qualities belong to Double Positive (DPS) media which serves as standard dielectric materials. Epsilon Negative (ENG) materials exhibit negative permittivity and positive permeability, while Mu Negative (MNG) materials exhibit positive permittivity and negative permeability.

The Double Negative (DNG) materials which have both negative values for ε and μ [44]. The materials which scientists refer to as metamaterials or left handed materials demonstrate backward wave propagation with negative refraction, as shown in Figure 1.7.

The unique electromagnetic behaviour of DNG metamaterials has been extensively exploited in antenna engineering to overcome classical design limitations. By incorporating negative refractive index effects, metamaterials enable antenna shrinking, resonance shifting, bandwidth enhancement, and radiation pattern control without changing the physical size of the antenna. This has made metamaterials especially attractive for lightweight, low-profile, and multifunctional antenna systems.

Engineered resonant unit cells of which the Split-Ring Resonators (SRRs) and Complementary Split-Ring Resonators (CSRRs) are the most commonly used to practically realize metamaterials. While CSRRs, which are dual structures etched on metallic surfaces, are useful in achieving negative permittivity characteristics, SRRs are made up of metallic rings with splits that predominantly generate negative permeability near resonance. To customize the antenna's electromagnetic response, these resonators are frequently incorporated into superstrates, ground planes, or antenna substrates [45].

a) Split Ring Resonators (SRRs)

One of the simplest artificial structures for creating metamaterials with negative magnetic permeability is the SRR. Two concentric metallic rings with thin splits placed diametrically opposed to one another usually make up a traditional SRR. This arrangement creates a highly conductive resonant structure where the capacitance created by the tiny spaces between the rings balances the inductance caused by the current flowing around the rings. The geometrical factors of an SRR, such as the split width, ring diameters, ring spacing, and substrate characteristics, have a significant impact on its resonant behavior. Subwavelength electromagnetic manipulation is made possible by properly adjusting these parameters, which will allow SRRs to resonate at wavelengths significantly larger than their physical size. SRRs can operate as tiny resonant elements in microwave and radio-frequency applications thanks to this special property.

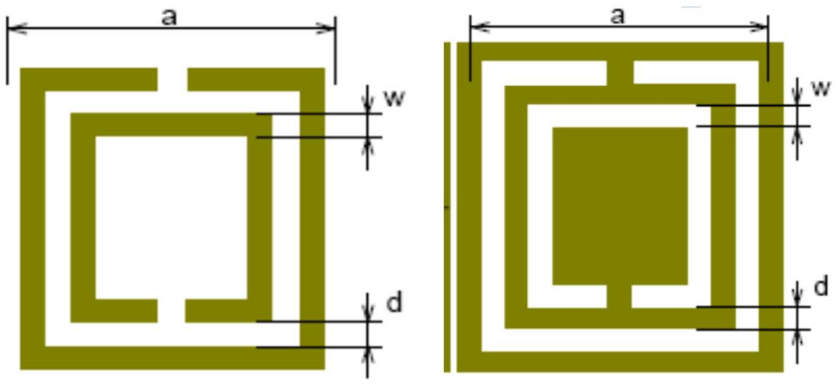


Figure 1.8. Square structure SRR & CSRR

Figure 1.8 shows square shaped SRR structure, while Figure 1.9 depicts the frequency dependent behavior of the effective permeability of the SRR. The shaded region in Figure 1.9 represents the frequency band in which the effective permeability ($\boldsymbol{\mu_{eff}}$) becomes negative.

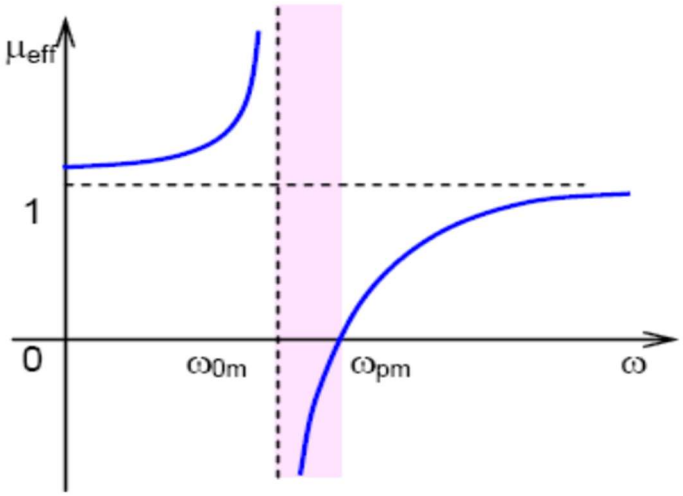


Figure 1.9. Frequency dependence of effective permittivity for a SRR

This negative permeability happens within a narrow frequency range around the resonant frequency, where ($\boldsymbol{\mu_{eff}}$) approaches positive or negative infinity. Due to this pronounced magnetic resonance and compact size, SRRs are widely regarded as the most commonly used and extensively considered building blocks for achieving negative permeability in metamaterial designs.

b) Complementary Split Ring Resonators (CSRRs)

The Complementary Split Ring Resonator (CSRR) is an electromagnetic dual of the conventional SRR. CSRRs are created by etching an aperture in the shape of a ring into a metallic surface rather than using a metallic ring like the conventional split ring. See Fig 1.8 for an example of CSRR's complementary form. The complementary nature of the CSRR, in comparison to the SRR, means that they exhibit similar resonant behaviour, however, their electromagnetic response is changed. In CSRRs, the small gaps between the fixed rings generate significant capacitance, which plays a dominant role in determining the resonant frequency of the structure. The capacitance is inversely proportional to the resonant frequency; hence, larger capacitance results in lower resonant frequencies for a given geometry. Unlike SRRs, which primarily exhibit negative magnetic permeability, CSRRs are capable of producing negative effective permittivity ($\boldsymbol{\varepsilon_{eff}}$) within a narrow frequency band close to their resonance.

Because of their flat shape and simple way they connect to both microstrip and coplanar waveguide systems, CSRRs are frequently used in making smaller filters, antennas, and microwave parts where a designer wants to control how electricity responds [46].

c) Key Application Areas of Metamaterials

Unmatched control over electromagnetic wave propagation has been made possible by metamaterials, opening up a plethora of creative applications in various technical fields [47]. Among the main areas of application are:

- Metamaterials are appropriate for current wireless and Internet of Things systems because they allow for the downsizing of antennas while improving gain, bandwidth, and radiation efficiency.
- The development of sophisticated electronic components with enhanced performance and smaller dimensions is made possible by the special electromagnetic properties of metamaterials.
- Super lenses that can image at subwavelengths beyond the diffraction limit are made possible by metamaterials that have both negative permittivity and permeability.
- Metamaterials can be employed for stealth applications, such as lowering the radar signature of naval platforms, by modifying the propagation of electromagnetic waves.

- To achieve reduced dimensions and improved functionality, metamaterials are commonly used in waveguides, phase shifters, filters, and couplers.
- Over certain frequency ranges, an object can be made virtually invisible by well crafted metamaterial structures that bend electromagnetic waves around it.

Because of their planar profile and ease of integration, metasurfaces the two-dimensional counterparts of bulk metamaterials have attracted a lot of attention recently. Periodic subwavelength elements can be used to create metasurfaces that can control surface waves, suppress undesired modes, increase gain, and improve impedance matching. They are ideal for contemporary antenna implementations due to their interoperability with traditional printed circuit technologies.

Metasurfaces

Metasurfaces function as engineered electromagnetic structures which exist in two dimensions and use subwavelength unit cells to create their periodic or quasi periodic patterns on a dielectric substrate. The practical use of antenna systems benefits from metasurfaces which provide compactness and low profile design and simple manufacturing and reduced energy losses in comparison to three-dimensional metamaterials. The tailored geometry and arrangement of metasurface unit cells enables users to control multiple electromagnetic wave properties which include propagation patterns and reflection phase and surface currents and antenna radiation behaviour.

Metasurfaces serve as vital components in modern wireless communication systems because they enhance multiple antenna metrics which include impedance bandwidth and gain and front to back ratio and radiation efficiency and polarization integrity and mutual coupling and electromagnetic compatibility. The most common metasurface structures used in antenna design include Electromagnetic Band-Gap (EBG) structures and Frequency Selective Surfaces (FSS) and Artificial Magnetic Conductors (AMC) [48].

a) Electromagnetic Band-Gap (EBG) Structures

Electromagnetic Band Gap (EBG) structures function as periodic metasurfaces which establish a frequency range that blocks all electromagnetic wave transmission. The structures create a periodic lattice through their two-dimensional design which uses printed metallic patches and vias on dielectric substrates to create subwavelength size elements. The structure's periodicity generates stopband behavior because Bragg scattering and resonant effects block surface waves from traveling through specific frequency ranges. The primary

application of EBG structures in antenna systems serves to control surface wave propagation which occurs at the substrate-ground boundary. Surface waves produce negative effects which include decreased radiation efficiency and altered radiation patterns and increased back radiation together with strong mutual coupling between nearby antenna elements. The performance of antennas improves through EBG structures which block the propagation of surface waves.

EBG metasurfaces are effectively utilized in:

- Mutual coupling reduction and decoupling in MIMO and array antenna systems
- Interference mitigation between closely packed radiating elements
- Improvement in radiation efficiency and gain
- Enhancement of pattern stability across the operating band

Due to these advantages, EBG structures are widely adopted in compact multi-antenna systems, wearable antennas, and high-density wireless devices [49].

b) Frequency Selective Surfaces (FSS)

Frequency Selective Surfaces (FSS) represent a distinct category of periodic metasurfaces which demonstrate different transmission and reflection patterns based on the frequency of incoming waves. FSS technology consists of periodically arranged metallic patches or apertures which operate on dielectric substrates to function as spatial electromagnetic wave filters. FSS devices can create band-pass and band-stop and high-pass and low-pass surfaces through different unit cell designs.

FSS structures in antenna engineering serve as EBG systems which control radiation patterns at particular frequency bands. FSS technology enables antennas to use FSS as superstrates or reflectors which control radiation patterns while improving overall system performance.

Key antenna enhancements achieved using FSS include:

- Radiation enhancement and gain improvement
- Bandwidth control and multi-band operation
- Suppression of unwanted harmonics and out-of-band radiation
- Pattern shaping and directivity enhancement

FSS-based metasurfaces are particularly beneficial in applications such as satellite communication, radar systems, and multiband wireless platforms, where selective frequency control is critical [50].

c) Artificial Magnetic Conductors (AMC)

Artificial Magnetic Conductors (AMC) are metasurface structures designed to mimic the characteristics of Perfect Magnetic Conductors (PMC), which do not occur in the natural world. Unlike Perfect Electric Conductors (PEC) which reflect electromagnetic waves with a 180° phase shift AMC surfaces show in-phase reflection at 0° reflection phase throughout a defined frequency range. The in-phase reflection property of AMC enables antennas to be placed very close to the reflecting surface without destructive interference. This results in low-profile antenna configurations. AMC structures are typically constructed from periodic metallic patches that engineers print onto grounded dielectric substrates which can include vias or exclude them.

In antenna systems, AMC metasurfaces provide several critical advantages:

- Improved gain and radiation efficiency
- Reduction of back radiation and enhancement of front-to-back ratio (FBR)
- Suppression of surface waves and radiation ripples
- Miniaturization and low-profile antenna design

Additionally, antennas utilizing asymmetric multiplexing channels (AMCs) reveal smoother radiation patterns, reduced sidelobe levels, and reduced pattern distortion compared to traditional antenna designs. These attributes make AMCs ideally suited for applications in wearable, vehicular and conformal antennas [51]. Furthermore, incorporating engineered surfaces, such as electromagnetic bandgap (EBG), frequency selective surface (FSS), and AMC structures into antenna design provides highly accurate control of electromagnetic emissions, which is difficult to achieve with more conventional approaches. These advanced structures are critical to satisfying the increasing requirements of today's high performance wireless communication systems, including miniature devices, multi-band operation, and electromagnetic compatibility. As a result, engineered surfaces provide a foundation for the development of next generation antennas in IoT, 5G/6G, multiple-input and multiple-output (MIMO), and advanced wireless technologies.

1.5. Significance of the study

- By attaining notable downsizing, increased gain, and higher radiation efficiency crucial for next generation wireless and IoT devices it overcomes the drawbacks of traditional antennas.
- Shows how hybrid fractal metamaterial antenna designs can effectively enable multiband and ultra wideband operation within small form factors.
- Through metasurface and SRR-based structures, impedance matching, surface wave suppression, and return loss performance are improved, guaranteeing dependable communication in intricate electromagnetic settings.
- Enhances isolation, directivity, and connection dependability to support high density and interference prone IoT installations, such as MIMO systems.
- Clears the path for next adaptive and reconfigurable antenna systems by offering a scalable and energy efficient antenna design framework appropriate for small, wearable, and environmentally friendly IoT applications.

1.6. Contributions of the study

- Offers a thorough analysis of hybrid fractal–metamaterial antenna topologies, showcasing notable antenna downsizing while maintaining radiation performance and allowing for small, unobtrusive designs appropriate for wireless and Internet of Things devices with limited space.
- By improving impedance matching and suppressing surface waves, metasurface and split-ring resonator (SRR) based integration effectively increases antenna gain, radiation efficiency, and directivity.
- Shows that impedance bandwidth, multiband behavior, and general matching qualities are greatly enhanced by double fractal topologies that include fractal radiating elements and fractal defective ground structures.
- Verifies that the suggested designs are appropriate for C-band and mid-band wireless applications, taking into account performance needs related to the IoT and new communication standards.
- The hybrid antenna structures are well suited for dense deployments and future MIMO-enabled IoT networks because they improve isolation, diversity performance, and overall system efficiency. They also provide the groundwork for future studies on reconfigurable and energy efficient antenna systems.

1.7. Organization of Thesis

This thesis is organized into six chapters, in which each addressing a specific aspect of the research, progressing from fundamental concepts to proposed designs, experimental validation, and conclusions.

Chapter 1 – Introduction

The context and rationale for the study are presented in this chapter, which also highlights the difficulties that conventional antennas confront in contemporary wireless and IoT applications. Miniaturization, multiband operation, broad bandwidth, and improved radiation characteristics are among the needs for next generation antennas that are covered. The chapter offers a thorough analysis of metamaterials, metasurfaces, and fractal antennas, covering their basic characteristics and applicability to improving antenna performance. To define the thesis's scope and direction, the study's importance, research contributions, and goals are all given in detail.

Chapter 2 – Literature Review

The research on fractal based antennas, antenna designs aided by metamaterials and metasurfaces, and hybrid fractal metamaterial topologies is thoroughly reviewed in this chapter. Antenna downsizing, bandwidth enhancement, gain improvement, multiband behavior, and isolation performance are all critically examined in relation to previous efforts. The constraints and research gaps found in the literature offer compelling technical justification for the suggested antenna designs proposed in the following chapters.

Chapter 3- An Asymmetrical Notch Fractal Antenna with Metasurface Integration at 5.2 GHZ

It describes the design process, simulation, construction, and experimental verification of a 5.2 GHz asymmetrical Notch fractal antenna with a metasurface incorporated. The antenna shape, substrate choice, fractal ground configuration, notch properties, and metasurface integration are all covered in detail in this chapter. Through simulated and measured results, performance parameters like return loss, impedance bandwidth, VSWR, gain, directivity, radiation patterns, axial ratio, efficiency, and ground plane effects are examined, proving the antenna's appropriateness for mid-band wireless communication applications.

Chapter 4- Performance Enhanced Star Fractal Antenna with Fractal DGS And Metasurface Integration

It describes the design, analysis, and experimental verification of a star-shaped fractal antenna with improved performance for C-band applications that incorporates a metasurface superstrate and a Sierpinski triangle fractal defective ground structure. The chapter describes the metasurface integration strategy, mathematical modeling, and design approach based on fractal geometry. Return loss, impedance bandwidth, VSWR, gain, directivity, radiation efficiency, and radiation intensity are examined in relation to the measured and simulated results. The suggested hybrid architecture for next-generation wireless and Internet of Things systems is validated by the notable improvements in bandwidth, gain, and radiation characteristics that are shown when fractal DGS and metasurface are used together.

Chapter 5- Conclusion and Future work

The main conclusions and contributions of the suggested fractal metamaterial antenna designs are compiled in this chapter, which wraps up the thesis. In addition to outlining future research directions such reconfigurable antennas, improved metasurface, bandwidth expansion, and intelligent optimization strategies for next-generation wireless and IoT systems, it emphasizes achieved performance increases in bandwidth, gain, efficiency, and compactness.

CHAPTER 2

LITERATURE REVIEW

2.1. Introduction

An extensive review of current studies on sophisticated antenna design methods pertinent to contemporary wireless and IoT communication systems is provided in this chapter. Conventional antenna structures have increasing challenges in achieving the demanding requirements of downsizing, multiband operation, radiation efficiency, and overall performance as a result of the rapid growth of wireless devices that are tiny, multifunctional, and have high data rates. As a result, significant research focus has been placed on novel antenna design approaches that can get around these restrictions while guaranteeing real world application. Two very successful and complementary methods for antenna engineering have arisen inside this research environment: fractal geometry and metamaterial ideas. Antennas based on fractal geometry make use of self-similarity and space-filling properties to provide improved bandwidth performance, multiband functionality, and smaller physical dimensions. In parallel, a significant amount of research has been done on metamaterials and metasurfaces, which are intentionally manufactured structures with specific permittivity and permeability, to enhance antenna properties like gain, impedance matching, bandwidth control, surface wave suppression, and mutual coupling reduction. According to the research currently under publication, combining fractal geometries with metamaterial or metasurface structures can result in significant performance gains over traditional antenna designs. Specifically, design strategies, performance enhancement mechanisms, and application relevance to next-generation wireless and IoT systems are highlighted in this review, which summarizes important contributions in the fields of fractal antennas, metamaterial-assisted antennas, and hybrid fractal-metamaterial configurations. In order to provide a clear reason and technical basis for the hybrid antenna designs created in the next sections of this work, a critical review of previous studies also identifies current limits and research gaps.

2.2. Fractal Based Antennas: Concepts and Applications

The emergence of fractal-based antennas has also generated substantial academic research with some significant findings regarding measured performance. As wireless communication systems demand the use of small, multiband and highly efficient antennas, many researchers are considering using fractal-based antennas as a solution. Unlike traditional Euclidean-based antennas, fractal-based antennas are developed from mathematical fractal concepts. The essential attributes of fractal based antennas (i.e., self-similarity, scale invariance, and space-filling properties) enable the creation of electrically small antennas that exhibit superior radiation characteristics, making them ideal for space-constrained and multifunctional wireless devices. Early research on fractal antennas had primarily focused on traditional (Euclidean-based) fractal geometries generated through Iterated Function Systems (IFS). An IFS is a systematic method to create complex self-similar structures, such as those exemplified by Sierpinski, Koch and Minkowski fractals. These types of fractals exhibited inherent multiband characteristics due to their recursive structure and compactness. In addition to traditional (Euclidean-based) fractal geometries, hybrid fractals have emerged as a means for developing new antennas and improving antenna performance by alternating combinations of multiple fractals or improving traditional (Euclidean-based) or hybrid (Euclidean/fractal) designs using optimization and intelligence-based techniques such as artificial neural networks and evolutionary algorithms to develop optimized impedance matching, improve bandwidth and improve radiation efficiency. Simultaneously, a significant quantity of application-based research reports that use fractal antennas to create electrically small antennas, multiband antennas, wideband antennas, UWB communications, arrays of antennas and multiple input and multiple output (MIMO) configurations, and wearable and body centric devices, and support emerging terahertz (THz) applications. These studies demonstrate that fractal antennas may be a highly adaptable and scalable design method that meets the performance demands of next-generation wireless and IoT technologies across many different types of applications.

Ezhumalai et al [52] presented an extensive survey on fractal patch antennas designed using the Iterated Function System (IFS) technique. The research examined multiple Euclidean fractal geometries which included Sierpinski, Koch, Cantor, Minkowski, and hybrid structures to show their ability to fill space for antenna miniaturization and multiband, wideband operation. The study demonstrated that MIMO antennas achieved

performance enhancements by decreasing mutual coupling between antennas and increasing their gain and efficiency. Nevertheless the review showed three main limitations which included difficulties in manufacturing high performance products and requirements to use specific substrates and difficulties to maintain consistent efficiency throughout different frequency ranges.

Chinnamuthu et al. [53] introduced a compact quad port THz MIMO antenna which uses fractal radiating elements and graphene based tunability and metasurface components and a defective ground structure to achieve ultra wideband transmission with high isolation performance. The technique brought about substantial improvements to the design which enabled 6G and TWPAN and sub THz IoT applications through better bandwidth and gain and MIMO diversity essential for these systems. The research study achieved important results through its development of a small system that allows changing operating frequencies. The project depended on computer simulations for most of its work because it faced difficulties in testing and running actual operations at THz frequencies.

Ghadeer et al. [54] introduced a new sub 6 GHz fractal monopole MIMO antenna design for 5G systems that uses Sierpinski triangle fractal radiators that receive power through CPW open-circuited feedlines. The system used a low, high impedance ground design together with a Hilbert-fractal CRLH band reject filter to achieve two functions, reduction of mutual coupling and expansion of operational bandwidth. The design achieved suitable performance because it met all three testing requirements of gain, isolation, and MIMO diversity that showed similar results between simulations and actual tests. The antenna functioned exclusively within sub-6 GHz frequency ranges, which restricted its use in higher frequency 5G and beyond 5G applications.

Kaur and Sivia [55] developed a hybrid fractal antenna that combines Giuseppe Peano, Cantor set, and Sierpinski carpet geometries for use in ISM band applications. The design used Artificial Neural Networks together with the Firefly Algorithm to optimize the microstrip feed position and achieve better impedance matching results. The antenna reached a compact size while maintaining stable resonance at 2.44 GHz that produced results that matched both simulated and measured data. The study showed how AI based optimization works for designing fractal antennas. The antenna functioned only within a restricted ISM bandwidth because it did not support multiple frequency bands or reconfiguration features.

In order to create a self-powered Solant-Rectenna system, Imran et al. [56] created a wearable, low profile Hilbert shaped metamaterial antenna that is integrated with a flexible solar panel and EBG ground plane flaws. SAR research confirmed that the design minimized exposure to the human body while combining solar energy collection with radiofrequency. For UWB wearable applications, the antenna demonstrated wideband functioning from 0.8 to 10 GHz with consistent gain and low distortion. It was important because it allowed wearable gadgets to integrate two energy sources in a small package. At higher frequencies, the RF to DC conversion efficiency was constrained, and long term performance might be impacted by real world bending effects.

Mohanty and Sahu [57] added an Artificial Magnetic Conductor (AMC) reflector to a small wideband hybrid fractal monopole antenna in order to increase radiation characteristics and gain. The semi elliptic stepped ground enhanced impedance matching and cross polarization, while the hybrid fractal design offered self-similarity, size reduction, and wideband performance. The AMC reflector decreased back lobe radiation and increased boresight gain. The antenna had a high efficiency and unidirectional radiation between 3.7 and 7.0 GHz. Compact, high gain wideband operation for hybrid cellular networks was its main benefit; nevertheless, its use was restricted to sub 7 GHz frequencies, which prevented the adoption of higher band 5G or beyond 5G.

Naderi et al. [58] to lessen mutual coupling in micro strip patch antenna arrays operating at 5.9 GHz created a new fractal shaped mushroom EBG structure. The method reduced the coupled current ratio from 18% to 0.3% by increasing the unit cell capacitance and inductance in order to miniaturize the EBG and generate a bandgap that decreased S21 by more than 30 dB. In comparison to earlier models, the design showed improved shielding and compactness. However, the strategy limited overall radiation performance by reducing antenna gain because of interactions between the patch elements and the EBG.

Rajabloo et al. [59] used a metamaterial ELC coupling element in conjunction with a Koch fractal form to create a small, triple band microstrip slot antenna. For GPS, WiMAX, and WLAN applications, the CPW fed antenna operated at 1.5, 3.5, and 5.4 GHz. At 3.5 GHz, circular polarization was attained. Miniaturization to 40×40 mm and better current distribution for the intended resonances were made possible by the technology. It was significant since it supported several bands at 1.5 GHz and was small enough to be

implanted. The antenna's low gain at the lower band, however, limited its usefulness in some applications.

To achieve wideband and multiband operation, Kaur et al. [60] improved a circular fractal antenna with rectangular stubs and SRR. Iterative fractal geometries from 0th to 3rd order were used in the design, and bandwidth and impedance matching were enhanced via SRR and stubs. With dual wideband coverage of 1.30 to 12.73 GHz and 14.83 to 20.0 GHz, the finished antenna was appropriate for a number of wireless protocols, such as Bluetooth, WiMAX, WLAN, and several satellite bands. The study's multiband capacity in a small 36 x 32 mm^2 size made it significant, but there are still issues with higher frequency performance and realistic production complexity.

For sub 6 GHz MIMO systems, Hussein et al. [61] suggested a miniature two element microstrip antenna array that minimized mutual coupling by utilizing a Minkowski shaped metamaterial column in conjunction with a monopole element, meander line, and interdigital capacitor. For optical reconfiguration, the design used light dependent resistances (LDR), which removed the need for intricate biasing circuits. With a maximum gain of 4.5 dBi and a bandwidth of 3 to 5.5 GHz, the antenna showed low BER and great channel capacity in massive MIMO simulations. Although 64×64 arrays may be difficult to fabricate on a wide scale and integrate in practice, the study proved important for small, reconfigurable MIMO arrays.

With their ability to meet the demands of wideband performance, multiband operation, compactness, and improved radiation efficiency, fractal-based antennas have become a very flexible option for contemporary wireless communication systems. These antennas, which naturally support multiband and ultra wideband operation, allow electrically compact designs appropriate for devices with limited space by utilizing the self-similar, space-filling, and scale-invariant characteristics of fractal geometries. A systematic framework for creating complicated geometries like Sierpinski, Koch, Minkowski, and Cantor shapes, which exhibit compactness and effective current distribution is provided by traditional fractal structures created with Iterated Function Systems (IFS). Impedance matching, gain, bandwidth, and radiation performance are further improved by developments in hybrid fractal designs, which are frequently paired with optimization and intelligence based approaches. Multiple applications exist for MIMO systems, antenna arrays, wearable devices, body centric technology, terahertz communication, and energy

harvesting systems, which successfully demonstrate their ability to work with future IoT and wireless network systems. The system gains additional advantages through its combination of metamaterial and metasurface components, which include AMC and EBG design elements that enhance its performance by improving gain and reducing mutual coupling while providing frequency band notching and better isolation between array elements. The design shows good simulation results, but its actual production, testing processes, and ability to perform throughout all frequency ranges face difficulties. Fractal based antennas with their metamaterial integration capabilities emerge as a powerful design solution that meets modern wireless communication system requirements which continue to grow more demanding.

2.3. Metamaterials and Metasurfaces for Antenna Performance Enhancement

The advent of metamaterials and metasurfaces has fundamentally changed how antennas are designed and developed today, giving antenna engineers a new level of control over how electromagnetic waves will propagate as well as enabling performance improvements that would not have been possible without them or with ordinary materials. Metamaterials are engineered material systems made from repeating periodic subwavelength-sized unit cells (e.g., split-ring resonators (SRRs) and complementary split-ring resonators (CSRRs)) that have been designed to have specific electrical properties (e.g., permittivity and permeability) depending on the number of unit cells used to form an overall metamaterial structure. By creating specific material characteristics, metamaterials provide the ability to create unique electromagnetic behavior (e.g., negative index of refraction, backwards waves, electromagnetic band gaps), which can be used to improve the key performance parameters of an antenna. Similarly, metasurfaces are two dimensional equivalent metamaterial structures that have also received considerable attention in recent years due to their flat geometry, ease of manufacturing, and ability to be integrated with printed antennas. When arranged in periodic or quasiperiodic arrays, the unit cells of a metamaterial can be used to create AMCs, frequency selective surfaces (FSSs) and electromagnetic band-gap (EBG) structures. By developing these types of metamaterial combinations, the surface wave property of antennas can be controlled, the radiation patterns can be enhanced, and impedance matching can be improved through the use of metasurfaces, thus, they are an excellent candidate for new, compact, high-performance antenna designs.

The application of metamaterials and metasurfaces leads to significant benefits in various areas of antenna design (e.g., antenna miniaturization, improved bandwidth and gain, band notch filtering, reduced specific absorption rate (SAR), reduced radar cross section (RCS), polarization conversion, and improved isolation of antennas in arrays or MIMO systems). These advantages can be achieved through a variety of different implementation strategies, including patch loading, ground plane etching, substrate modification, or the integration of superstrates into conventional antenna designs. Together, metamaterial and metasurface based solutions offer an innovative and flexible way to achieve enhanced performance from antennas so that next generation wireless, IoT and high frequency communication systems can successfully address demanding constraints on size, efficiency, and functionality.

By combining an epsilon-negative transmission line (ENG-TL) with a single split-ring resonator (SSR) and loading it with a via-free artificial magnetic conductor metasurface (AMC-MS), Ameen and Chaudhary [62] created a compact circularly polarized metamaterial antenna. The method used image theory to determine the active input impedance and took advantage of zeroth-order resonance for downsizing. The antenna demonstrated compact, bandwidth-enhanced performance with an impedance bandwidth of 16.36%, a CP bandwidth of 11.93%, a gain of 5.62 dBic, and a radiation efficiency of 72.1%. However, applications in high-gain or ultra-wideband scenarios were limited by the design's modest radiation efficiency and operational bandwidth.

By combining the Moore and Koch curves and adding Split Ring Resonators (SRRs) to improve gain, bandwidth, and impedance matching, Sharma and Bhatia [63] created multiband hybrid fractal antennas. To maximize performance, two feed line positions left (LFL) and right (RFL) were examined. With peak gains of up to 8.56 dB and bandwidths of around 750 to 770 MHz, the antennas, which were built on 25×25 mm² FR4 substrates, demonstrated various resonances across ISM, WiMAX, WLAN, and X-band satellite frequencies. The achievement of compact, multiband operation was the study's key contribution; yet, the design's intricacy and restricted ultra high frequency scalability still pose possible limitations.

A small ultra wideband monopole antenna with symmetric split ring resonator (SSRR) metamaterial unit cells that have single negative (SNG) and near zero refractive index (NZRI) characteristics was proposed by Al-Bawri et al. [64]. In comparison to

traditional designs, the metamaterial integration improved gain, increased radiation efficiency by up to 97%, and expanded bandwidth from 3.08 to 14.1 GHz while keeping a small 14.5 × 22 mm² footprint. In order to achieve high performance UWB operation with metamaterial loading, the study was important. Manufacturability and uniformity in mass production, however, may be constrained by the design's intricacy and sensitivity to exact unit cell placement.

For Wireless Body Area Sensor Networks (WBASNs), Douhi et al. [65] created a flexible, wearable ultra wideband (UWB) antenna that is integrated with a 7×7 artificial magnetic conductor (AMC) metamaterial array. The AMC reflector improved gain by 6.59 dBi between 5.1 and 13 GHz, decreased back radiation, and decreased the Specific Absorption Rate (SAR) by an average of 96.84%. With experimental findings closely matching predictions, the antenna that was made completely of textile materials showed conformal flexibility, durability, and ease of fabrication. The design's reliance on exact AMC placement may make large-scale manufacture and integration with intricate wearable devices more difficult, despite its importance for safe, high-performance wearable applications.

Using double negative (DNG) metamaterial structures, Ez-Zaki et al. [66] created Koch fractal antennas in single, two and four element MIMO configurations for IEEE 802.11p and sub 6 GHz V2X applications. By reducing mutual coupling and improving isolation, the metamaterials such as electrically linked square split-ring resonators with negative permittivity and permeability and broadside resonators achieved -45 dB between elements. By providing polarization variety, orthogonal placement enhanced MIMO performance. The study showed improved surface current distribution and radiation patterns. Although important for high-isolation vehicle MIMO antennas, the intricate manufacture of metamaterials and the need for exact alignment in vehicular conditions may limit their practical application.

Alibakhshikenari et al. [67] suggested a fractal isolator that suppresses mutual coupling between two closely separated microstrip patch antennas using electromagnetic bandgap metamaterials (EMBG-MTM). With a maximum gain enhancement of 71% and no reduction in radiation patterns, the technique allowed the inter-element gap to be lowered to 0.65λ while improving isolation by up to 37 dB across the X, Ku, K, and Ka bands. With its wideband functioning and good isolation, the method was important for radar, RFID, and

small MIMO applications. However, realistic large scale deployment may be limited by the design's intricacy and sensitivity to exact fractal geometry.

Utilizing metamaterial techniques, Aggarwal et al. [68] created a high-gain super wideband (SWB) antenna that incorporates a flower-shaped slot to produce SWB features and inverted U-shaped slots for dual notches at 3.5 GHz and 5.5 GHz. To increase gain, a 3x3 array of metamaterial unit cells was used as a superstrate. With notched bands for WLAN and WiMAX, the antenna, which was built on a 30x35x1.5 mm^3 FR4 substrate, has a measured bandwidth of 3.1-15 GHz. Although the design's performance depended on exact slot and metamaterial alignment, which could make manufacture more difficult, the study proved important for small, gain enhanced SWB wireless applications.

For ISM band applications, Reddy [69] combined Minkowski fractal edges with a metamaterial inspired reactive impedance substrate (MRIS) to create a circularly polarized fractal patch antenna. The metamaterial loading improved the CP bandwidth, and the asymmetrical fractal curves produced circular polarization. The antenna's 3 dB axial ratio bandwidth was 7.47% and its 10 dB return loss bandwidth was 40.7%. The development of small, wideband CP antennas with enhanced polarization purity was made possible by this method. However, large scale production and repeatability in real world deployments may be constrained by the intricacy of fractal patterning and accurate MRIS implementation.

In order to lessen mutual coupling between elements, Reddy et al. [70] created a small ultra-wideband (UWB) MIMO fractal antenna combined with metamaterial structures. With a peak gain of 6.2 dBi, radiation efficiency above 88%, and an impedance bandwidth of 5.8 to 15 GHz with mutual coupling below -25 dB, the antenna was printed on a 30×30×1.6 mm^3 FR4 substrate. Diversity performance was confirmed with DG ≈9.98 dB, TARC <-10 dB, MEG <3 dB, and ECC <0.07. Although accurate metamaterial fabrication and integration may limit the viability of mass production and increase design complexity, the work proved important for small, high-performance UWB MIMO applications.

For millimetre wave applications, Tariq et al. [71] created an ultra miniaturized 1×2 antenna array by combining rectangular-slotted patches with a single layer metasurface made of a 2×4 diamond shaped split ring unit cell array. By placing the metasurface 0.5 λ above the array, a Fabry-Perot cavity was created, improving impedance matching, gain, and bandwidth. The antenna achieved 94% radiation efficiency, a peak gain of 12.7 dBi, and a 5.96 GHz bandwidth (27.38–33.34 GHz). For small, high performance mmWave systems,

this strategy was important; but, large scale deployment may be constrained by the intricate fabrication process and exact alignment of the metasurface.

In order to improve stealth and lower radar cross-section (RCS) in a four element slot antenna based MIMO setup, Rangula et al. [72] suggested an ultra broadband polarization converter metasurface. In order to create a 10x10 chessboard metasurface, the design used a low-profile meta-atom with horizontal edge strips and a diagonal metallic strip. The setup maintained angular stability up to 60° incidence while achieving strong isolation (>25 dB), a peak gain of 6.95 dBi, and a polarization conversion efficiency of over 90%. Although the technology proved important for stealth MIMO systems and RCS mitigation, actual scalability may be limited by the intricate fabrication process and exact alignment of metasurface pieces.

The performance of modern antennas has improved significantly with metamaterials and metasurfaces, which provide designers with greater flexibility and control over the electromagnetic properties compared to traditional materials. Properties of antennas such as gain, bandwidth, impedance matching, isolation, and polarization control can all be optimized using engineered structures including split-ring resonators (SRRs), complementary split-ring resonators (CSRRs), and frequency selective surfaces (FSS). Metamaterials and metasurfaces also enable practical applications of printed antennas as planar implementations of metamaterial concepts in wearable, multiple-input many-output (MIMO), and high-frequency antenna applications. Reported systems exhibit capabilities such as miniaturization, ultra-wideband operation, reduced mutual coupling, band notching, and reduced specific absorption rate (SAR) and radar cross-section (RCS). Implementation strategies include loading of patch antennas, etching of ground planes, modification of substrates, integration of superstrates, and creation of Fabry-Perot cavities; these illustrate the flexibility of these design approaches for both traditional and hybrid antenna systems. Significant improvements in performance metrics like gain, radiation efficiency, isolation, and polarization purity have been achieved with these designs; however, challenges to precision in fabrication, precise alignment of metamaterial components, and scalable mass production remain an issue for this technology. Overall, metamaterials and metasurfaces provide a robust and adaptable framework for next-generation antenna design, enabling high performance, compact, and multifunctional solutions suitable for wireless, IoT, wearable and high frequency communication systems.

2.4. Hybrid Fractal-Metamaterial Antennas

The combined use of fractal geometries and metamaterials creates a unified method that engineers antennas to address the basic design restrictions of both fractal and metamaterial systems. Fractal antennas are well known for their self-similar and space-filling properties, which enable compact dimensions, multiband operation and broadband behavior. The advantages of fractal antennas become limited because extreme miniaturization results in three main problems that decrease their performance. The antennas which use metamaterials and metasurfaces for their operation, exhibit better performance because they can increase gain and control bandwidth, while their surface waves are suppressed and their array systems achieve isolation, but their design does not automatically deliver multiband operation and ultra-compact performance. The performance benefits and main features of fractal antennas and metamaterial-inspired antennas appear in Figure 2.1, which shows their ability to reduce size, operate on multiple frequency bands, boost their signal strength, and support MIMO and energy harvesting systems.

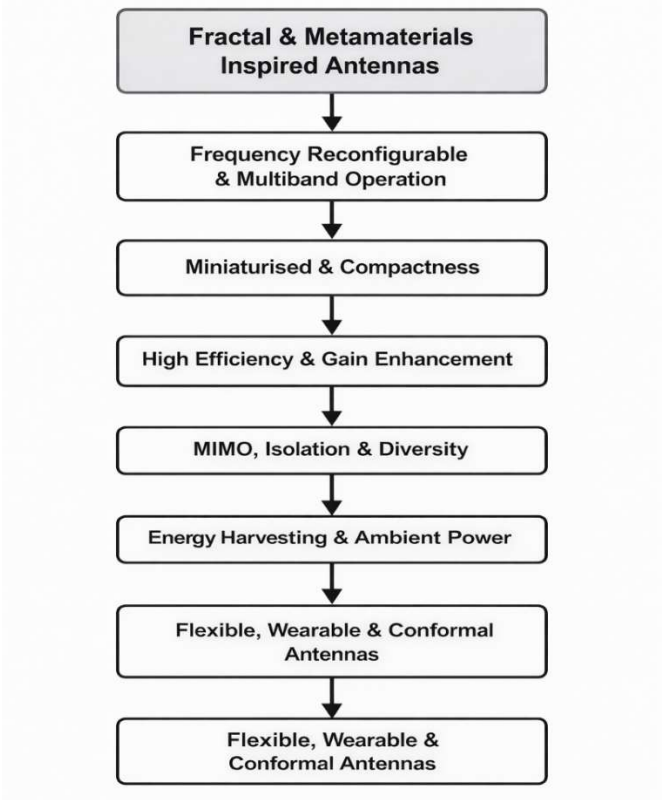


Figure 2.1. Key features and performance advantages of fractal and metamaterial-inspired antennas

Hybrid antenna designs use fractal and metamaterial concepts together to achieve better electromagnetic performance because both methods create different advantages. Fractal structures can be employed to generate wideband or ultra-wideband response, while metamaterial elements, such as AMC or EBG metasurfaces, can selectively enhance gain at target frequencies, suppress unwanted modes, or provide band notching capabilities. Multiple input multiple output (MIMO) systems and antenna array configurations benefit from this hybridization because it helps to achieve better isolation and lower mutual coupling that supports both signal integrity and system performance.

Recent research has demonstrated that hybrid fractal metamaterial antennas can simultaneously achieve compact size, multiband operation, high radiation efficiency, enhanced gain, and precise control over frequency responses. Such designs are essential for next-generation wireless communication and IoT applications because they require devices to be smaller while supporting multiple operations and resisting interference. Overall, the hybrid fractal metamaterial antennas create a flexible and strong framework, which engineers use to build antennas that meet the strict requirements of present day and future wireless communication systems.

Sabban [73] developed new meta fractal wearable antennas and sensors which use fractal geometries together with metamaterial CSRRs for applications in 5G, IoT, and medical fields. The research produced compact designs that operate at wide frequency ranges and maintain low manufacturing costs while achieving better performance through enhanced gain and directivity plus lower resonant frequency. The integration of active sensors with low-noise amplifiers boosted system efficiency. The research depended mostly on simulations while actual world testing showed restricted results and the study did not extensively examine long-term performance close to human bodies or the ability to produce large quantities.

Saraswat [74] developed a hybrid multiband antenna that uses fractal and metamaterial design principles to create wireless operating bands through the integration of SRR and CSRR elements on an FR4 substrate. The antenna achieved compact dimensions with acceptable gain and radiation efficiency across multiple bands, demonstrating its suitability for modern multistandard communication systems. The research demonstrated effective bandwidth use throughout the study while maintaining stable radiation patterns and achieving more than 70% efficiency in all resonant modes. The study results showed that

the FR4 substrate affected high frequency performance while the research did not demonstrate performance testing for on body or real world conditions.

In order to accommodate Bluetooth, WLAN, WiMAX, and X band applications, Elhabchi et al. [75] created a multiband fractal wide slot metamaterial antenna by combining fractal slot geometry with loop resonators and meandering metamaterial structures. Through CST and HFSS simulations, the antenna's multiband and broadband features were confirmed, along with an adequate gain throughout resonant frequencies. The impact of fractal and metamaterial dimensions on performance was brought to light using parametric analysis. However, experimental manufacturing, measurement validation, and practical integration aspects were not addressed; instead, the work was based entirely on simulation results.

A circular fractal microstrip patch antenna with a metasurface layer was proposed by Habib et al. [76] to increase gain and bandwidth for satellite communication applications. A periodic metasurface served as a focusing lens to enhance radiation characteristics, and fractal circular slots were added to increase the bandwidth. With better impedance matching, the antenna significantly increased its gain and bandwidth. However, experimental fabrication, measurement findings, and performance under real world operating conditions were not disclosed, and the work was restricted to simulation based validation utilizing CST.

In order to achieve wideband operation with triple band rejection characteristics, Sudarsan et al. [77] presented a dual port square fractal MIMO antenna that uses edge chamfered fractal geometry, defected ground structure (DGS), and metamaterial elements. Mutual coupling was successfully decreased by the metamaterial loaded ground, and overall performance was improved over a broad impedance bandwidth by the MIMO design. Compactness and appropriateness for broadband wireless systems were demonstrated by fabrication and measurement, which confirmed the simulated findings. However, compared to single-element antennas, the design required a comparatively larger footprint, and there was nothing in the way of in depth investigation of radiation efficiency and on body performance.

With the objective to improve spectral efficiency, Bespalov et al. [78] studied MIMO antenna systems using fractal radiators on biisotropic and bianisotropic chiral metamaterial substrates. Electrodynamic modeling and Shannon based capacity formulations were used to examine fractal geometries, including the Sierpinski triangle, Koch, and Gilbert curves.

The study demonstrated reduced mutual coupling and improved spectral efficiency across multiple frequency ranges compared to conventional antennas. With no experimental validation, fabrication feasibility study, or evaluation under real world channel and hardware limitations, the work was still primarily simulation based.

With a focus on polarization insensitive and wide angle absorption properties, Costanzo and Venneri [79] suggested a fractal based metamaterial unit cell for ambient RF energy harvesting in the 2.45 GHz Wi-Fi band. Numerical analysis of a small 9 x 9 metamaterial harvester revealed very high absorption and RF to AC efficiency, indicating its use for wireless sensor networks and the IoT. The study emphasized the possibility of high efficiency, ecologically friendly harvesting methods. Nevertheless, rectifier integration was absent, multiband operation and actual measurements were not covered, and the study was restricted to simulation based validation.

In an attempt to achieve extreme downsizing and ultrathin profiles, Venneri et al. [80] presented a dual band fractal metamaterial absorber sensor that operates in the UHF range using Minkowski fractal metallic patches. Simulations and actual observations confirmed the absorber's dual band near perfect absorption, high angular stability, and the efficient dielectric sensing with good sensitivity and quality factor. The possibility of low frequency metamaterial based sensing was validated by the investigation. Nevertheless, dynamic reconfigurability and real time sensing integration were only mentioned as potential future study areas, and the design was restricted to fixed frequency operation.

Manoharan et al [81] developed a monopole antenna that operates at four frequency bands and uses a fractal square design together with a CSRR metamaterial ground plane to improve both bandwidth and impedance matching. The Chinese coin inspired fractal geometry enabled multiband operation across sub 6 GHz, C, and X bands with stable radiation characteristics. The design concept received validation through characteristic mode analysis and equivalent circuit testing. The antenna required a larger space than standard designs but its performance tests only measured free space conditions without testing on body effects or actual system level integration.

Iyampalam and Ganesan [82] proposed a penta band fractal antenna inspired by meta-materials. It integrates a CSRR based metamaterial layer on a FR4 substrate, a Koch loop radiating element, and a decagon fractal geometry. Five different resonant bands with acceptable gain and bandwidth were made possible by the three-layer structure, which made

the antenna appropriate for a range of wireless and emergency communication applications. Through measurement validation, the study showed consistent impedance characteristics and effective multiband behavior. Nevertheless, the antenna's gain levels were moderate, and using a lossy FR4 substrate might not be as effective at higher frequencies.

By fusing the benefits of both fractals and metamaterials into the same antenna, hybrid fractal/metamaterial antennas improve upon the limitations associated with each standalone fractal or metamaterial antenna to create superior design alternatives. Fractal antenna geometries provide advantages such as compactness, inherent self-similarity and multi band ,wideband operation, while metamaterial, metasurface structures (AMCs, EBGs, and CSRRs) allow for improved gain, suppressed surface waves, impedance matching and reduced mutual coupling in MIMO array applications. Antennas constructed using a combination of fractals and metamaterials are capable of achieving high radiation efficiencies, highly accurate frequency control, frequency band notching, and excellent isolation all within the small form factors required for modern wireless, IoT, wearable, and satellite communications. Several studies conducted within the past year have validated that hybrid fractal/metamaterial antennas can provide support for multiband, ultra wideband operation, reconfigurable sensitive responses, and energy harvesting capabilities, thus making them highly versatile for multiple application environments. Although there have been no validations via simulated studies or parametric analyses that have not shown performance to be improved via hybrid fractal metamaterial designs, there are still challenges to overcome related to manufacturing complexity, precise assembly of metamaterial components, substrate losses, and successful scaling for real-world application deployment. Overall, hybrid fractal metamaterial antennas provide a robust and scalable framework for designing high-performance, multifunctional antennas that meet the stringent demands of next generation communication systems, offering a pathway to compact, efficient and interference resilient devices suitable for IoT, 5G, 6G and beyond.

2.5. Research Gaps

Significant advancements have been made in the design of fractal antennas, hybrid fractal metamaterial antennas, metamaterials, and metamaterial assisted antennas, but several critical gaps exist in research on antennas. Fractal antennas are inherently compact and multiband capable, however, they suffer from decreased gain and efficiency, as well as increased surface wave losses when the antennas are miniaturized to extreme proportions.

Conversely, metamaterial and metasurface assisted antennas tend to outperform traditional antennas in terms of gain, bandwidth, and isolation, but they suffer from substrate dependency, which limits the scalability and practical deployment of these antennas due to the cost and complexity associated with precise fabrication. Hybrid fractal metamaterial antennas could provide an ideal combination of advantages of the two types of antennas; however, achieving consistent performance across multibands or over ultra wide bands of frequencies continues to be difficult. Additionally, integrating antennas into small IoT, wearable, and high frequency applications is complicated, and the vast majority of hybrid fractal metamaterial antenna designs in previous studies were experimentally evaluated only using simulation data, with no empirical validation. Additionally, the potential to manufacture antennas on a large scale and to implement cost and supply efficient solutions remains an area of research. Finally, advanced features such as tunability and dynamic reconfigurability have not been fully explored. Research directed at addressing these knowledge gaps is critical for providing high performance antenna solutions that are scalable and flexible to serve the next generation of wireless communications, IoT and wearable applications.

2.6. Motivation

Due to the fast pace at which wireless communication and IoT are evolving, antennas need to be small, perform well, and work in multiple frequency bands. Typical designs do not meet all of these standards; therefore, space-constrained (such as wearables) and miniaturisation will often result in less gain and less efficient antennas. Fractal geometries allow for compact multiband structures, while metamaterials and metasurfaces offer a high-quality way to control the electromagnetic wave in such a way that it can enhance performance. However, using only one approach (fractal antennas or metamaterial, metasurface designs) will not satisfy all performance requirements, especially next-generation IoT, MIMO, or high-frequency systems. This research is motivated by a need to combine both these complementary features (fractal and metamaterial) to create hybrid antennas that can deliver the following: High Gain, Wideband, Multiband, Improved Isolation, and Consistent Performance Across Varying Operational Environments. These antennas will help make communication devices more reliable, consume less energy, and offer greater functionality and therefore enabling the next-generation of applications for wearable electronics, high data rate IoT networks, and beyond 5G wireless systems.

Furthermore, by addressing their physical construction, tuning, and integration challenges this research aims to provide a scalable solution framework at the next-generation of antenna solutions that balances miniaturisation with either performance or practical deployment.

2.7. Research Objectives

- To increase impedance bandwidth and optimize effective electrical length for downsizing, analyze and create new fractal antenna geometries, particularly an asymmetrical star-shaped patch and a Sierpinski triangle fractal Defective Ground Structure (DGS).
- Create an Artificial Magnetic Conductor (AMC) behavior that suppresses surface waves and lowers mutual coupling by designing and characterizing a metamaterial inspired metasurface using Rectangular Split-Ring Resonators (RSRR).
- To maximize constructive interference and broadside radiation, do thorough parametric studies on the Fabry-Perot cavity height (h) between the radiator and the metasurface superstrate in order to optimize the antenna's directional gain. thereby reducing losses in intricate electromagnetic environments and squelching surface waves.
- Create antennas that support low power and sustainable operation for wearable technology and devices with limited space.
- By building prototypes on substrates and testing them experimentally in an anechoic chamber, validate the theoretical and simulated models and make sure that the radiation patterns, voltage standing wave ratios (VSWR), and measured scattering parameters (S11) match the predictions of the simulations.

CHAPTER 3

DESIGN-1 METHODOLOGY AND RESULT AND DISCUSSION: AN ASYMMETRICAL NOTCH FRACTAL ANTENNA WITH METASURFACE

3.1. Introduction

This chapter will provide an overall appraisal of performance characteristics of the antenna system assessed in the study. A primary purpose of this section will be to examine how well the proposed technique addresses the core requirement of modern mid band wireless communications systems regarding signal integrity, impedance characteristics, radiation characteristics, and overall operational performance stability. This chapter will attempt to demonstrate feasibility for practical wireless applications by correlating simulated results with results obtained through experimental measurement under controlled conditions. The analysis of key antenna parameters required for reliable communication, including impedance matching characteristics, reflection properties, radiation limitations, efficiency, and directivity over the frequency range of interest, is the basis of the performance assessment. There is a focus on determining the consistency of the performance of the antenna at the frequency band specified for operation, as well as evaluating the suitability of the antenna for use in environments with stable signal transmission, receipt requirements. The findings documented in this chapter provide an indication of the capacity of the antenna to maintain effective power transfers, to reduce signal losses, and to produce stable radiation patterns in realistic deployment conditions. This chapter also looks at how structural and environmental elements affect antenna performance, providing a thorough explanation of how configuration changes affect overall behavior. The study's accuracy and dependability are established by comparing the simulated and measured results, guaranteeing that the conclusions are not restricted to perfect circumstances. Overall, this chapter offers a critical analysis of the performance patterns that have been noticed and emphasizes the antenna system's usefulness in meeting the demands of modern wireless communication.

3.2. Method

The proposed antenna system development proceeds according to the design process which Figure 3.1 shows. The process begins with the conceptualization of a Novel Fractal Geometry, which engineers the design to achieve the Target Resonant Frequency and continues with the MTM Unit Cell selection and optimization process. The design process proceeds to Metasurface Simulation and parameter measurement after the workflow demonstration and the team conducts a Parametric Study of Placement to identify the configuration that produces maximum gain and bandwidth. After selecting the final model the team builds the hardware through Fabrication on a Substrate with an AMC to enter the empirical validation phase. The testing phase requires a dedicated Prototype Testing Setup, which performs physical measurements to gather data for the Analyzed Performance phase that compares simulated and experimental results to verify design strength.

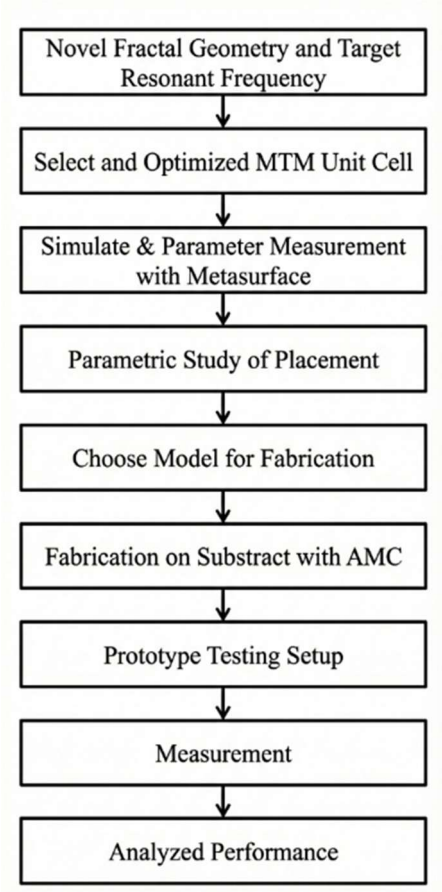


Figure 3.1. Design flow of the proposed fractal antenna integrated with a metasurface

This research describes an antenna designed and optimized with ANSYS HFSS software, manufactured on an FR4 substrate material, and tested in an anechoic chamber environment. The antenna uses an asymmetrical five-pointed star fractal radiator and an additional metasurface layer comprising an array of periodically arranged rectangular SRR unit cells. Together these two parts function to minimize the effects of surface waves, improve impedance matching, and improve directionality of the radiated energy. This helps to alleviate many of the problems associated with traditional microstrip patch antennas, including their narrow bandwidth and high return loss. Using both the fractal shape and the metasurface synergistically reduces the power reflected back to the antenna, improves impedance characteristics, and increases the antenna's overall performance at mid-band frequencies. Figure 3.2 shows a simulated triangular fractal ground plane, while Figure 3.3 offers a comprehensive view of the multilayer structure. It highlights the R-SRR metasurface, the dependent notches on the radiating patch, and the microstrip feed line. This clarifies the manufacturing geometry by clearly illustrating how the radiating element, feed system, and metasurface layer are structurally combined into a unified antenna system.

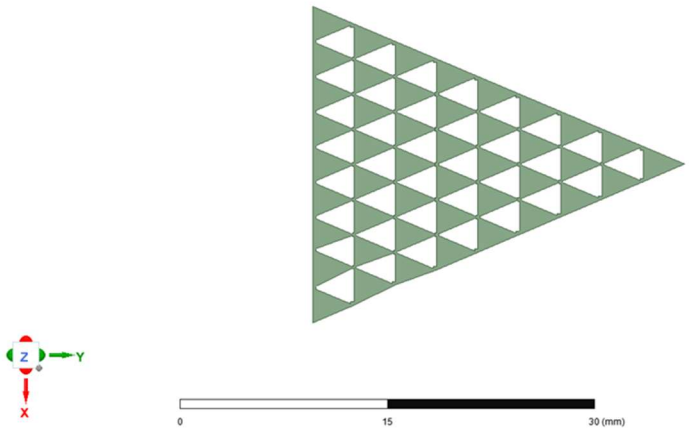


Figure 3.2. Triangular fractal ground plan

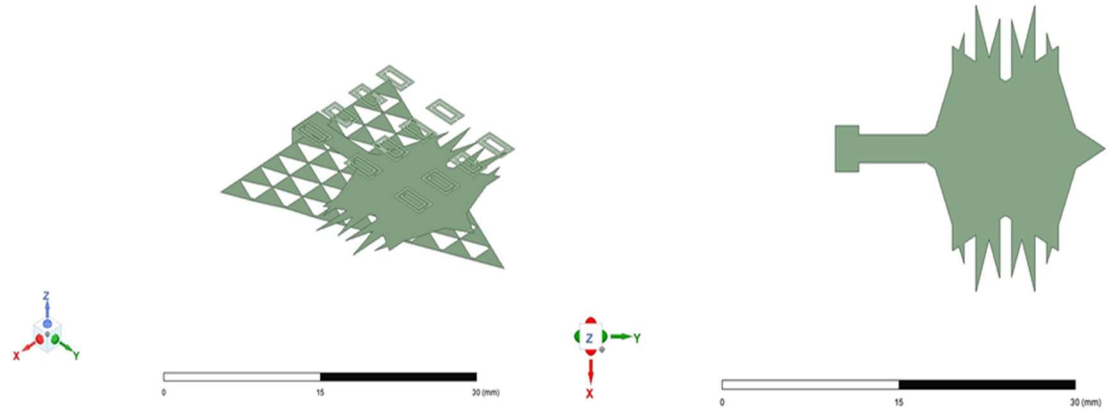


Figure 3.3. Multi-layered configuration R-SRR Metasurface, Fractal Patch-Feedline, Fractal Ground & Detail view of Asymmetrical Notch Patch

The triangular fractal ground plane is shown in Figure 3.2, and the detailed geometry of the asymmetrical notch fractal radiating patch is shown in Figure 3.3, along with the multilayer configuration of the proposed antenna. The ground plane fractalization creates controlled phase discontinuities that improve electromagnetic coupling with the radiating element. The patch fractal geometry enables extension of surface current paths, leading to better resonance performance. The combination of these features improves impedance bandwidth, decreases return loss, and boosts overall radiation efficiency.

3.3. Antenna design Specifications

The proposed antenna prototypes are built using FR4 substrates that combine asymmetrical star-shaped fractal patterns with metasurface technology to enhance their radiation efficiency and directivity and impedance matching capabilities. The complete antenna configuration is illustrated in Figure 3.4, while the principal design parameters are listed in Table 3.1. The parameters for this project include substrate properties, fractal iteration level, notch width, metasurface specifications, and ground plane design.

FR4 was selected as the board material because of its consistent dielectric constant (εr=4.4), durability, and affordability. These attributes make it an excellent choice for creating prototypes. The small size of the substrate at 32 by 23 by 1.6 mm^3 with a standard thickness of 0.035 mm of copper will provide both miniaturization and physical integrity. The use of a triangular fractal pattern for the ground plane at the back of the board introduces

phase discontinuities, increasing electromagnetic coupling between ground and radiating patch while improving radiation efficiency overall.

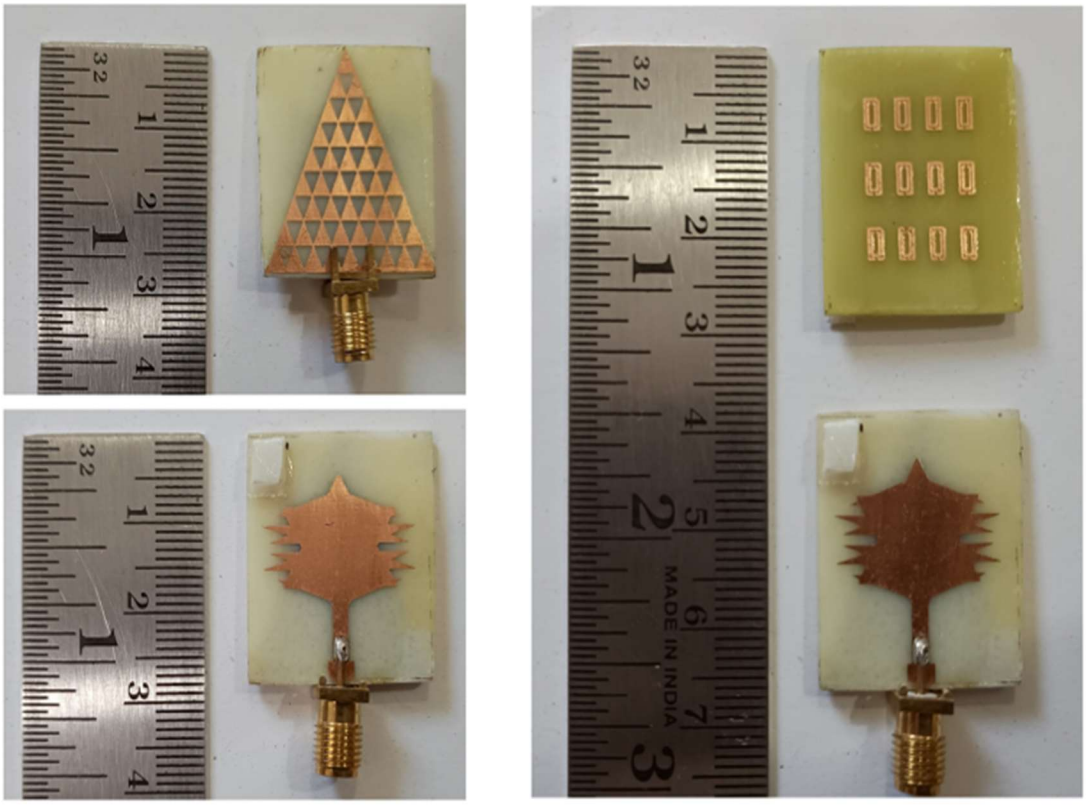


Figure 3.4. Fabricated proposed asymmetrical star-shaped fractal antenna incorporating a metasurface and fractal ground.

Table 3.1. Design parameters of the proposed asymmetrical star-shaped fractal antenna

Parameter	Value
Substrate material	FR4 (εr = 4.4)
Substrate dimensions	32 × 23 × 1.6 mm³
Fractal iteration level	2 (asymmetrical star-shaped fractal)
Notch width	3 mm
Patch thickness	0.035 mm (copper)
Metasurface unit-cell pitch	4 × 4 mm
Metasurface layer thickness	0.5 mm
Ground plane configuration	Full / partial (defected ground)

3.3.1. Fractal Antenna Design

To increase directivity and enable multi band operation, the suggested antenna makes use of an asymmetrical star shaped fractal design. Multiple radiating arms and sharp edge discontinuities are incorporated into the star shaped geometry, which successfully extends the surface current courses and adds more modes that are resonant. The design improves impedance bandwidth while achieving compact physical dimensions by the integration of asymmetrical notch features. Additionally, the effective distribution of electromagnetic fields across the radiating patch made possible by the fractal arrangement results in better overall antenna performance, expanded impedance bandwidth, and changed radiation characteristics.

3.3.2. Notch Characteristics

The proposed antenna has a copper radiating patch, which includes dependent notches placed in a way that will enable the radiating characteristics to be frequency selective. The notch width was established at wn = 3mm, and was optimized using HFSS by analyzing many different parameter values. It was found that a narrow notch had less electromagnetic coupling than a more widely spaced notch, and that too wide of a notch resulted in impedance mismatches and poorer matching performance. By properly locating the dependent notches on the patch surface, the dependent notches will disturb the surface current distribution, which increases the effective electrical length along the resonant paths, helping to excite new resonant modes. Therefore, the antenna provides an increase in impedance bandwidth while maintaining small dimensions. Additionally, the dependent notches act as bandstop filter elements, which reduce unwanted harmonic responses while providing minimized spurious radiation effects. In addition, the dependent notches reinforce the intended resonant frequencies and therefore improve frequency selectivity and spectral purity of the antenna. The combination of these two factors provides more stable and reliable antenna performance in the midband frequency region, allowing this antenna design to be used for multiband and interference less wireless communications.

3.3.3. Metasurface integration

To improve radiation performance and overall electromagnetic performance of the antenna, the proposed plan utilizes a metasurface layer. The unit cell has a periodic distance of 4mm, which has been determined to provide the best level of structural compactness and lowest amount of effective surface wave suppression, matching previous studies [83]. In this way, there are improvements in the impedance bandwidth and directivity of the antenna

without significantly increasing its physical size due to the addition of the metasurface layer. Furthermore, the metasurface also modifies the distribution of the surrounding electromagnetic field, resulting in better directional radiation and more uniform energy confinement in the desired directions of propagation. The metasurface allows for tight control over either the phase or the amplitude of the radiated fields that will be helpful for applications that require high polarization purity or directional selectivity. The metasurface supports surface current flow and limited surface wave losses to suppress harmonics and significantly suppress back radiation [84]. Therefore, collectively these improvements would provide stable gain characteristics, low return loss, and highly efficient antenna operation within the designed mid-band frequency range.

3.4. Anechoic Chamber Testing of the Fractal Antenna

For the purpose to estimate important performance parameters such radiation characteristics, return loss, gain, and directivity under idealized conditions, the asymmetrical notch based fractal antenna was first developed and examined using ANSYS HFSS. To confirm the simulated results, the antenna prototype was experimentally characterized inside an anechoic chamber after being fabricated on a FR4 substrate. As illustrated in Figure 3.5, the chamber simulates free-space conditions by using pyramid-shaped radiofrequency absorbers that successfully reduce electromagnetic reflections, allowing for precise and interference free measurements.

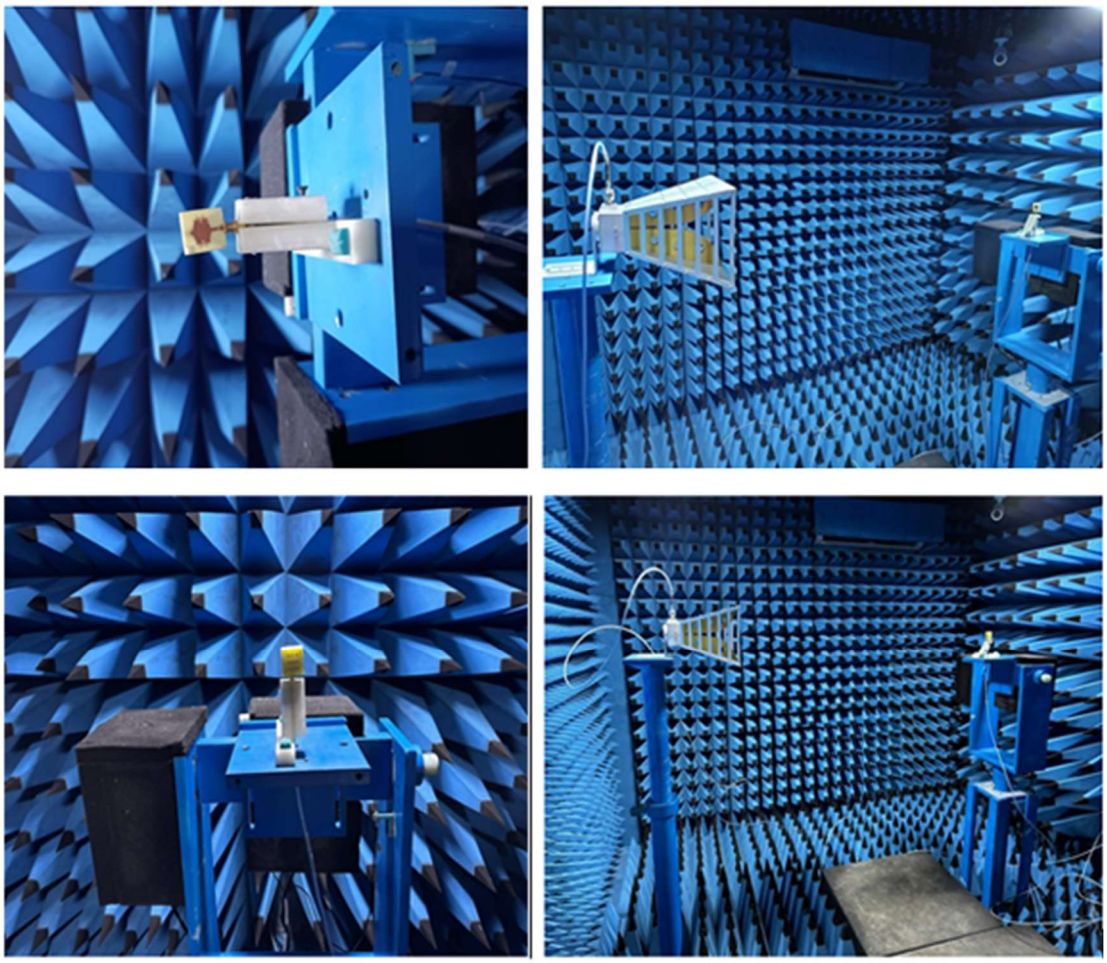


Figure 3.5. Experimental setup of the fractal antenna inside the anechoic chamber

A calibrated vector network analyzer (VNA) was utilized in the measurement setup to connect to the antenna via high-quality, low-loss cables. The VNA enabled the direct recording of the return loss and voltage standing wave ratio (VSWR) of the antenna. Gain and directivity were calculated from standard gain comparison using a reference horn antenna. The measurement environment also provided an anechoic setting, which helped limit external interference. To thoroughly explain minor experimental deviations, potential sources of noise and measurement uncertainty must be discussed; specifically, intrinsic VNA calibration tolerances, high-frequency connector losses, and slight positioning errors during anechoic chamber testing. Therefore, after completing several validation trials with the same equipment, the uncertainty margins were firmly estimated to be within ±0.2 dB for return loss, and ±0.5 dB for gain and directivity. These negligible errors compared to the measured performance of the antenna confirm the robust validity of the experimental data.

3.4.1. Ground Plane Configurations

Three different ground plane configurations were developed through the High Frequency Structure Simulator (HFSS) and then fabricated to facilitate comparative analysis. The full ground configuration served as a reference model by utilizing a continuous copper layer on the backside of the substrate. The partial ground configuration used an intentionally shortened ground plane to create defected ground structure (DGS) effects and changed the surface current distribution, as well as improved impedance matching characteristics. By omitting the metasurface layer, the triangular fractal ground plane was maintained in the no metasurface configuration; thus, allowing for the specific effect of the metasurface to be independently analyzed. A systematic evaluation of the full ground, partial ground, and no metasurface configurations will provide a means of assessing the impact of ground configuration types on the key measures of performance, such as return loss, impedance bandwidth, and radiation efficiency.

3.4.2. Performance Optimization

The performance of the antenna is assessed using several essential parameters, including radiation efficiency, return loss, gain, directivity, and voltage standing wave ratio (VSWR). High radiation efficiency indicates minimal power dissipation, while low return loss reflects effective impedance matching and reduced signal reflection. The evaluation of these performance indicators is conducted through specific mathematical equations.

Radiation efficiency, represented by $\boldsymbol{\eta_r}$, defines the ratio of the radiated power to the total power supplied to the antenna and is given by:

$$\boldsymbol{\eta_r} = \frac{\boldsymbol{P_r}}{\boldsymbol{P_t}} \times \mathbf{100}\% \tag{3.1}$$

Where, $\boldsymbol{P_r}$ denotes the radiated power ($\mathbf{W}$) and $\boldsymbol{P_t}$ represents the total input power delivered to the antenna (W).

Return loss (RL), which characterizes the amount of power reflected due to impedance mismatch, is expressed as:

$$\boldsymbol{RL} = -\mathbf{20}\mathbf{log_{10}}\left(|\boldsymbol{S_{11}}|\right) \tag{3.2}$$

Where, $\boldsymbol{S_{11}}$ is the reflection coefficient.

Antenna gain ($\boldsymbol{G_a}$), indicating the capability of the antenna to direct radiated energy in a specific direction, is defined as:

$$\boldsymbol{G_a = 10\log_{10}\left(\frac{U(\theta,\phi)}{P_t/4\pi}\right)} \tag{3.3}$$

Where, $\boldsymbol{U(\theta,\phi)}$ represents the radiation intensity ($\mathbf{W/sr}$) in the direction ($\boldsymbol{\theta,\phi}$), and $\boldsymbol{P_t}$ is the transmitted input power (W).

Directivity ($\boldsymbol{D_a}$), which measures the maximum concentration of radiated power, is given by:

$$\boldsymbol{D_a = \frac{4\pi U_{max}}{P_r}} \tag{3.4}$$

Where, $\boldsymbol{U}_{\max}$ is the peak radiation intensity (W/sr).

The voltage standing wave ratio (VSWR), used to assess the degree of impedance matching, is defined as:

$$\boldsymbol{VSWR = \frac{1+|\Gamma|}{1-|\Gamma|}} \tag{3.5}$$

Where, $\boldsymbol{\Gamma}$ denotes the reflection coefficient.

3.5. Results and Discussion

3.5.1. Return Loss and Bandwidth

Figure 3.6 shows the simulated reflection coefficient (S11) of the antenna in the frequency range of 2.0-7.0 GHz. The antenna resonates at 5.2075 GHz with a return loss of −32.67 dB and an impedance bandwidth of 8.5%. The results show efficient power transfer with minimal signal reflection. The improved impedance matching at this frequency band can be attributed to the cumulative effect of the metasurface integration, which suppresses the surface wave, and the asymmetric notch design, which maximizes the surface current path and ensures robust resonance.

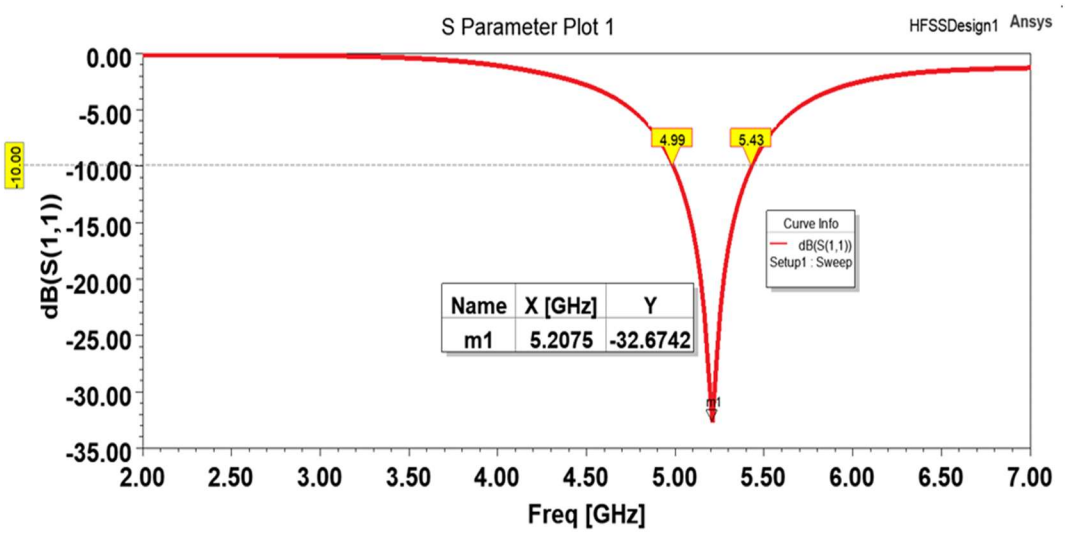


Figure 3.6. Simulated S-parameter (S11) plot across 2.0–7.0 GHz



(a) (b)

Figure 3.7. Measured reflection loss (S11) of the fabricated antenna: (a) higher-frequency resonance and (b) lower-frequency resonance

The results obtained from examining the VNA measurements for reflection losses are depicted in Figure 3.7, which includes both the high-frequency resonance curve (Figure 3.7 (a)) and the low-frequency resonance curve (Figure 3.7 (b)). Analyzing the data has shown that there is a 5.2075-GHz resonance point with a -32.67-dB minimum return loss and an impedance bandwidth of 440 MHz (4.99-5.43 GHz). It was found that there was a high degree of correlation between simulation and experimental results based on measurements having an average <0.2% frequency difference and 0.77 dB difference in return loss. High correlation of the measured data with the simulated data supports the validity of the simulation model to accurately represent aspects of the physical

characteristics utilized in the experiment. Overall, the similarities of simulation and measured results indicate that the configuration proposed for a wireless communication application provides increased impedance bandwidth, improved return loss characteristics, and therefore presents an excellent opportunity for their use as a wireless communication device.

3.5.2. Voltage standing wave ratio analysis

In Figure 3.8, the antenna's VSWR behaviour is presented to show how impedance matched across the 1.00-9.75 GHz frequency range, where a VSWR equal to 1.0 represents perfect impedance match and a VSWR less than 2.0 can be classified as acceptable for practical use. The antenna exhibited maximum performance at 5.2075 GHz with a VSWR of 1.0476, closely approaching an ideal condition where power will be absorbed efficiently and the maximum amount of power will not be reflected.

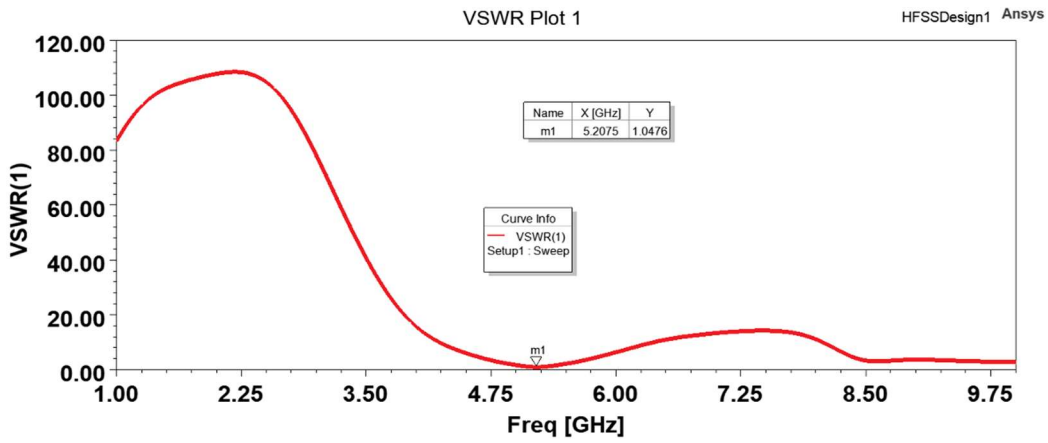


Figure 3.8. VSWR plot across a wide frequency range for the proposed fractal antenna

This is due to the good impedance matching. Below 4.50 GHz, the VSWR increases substantially, showing a poor match and higher reflection losses. After the resonant frequency, the VSWR levels remain constant, showing a good tuning around the mid-band and suitability for Wi-Fi and ISM applications.

3.5.3. Gain and Directivity

The gain and directivity characteristics of the antenna are presented in Figure 3.9, which shows how the antenna radiates and how it directs signals.

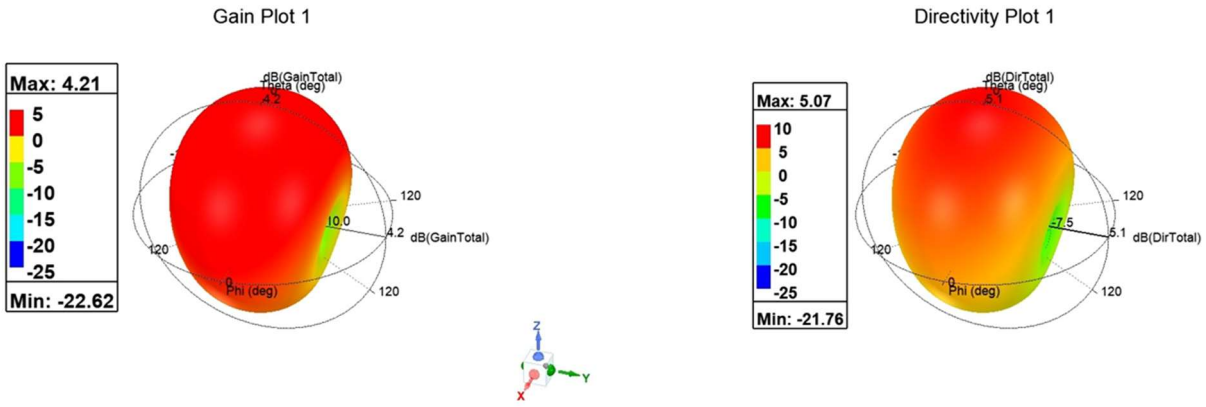


Figure 3.9. Gain and directivity plots with maximum and minimum values across various angles

The gain plot illustrates the antenna's ability to receive and transmit signals over different angular orientations, showing a maximum gain of 4.21 dBi and a minimum value of −22.62 dBi in certain directions. The directivity plot shows that the antenna produces directional radiation patterns that reach a peak directivity of 5.07 dBi while displaying minimum directivity values of −21.76 dBi when compared to an isotropic reference.

The antenna results show both its strong radiation areas and its weak radiation areas. The measurement results show that the system can direct energy to specific areas that enables communication systems to use concentrated beams. The negative minimum values show radiation nulls, which represent a typical characteristic of practical antenna radiation patterns that show areas with extremely low or absent radiated energy. The combined gain and directivity results show that the antenna performs effectively for directional point-to-point communication systems, which produce better signal quality and less interference.

3.5.4. Radiation Patterns and Axial Ratio

Three distinct angle positions lying adjacent to the antenna were used to compare its axial ratio characteristics and polar radiation pattern. The various results are shown in Figures 3.10 and 3.11. From Gain Plot 2 shown by Figure 3.10(a), at angle position of 0 Degrees, radiation levels are shown to varying from -2 dB to -23 dB at the horizontal plane; and through -9 dB to -16 dB at the vertical plane for the same angle position of 0 degrees. As noted in Gain Plot 3 (Figure 3.10(b)), at the same operating frequency, the radiation patterns appear to have a similar behaviour regardless of their angle position with respect to the same frequency; therefore, demonstrating its stable radiation performances.

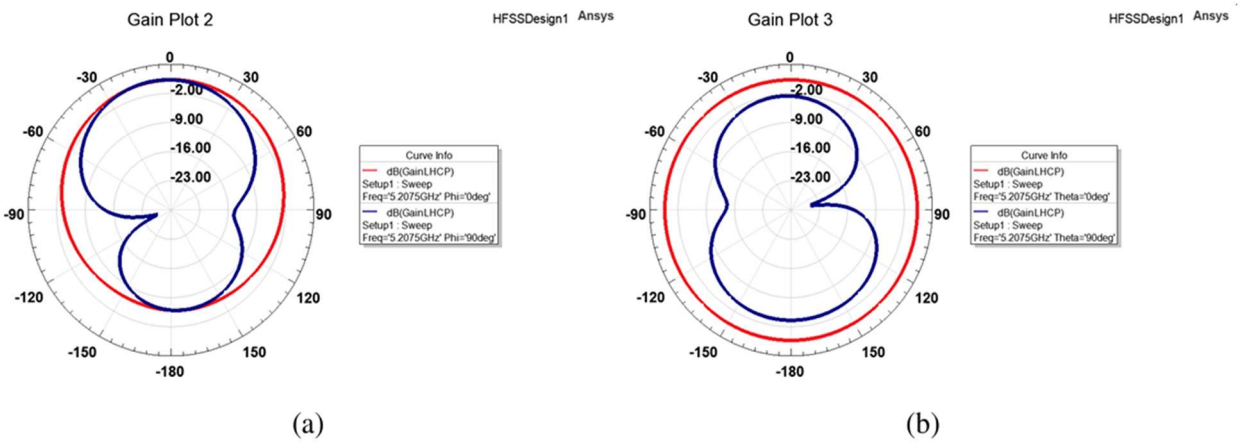


Figure 3.10. Polar radiation characteristics of the proposed antenna at f = 5.2075 GHz: (a) gain plot 2 for Φ=0◦ and Φ=90◦ and(b)gain plot 3 for Θ = 0◦ and Θ = 90◦

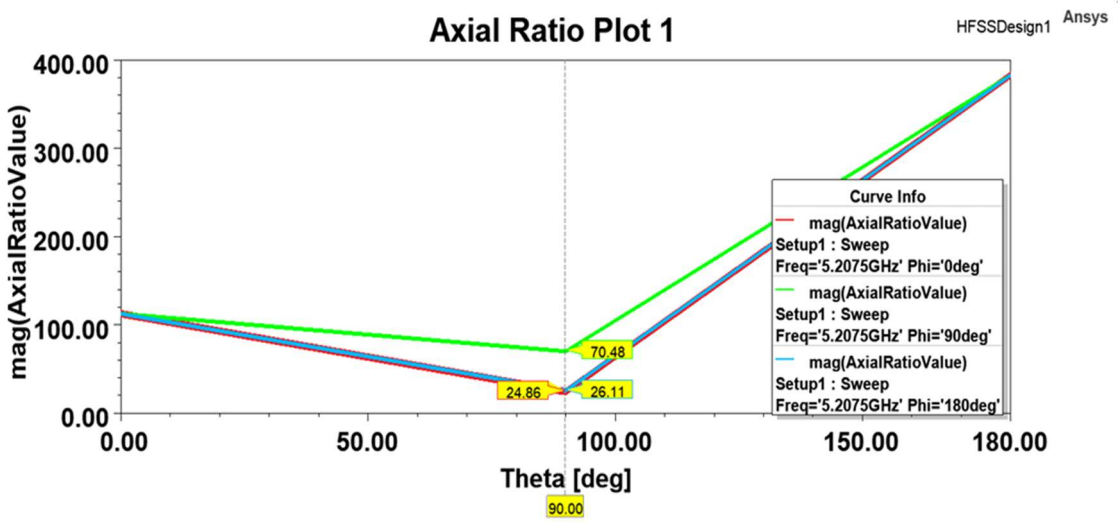


Figure 3.11. Axial ratio variations at 5.2075 GHz for Φ = 0◦, Φ = 90◦, and Φ = 180◦ orientations

The antenna has been shown to exhibit effective circularly polarized performance at φ=0° and φ=90°. Increased axial ratio seen in Figure 3.11 at φ=180° also implies decreased purity of circular polarisation at this φ-value. Applications like satellite communications, RFID and IoT systems benefit from the circular polarised nature of an antenna due to this decreased potential for misalignments between polarisation types leading to increased transmission reliability. Overall, the steady nature of the axial ratio at the majority of the φ-

values indicates that this antenna would be suitable for these types of applications, although further optimisations may be necessary at φ=180°. The combined findings shown in this report further demonstrate that this antenna has great potential for mid-band applications requiring both polarised diversity as well as reliable performance levels.

3.5.5. S-Parameter and Impedance

The S-parameter representation of the antenna is shown in Figure 3.12, with a focus on its S11 response at 5.2075 GHz. The low reflection coefficient at this frequency demonstrates very good impedance match between the antenna and the feed network, allowing efficient power transfer between the antenna and feed network. Impedance matching is especially important for antennas operating at high frequencies since it reduces supply of the signal reflected back to the feed. The impedance plot of the antenna provides an idea of how the input impedance varies with frequency in relation to both its resistive component (real) and its reactive component (imaginary). The impedance provides balanced resistive and reactive components, showing that the antenna efficiently received high frequency signals with good impedance match and almost no mismatch. The S-parameter and impedance data show the antenna has stable impedance characteristics and provides good performance in mid-band wireless communications systems.

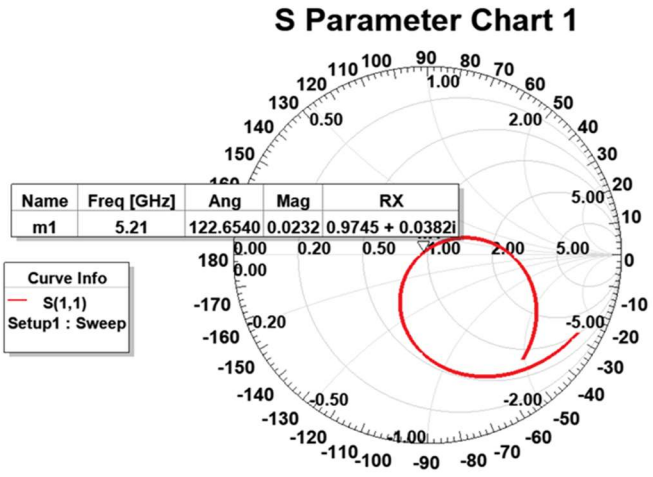


Figure 3.12. S-parameter chart showing reflection characteristics at 5.2075 GHz

The antenna's gain and directivity performance between 5.00 GHz and 6.00 GHz shows its operational frequency at 5.2075 GHz through the data presented in Figure 3.13. The antenna generates a 4.2132 dBi gain and a 5.0692 dBi directivity at this frequency which demonstrates its capacity to boost signal strength while directing radiated power more effectively than an isotropic radiator. The gain curve increases steadily toward 5.2075 GHz,

reaches its maximum at resonance, and then gradually decreases, highlighting that the antenna's optimal operating band is centred around this frequency.

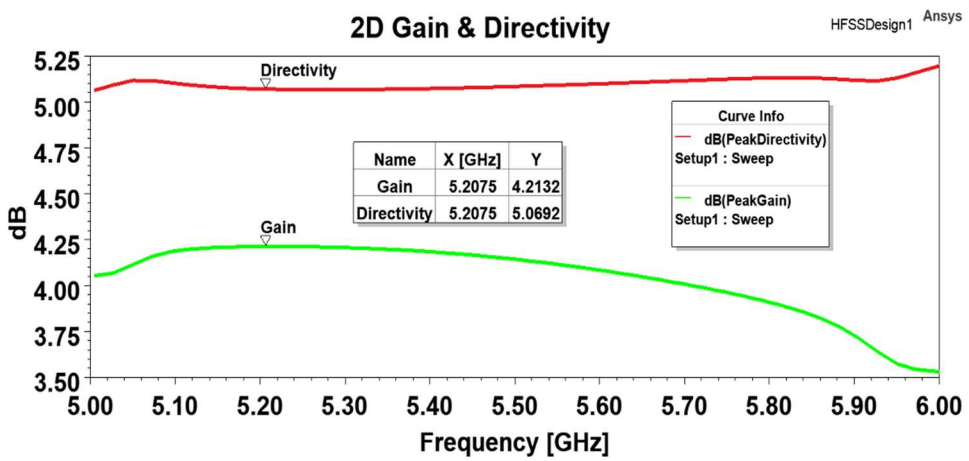


Figure 3.13. Antenna gain and directivity over the frequency range of 5.00–6.00 GHz

The directivity curve shows stable behavior throughout the entire frequency spectrum except for a minor peak which occurs at the resonant frequency. The consistent directivity behavior proves that the system produces a specific radiation pattern which enables efficient power use and dependable signal transmission. The antenna demonstrates suitable performance for specific communication tasks because its design delivers better signal reception and wider communication distances.

3.5.6. Efficiency and Radiation Intensity

The antenna shows its radiation efficiency and peak radiation intensity measurement results which remain constant from 5.00 GHz to 6.00 GHz. The antenna reaches its maximum radiation efficiency of 0.8211 at the 5.2075 GHz resonant frequency according to Figure 3.14a which shows that the antenna functions optimally at this frequency. The normalized radiation intensity field reaches its highest point of 0.2098 at the same operational frequency according to Figure 3.14b demonstration.

The peak performance of the antenna shows how well it can emit energy through specific directions which improves its transmission capabilities. The resonant frequency shows maximum efficiency and radiation intensity because accurate frequency tuning is essential for optimal antenna operation. The study demonstrates that systems need to maintain their operational frequency at the designed frequency to achieve high efficiency

and stable radiation patterns together with polarization performance which prepares them for top wireless communication performance in mid-band frequency systems.

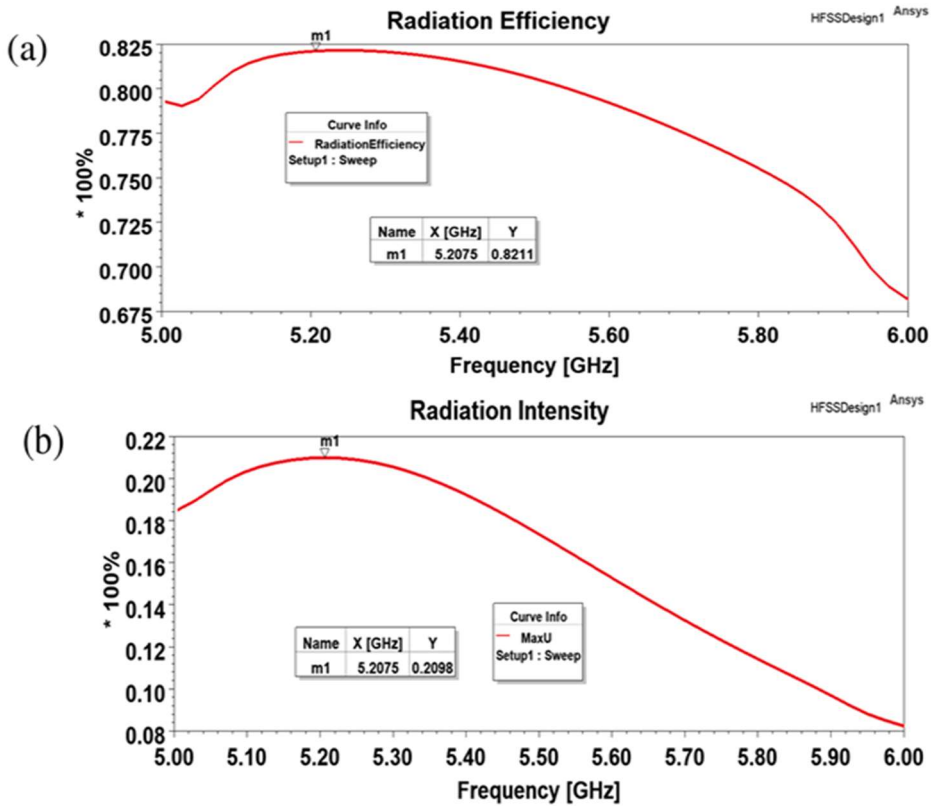


Figure 3.14. Antenna performance between 5.00–6.00 GHz: (a) radiation efficiency and (b) radiation intensity with peaks at 5.2075 GHz

3.5.7. Power Handling and Ground Effects

The diagram in Figure 3.15 shows the antenna power handling operates under different ground plane setups. The antenna in Figure 3.15 demonstrates its operational capability to handle 29.9977 dBm of input power at 5.2075 GHz while its output shows a power level of 29.1417 dBm. The difference between these values corresponds to a modest power loss of 0.856 dB which can be attributed to resistive and dielectric losses within the antenna structure. The power accepted by the system remains constant throughout the frequency range under study whereas the system shows decreasing radiated power at higher frequencies which indicates potential for future performance improvement

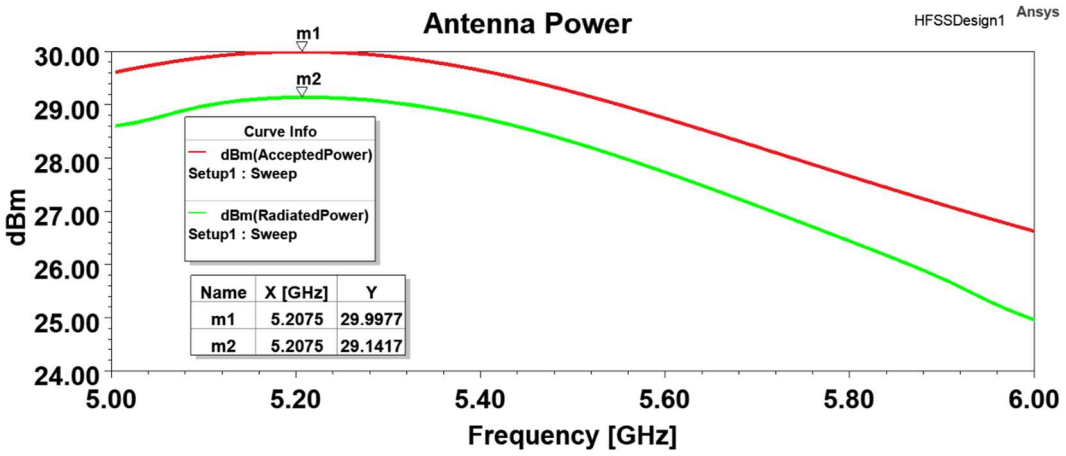


Figure 3.15. Antenna performance showing power handling capability

The study compares three different ground plane setups that include full ground and partial ground and a setup that lacks the metasurface element. The partial ground configuration achieves better impedance matching results that show a return loss of about 30 dB at 5.46 GHz. The full ground and no metasurface setups show weak matching performance that leads to significant changes in their resonance behavior. The study shows that designers can achieve better impedance stability through proper ground plane design that reduces losses and boosts antenna performance.

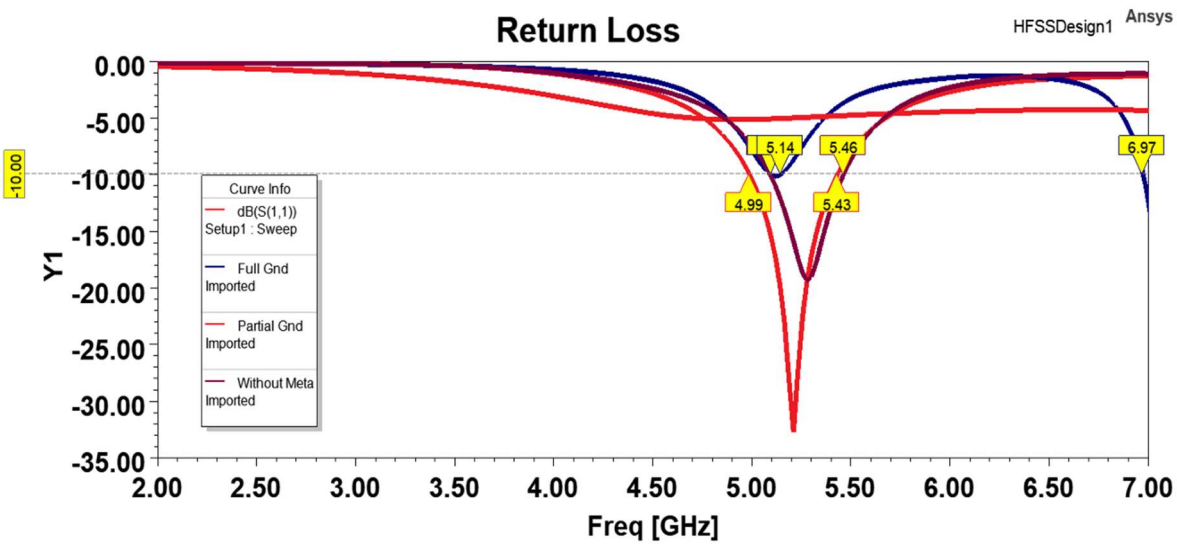


Figure 3.16. Antenna performance showing return loss for different ground configurations.

Table 3.2: Summary of Antenna Performance Metrics across Various Measurements

Parameter	Description	Configuration	Frequency (GHz)	Value	Performance Insights
Radiation Efficiency	Peak efficiency measured	Standard Configuration	5.2075	82.11%	Indicates optimal radiation efficiency
Radiation Intensity	Peak intensity measured	Standard Configuration	5.2075	20.98%	Represents maximum directional radiation
Accepted Power	Maximum power accepted by the antenna	Standard Configuration	5.2075	29.9977 dBm	The highest power handling capability was observed
Radiated Power	Maximum power radiated by the antenna	Standard Configuration	5.2075	29.1417 dBm	Highest power effectively radiated
Return Loss	Measure of impedance matching	Full Ground Imported	5.14	-25 dB	Effective matching at this frequency
Return Loss	Measure of impedance matching	Full Ground Imported	6.97	-10 dB	Lesser matching, indicating inefficiencies
Return Loss	Measure of impedance matching	Partial Ground Imported	5.46	-30 dB	Most effective impedance matching observed
Return Loss	Measure of impedance matching	Without Meta Imported	4.99	-15 dB	Moderate matching
Return Loss	Measure of impedance matching	Without Meta Imported	5.43	-20 dB	Better impedance matching compared to 4.99 GHz
Gain	Peak gain measured	Standard Configuration	5.2075	4.2 dB	Indicates effective signal amplification

Directivity	Peak directivity measured	Standard Configuration	5.2075	5.0 dB	Suggests efficient energy focusing in a specific direction

Table 3.3. Comparison of the proposed antenna with recent state-of-the-art designs

Study	Size (mm^3)	Bandwidth (%)	Peak Gain (dBi)	Efficiency
DSF [84]	20.42 × 22.71 × 4.72	12.95 @ 5.9 GHz, 10.89 @ 9.5 GHz	2.43 / 7.88	93.34 / 96 %
RIS-patch [85]	60 × 60 × 3.6	26 (4.98–6.48 GHz)	6.5	72–82
Varactor [86]	~0.51λ × 0.49λ × 0.013λ	5 (2.51–2.64 GHz), tuneable to 3.4 GHz	7.5	—
Proposed	**32 × 23 × 1.6**	**8.5 (4.99–5.43 GHz)**	**4.21 @ 5.2075 GHz**	**82.11**

The proposed asymmetrical notch fractal antenna design achieves an optimal performance balance through its compact dimensions that maintain consistent signal strength and deliver exceptional radiation efficiency according to Table 3.2. Antenna designs that exist today provide antennas with strong gain capabilities and improved flexibility but these features require users to accept larger antenna sizes and designs that are more complicated. The proposed antenna is optimized for mid-band frequencies, prioritizing compactness and stable performance over bandwidth expansion. The results demonstrate that it achieves competitive levels of gain and efficiency through its smaller design, which outperforms other designs according to Table 3.3. The system operates optimally for wireless communication and radar applications because it maintains stability while providing efficient performance in a compact form factor.

The results from the design, simulated, and actual experimental tests of a star-shaped, fractal-shaped antenna integrated with a metasurface demonstrate the suitability for mid-band wireless communication applications. Their performance characteristics include a distinct resonance at 5.2075 GHz with a deep return loss of -32.67 dB, yielding an impedance bandwidth of 8.5% (4.99-5.43 GHz) confirming power is transferred to the antenna

efficiently with minimal reflected signal. The VSWR of 1.0476 indicates a near-ideal impedance match at the operating frequency. Radiation performance reveals a peak gain of 4.21 dBi and a directivity of 5.07 dBi demonstrating the ability to provide directional communication with focused radiation. The measured efficiency of 82.11% along with much of the total anticipated radiation intensity peak of 20.98% demonstrate excellent energy utilization and strong ability for directional transmission. Power handling analysis reveals that most of the measured input power (29.99 dBm) was efficiently radiated (29.14 dBm), with only 0.856 dB being lost indicating that the antenna has low loss due to internal dissipation.

The study examined various ground plane designs that demonstrated that partial ground systems achieved better impedance matching by obtaining a return loss measurement of approximately −30 dB at 5.46 GHz that confirmed that ground alterations improve system performance. The study has two limitations, which restrict its findings because researchers only used FR4 substrates and conducted their measurements inside an anechoic chamber. The antenna design requires engineers to accept a compromise that limits bandwidth while making manufacturing more difficult because of the use of fractal designs and metasurface components. The chapter investigates different substrate materials that will boost bandwidth while testing antenna operations in actual multipath environments and developing a multi-band design from the original system. The research results will enhance the antenna's practical performance and operational strength and its ability to function in future wireless communication systems

CHAPTER 4

DESIGN-2 METHODOLOGY AND RESULT AND DISCUSSION: PERFORMANCE ENHANCED STAR FRACTAL ANTENNA WITH FRACTAL DGS AND METASURFACE INTEGRATION

4.1. Introduction

Due to the common evolution of wireless technology, there have been strict requirements for antenna requirements, especially with a compact size, a larger bandwidth and better radiating properties within a restricted amount of spectrum. Commercial microstrip antennas have generally remained very popular due to their planar form and ease of integration into systems; however, in many instances, these antennas suffer from narrow impedance bandwidth and modest gain, limiting their use in very high capacity and interference-prone applications. Therefore, new design methods are needed to satisfy these performance parameters to accommodate today's wireless services. The use of fractal geometries has attracted considerable interest in antenna design because their self-similarity and space-filling characteristics make them an effective method of reducing antenna size, achieving multi-band functionality, and improving impedance matching. Similarly, metamaterial-based techniques such as defected ground structures and metasurfaces have shown how the use of engineered materials can be an effective means of controlling electromagnetic fields, therefore enhancing antenna bandwidth, suppressing unwanted modes of operation, and improving pattern directivity. The combination of fractal geometries and metamaterials represents a potential method to achieve performance enhancement of antennas without increasing physical or implementation complexity. This chapter focuses on evaluating the combination of fractal radiating elements, fractal ground structures and metasurface-based enhancements for C band wireless services. This chapter explains three main aspects, which include the basic design principles, the electromagnetic characteristics, and the performance enhancements that result from these hybrid systems. With the goal to illustrate how these techniques impact impedance bandwidth, gain, and radiation patterns, the paper includes both simulation and experimental results. In addition to highlighting

possible areas for advancement in bandwidth flexibility and device operational adjustments, the chapter illustrates how fractal and metamaterial design approaches collaborate to create solutions that meet future wireless communication demands.

4.2. Fractal Geometry-Based Design and Its Impact on Antenna Performance

There are currently more opportunities to increase the effectiveness of telecommunications systems because of the application of fractal geometry in antenna technology. The self-similar and scale independent geometric characteristics of the fractal antenna give it an advantage over conventional antenna designs. Wideband and multiband designs, improved impedance matching, reduced size, and higher bandwidth are among the benefits. The idea of fractal geometry has allowed for the creation of an antenna with a compact and flexible structural design that can operate effectively across a wide frequency range. This section is dedicated to a star-fractal radiating element featuring a symmetric notch, which is added to enhance modal diversity and promote a uniform surface current distribution. The star shape, obtained from a symmetric notch fractal design, is very efficient in extending the electrical length of the surface currents and excites multiple resonant modes. This leads to an improvement in impedance bandwidth and frequency response. Compared with conventional patch shapes, the star-fractal designs facilitate either a smaller size for a given operating frequency or a lower operating frequency for a given size.

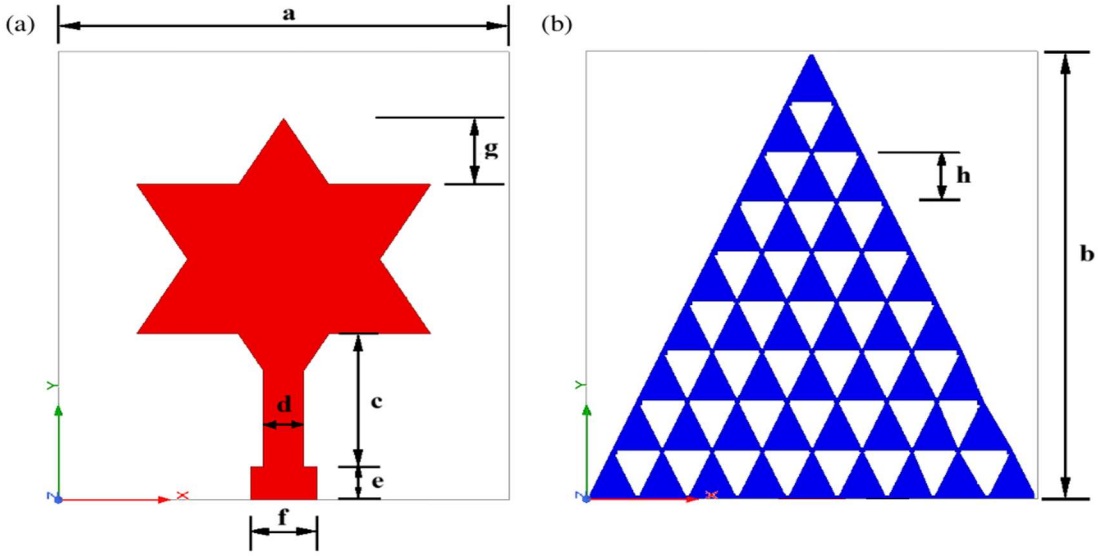


Figure 4.1. (a) Star-shaped fractal Patch with symmetric Notch (b) Sierpinski triangle fractal antenna with recursive design as defective ground structure.

Moreover, the introduced geometric complexity of the antenna contributes to improving the radiation properties (gain enhancement and radiation pattern control) due to the generating of more current paths and stronger fringing fields. To further facilitate the enhancement of the antenna, the structure of the ground plane is modified with a recursively generated Sierpinski triangle fractal structure created as a defective ground structure (DGS), illustrated in Figure 4.1. The addition of the DGS is used to help control surface wave propagation and to improve impedance bandwidth by taking advantage of the filtering and resonantly intrinsic properties of self-similar geometric figures. In addition to modifying the ground plane, a metasurface superstrate made up of an array of 3 x 4 split ring resonators (R-SRRs), illustrated in Figure 4.2, is placed above the radiating patch to manipulate the phase of the transmitted electromagnetic waves and improve constructive interference in the broadside direction. As a result, significant improvements (in terms of both gain and radiation directivity) were observed across the antenna's operating frequency range.

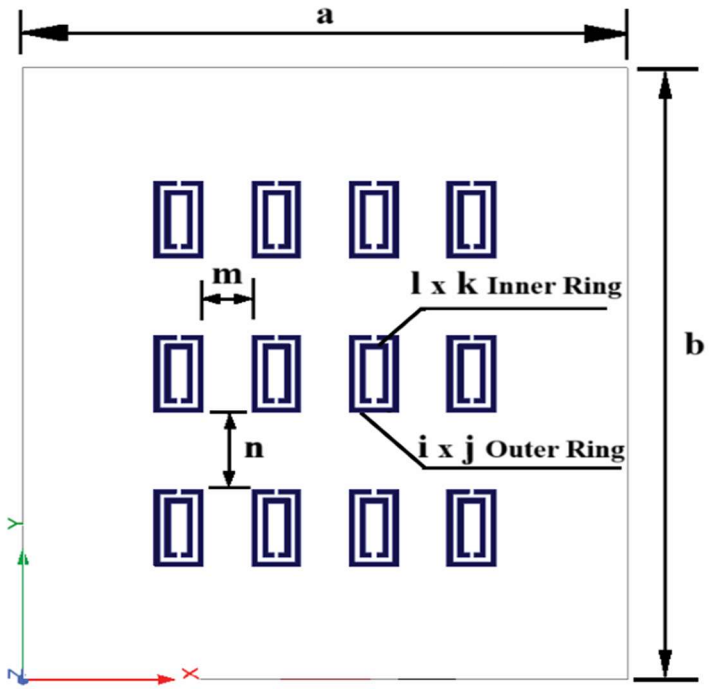


Figure 4.2. 3 × 4 Rectangular Split Ring Resonator (R-SRR) Metasurface as super substrate

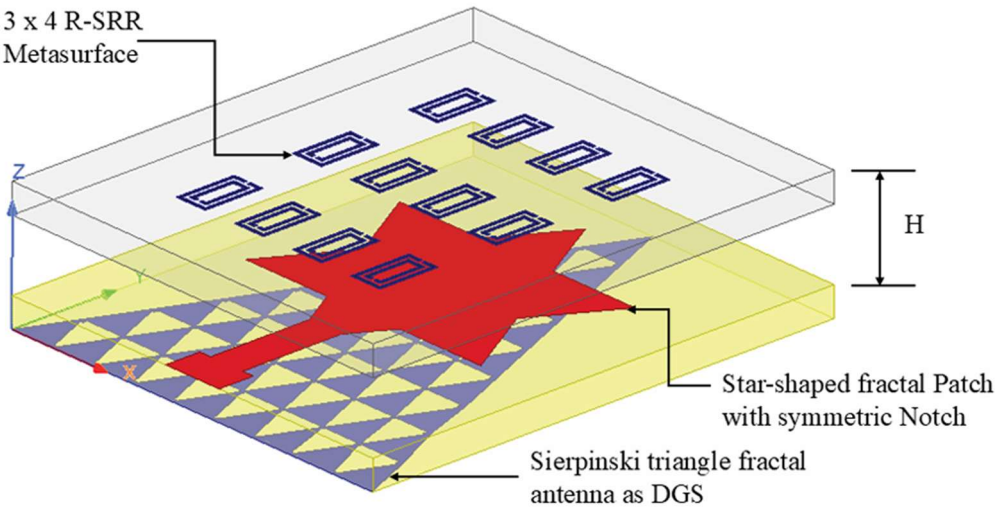


Figure 4.3. Star-shaped fractal antenna with fractal DGS and metasurface

In Figure 4.3, displays the complete integrated system that combines the fractal radiating patch with Sierpinski based fractal DGS and R-SRR metasurface superstrate elements to enhance antenna performance through their combined operation.

4.2.1. Design Architecture

The section below will discuss a star shaped fractal antenna with a symmetrically structured radiating patch and a Sierpinski triangle fractal ground configuration. The purpose behind both designs was to maximize the operating performance of the system while reducing the physical size of the system as much as possible. The design of these antennas was accomplished by using recursive triangular iterations of various shapes within the geometry of an overall triangular area that continually decreases in size. As can be seen in Figure 4.1, the use of recursion to achieve maximum surface area permits an efficient use of multiple resonant paths through a single finite area. Each figure illustrates two different types of fractal antennas: a star patterned fractal type geometric radiator, and the Sierpinski triangle based fractal structure. Each type contains the basic feature of a radiator and the critical geometric elements, such as point of feed and overall length of antenna. Along with these two fractal designs, Figure 4.2 shows the metasurface configuration used to enhance the performance of the antenna. The fractal antenna's structure was developed through an iterative design process that incorporated analytical modeling and full-wave electromagnetic simulations performed using ANSYS HFSS.

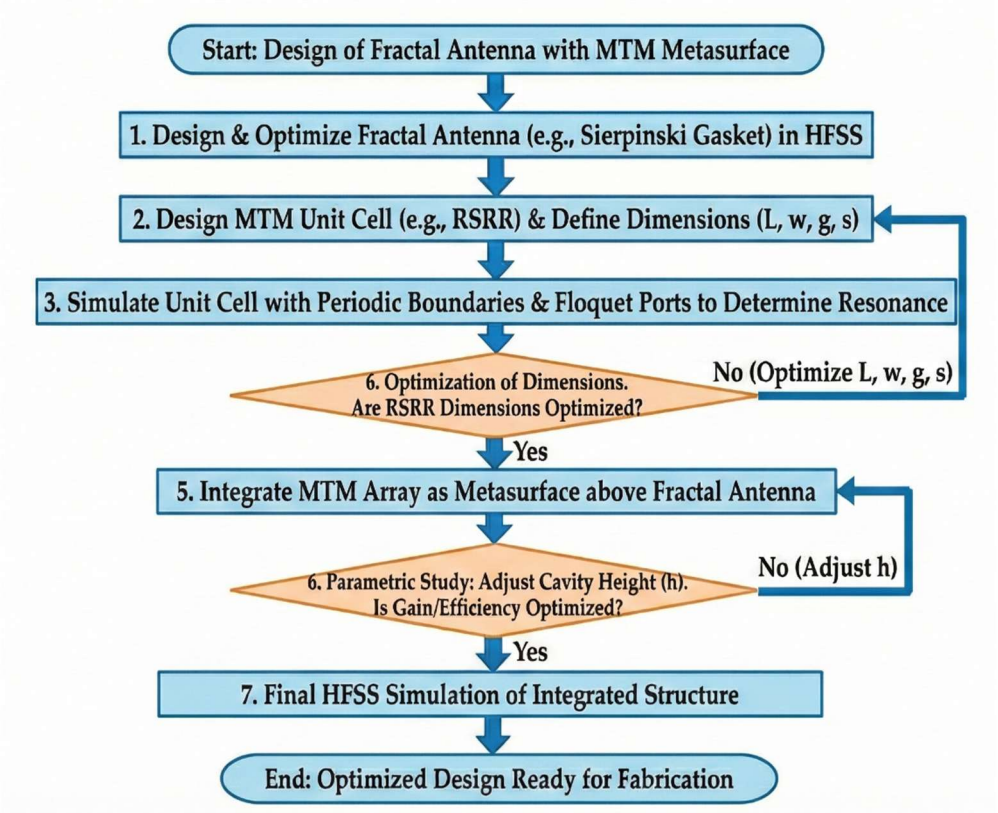


Figure 4.4. Design Flow for Fractal Antenna with Meta Material Inspired metasurface

The procedure used to create a fractal radiator with a metamaterial-influenced metasurface antenna consists of a number of steps outlined in Figure 4.4. To set the characteristics of the first radiator at the frequency required will be to have defined the Novel Fractal Geometry and the target frequency of resonance in relation to the electrical properties of the radiator. Along with this step will be the selection and refinement of the Metamaterial (MTM) Unit Cell (e.g. RSRR) to develop the required electromagnetic characteristics of near-zero and negative values of permittivity and permeability. The design of the two elements (radiation patch & metasurface) will be considered together in one environment (usually Ansys HFSS) to determine how they interact when the radiation output is applied.

The parametric study of placement which tests various vertical separation heights between the fractal patch and the metasurface to achieve maximum Fabry-Perot cavity effect and improved directive gain operates as a crucial step within this design process. The team selected their final model after they optimized the physical dimensions to achieve maximum efficiency and bandwidth performance which they would manufacture on a substrate that

possessed AMC (Artificial Magnetic Conductor) properties. The physical prototype undergoes testing, with setup and measurement execution, to confirm the simulated S_{11} parameters and radiation patterns against the performance analysis results. The complete technique establishes all elements necessary to achieve resonant coupling between the metasurface and the patch, meeting the high-gain requirements of contemporary wireless applications. The design process requires optimization of essential variables that include the radiating patch geometry and substrate characteristics together with the dimensional parameters of the metasurface unit cells to achieve the targeted resonant frequencies and improved impedance matching and specific radiation patterns. Free-space conditions are accurately simulated through radiation boundary conditions, which apply to all external surfaces while a discrete wave port system enables excitation of the antenna structure. The process of localized mesh refinement focuses on critical regions that include the symmetric notch star-shaped patch to improve numerical accuracy. The complete simulation system supports accurate measurement of essential antenna performance metrics, which include S-parameters and gain and radiation patterns thus enabling the optimal balance between antenna dimensions and bandwidth and gain for the specified application.

4.2.2. Mathematical Modeling of Fractal Geometry

The basic principles of fractal antenna design exist because researchers study how fractal dimensions impact important antenna properties which include their resonant frequency and impedance bandwidth. The fractal dimension, which researchers represent as D, functions as a measurement tool to assess geometric intricacy while it specially applies to self-similar patterns which include the Sierpinski triangle. It is mathematically defined as

$$\boldsymbol{D = \frac{\log (N)}{\log (\text{ Scale Factor })}} \tag{4.1}$$

where the scale factor indicates the reduction ratio applied to each subsequent iteration, and $\boldsymbol{N}$ is the number of self-repeating duplicates produced at each iteration. With a scaling factor of two, three self-similar copies of the Sierpinski triangle are generated. Substituting these values yields

$$\boldsymbol{D = \frac{\log (3)}{\log (2)} \approx 1.585} \tag{4.2}$$

According to this fractal dimension, the defected ground structure (DGS) based on the Sierpinski triangle has a significantly longer effective electrical length than a traditional

solid planar triangular geometry, thereby improving the overall radiation performance. Multiple current routes at various scales are supported and resonance behavior is improved by the longer electrical channel. Because fractal geometry is recursive, surface currents are dispersed among several hierarchical layers, which encourages wave localization and scattering. As a result, the uninterrupted surface wave propagation is disrupted, which improves electromagnetic isolation and decreases mutual coupling. Fractal geometries have better surface wave suppression than conventional planar ground structures because of these intrinsic scaling characteristics. Additionally, adding fractal features directly affects antenna radiation performance and modifies the effective radiating area. The effective area ($\boldsymbol{A}_{\text{eff}}$), gain ($\boldsymbol{G}$), and wavelength (λ) are related in the following way,

$$\boldsymbol{A}_{\text{eff}} = \frac{\lambda^2}{4\pi} \times \boldsymbol{G} \tag{4.3}$$

These expressions highlight how changes in effective area, induced by fractal geometry, contribute to gain enhancement and improved radiation efficiency.

4.2.3. Procedure for Designing the R-SRR Metasurface

Fractal geometry creates a major impact on the antenna's radiation characteristics and its impedance performance. The antenna maintains constant performance because its self-similar design with recursive elements produces identical radiation patterns throughout all its operating frequencies. The fractal design enables easier impedance matching at different resonance points which results in reduced return loss and increased overall radiation efficiency.

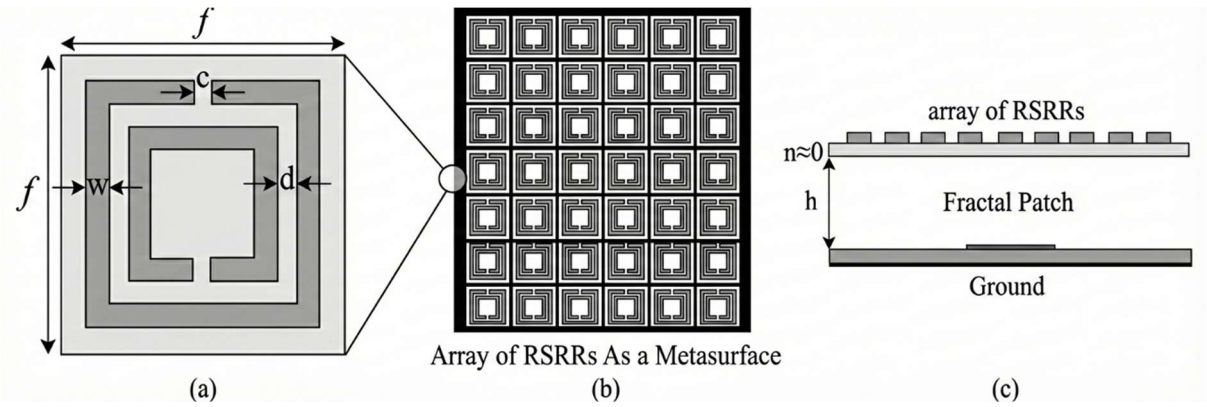


Figure 4.5. Figure Super-subtract Based Arrangement

A simulation oriented design approach is adopted to realize a metasurface-assisted fractal patch antenna on an FR4 substrate. Initially, electromagnetic design objectives are established by defining the desired resonant frequency and accurately modeling the FR4 substrate parameters. An equivalent LC-based model of the rectangular split-ring resonator (R-SRR) unit cell is then developed to provide initial design insight and parameter estimation. This is followed by periodic analysis using Floquet ports to extract S-parameters and evaluate resonance behavior and transmission phase characteristics under normal incidence. Subsequently, finite-sized metasurface array simulations are conducted to investigate inter-element coupling and edge-truncation effects. Based on these results, iterative tuning of the unit cell dimensions is performed to achieve the required phase distribution suitable for low-profile Fabry-Perot cavity operation [87,88], as illustrated in Figure 4.5. It shows the configuration of the proposed metamaterial-loaded antenna: (a) Geometry of the RSRR unit cell, (b) Top view of the RSRR array as a metasurface, and (c) Side view of the integrated layer structure showing the fractal patch and ground plane.

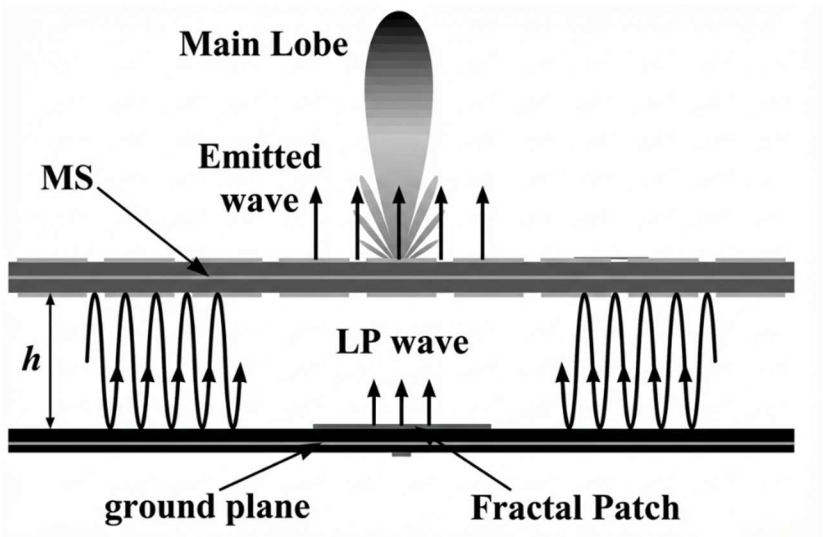


Figure 4.6. Fabry–Perot cavity-based arrangement in Proposed Antenna

The metasurface, composed of compact resonant elements, functions as a high-impedance surface that emulates an artificial magnetic conductor (AMC). By appropriately tuning the metasurface's resonance, the reflection phase can be controlled to ensure in-phase reflection with the radiating patch. This in phase condition within the Fabry–Perot like cavity formed between the patch and the metasurface leads to a substantial enhancement in antenna gain and directivity. The metasurface has a significant impact on the cavity behavior since it modifies the resonance conditions and electromagnetic field distribution, which directly

affects the overall performance of the antenna. An air filled Fabry-Perot cavity is created by maintaining an air gap of roughly $\lambda_0/10$, or 5.5 mm at 5.47 GHz, between the designed metasurface superstrate and the radiating patch. This Fabry–Perot cavity configuration, shown in Figure 4.6, enables strong constructive interference in the broadside direction while preserving a compact antenna profile. As a result, a gain improvement in the range of 4–7 dB and a competitive 3 dB bandwidth are achieved, consistent with recent studies on low-profile Fabry–Perot cavity antennas employing advanced metasurface unit cell designs [89-92].

The fabricated antenna configuration consists of two stacked RF structures implemented on a 25 mm × 30 mm FR4 substrate. The upper layer comprises the metasurface superstrate, while the lower layer consists of a symmetric star-shaped fractal patch on the top surface and a Sierpinski triangle–based fractal defective ground structure on the bottom layer of a 1.6 mm thick PCB, optimized for wideband operation. The fabricated star-shaped fractal antenna and its ground structure are shown in Figure 4.7 and 4.8 respectively. Experimental characterization is carried out in an anechoic chamber, as depicted in Figure 4.9, to minimize reflections and closely approximate free-space conditions.

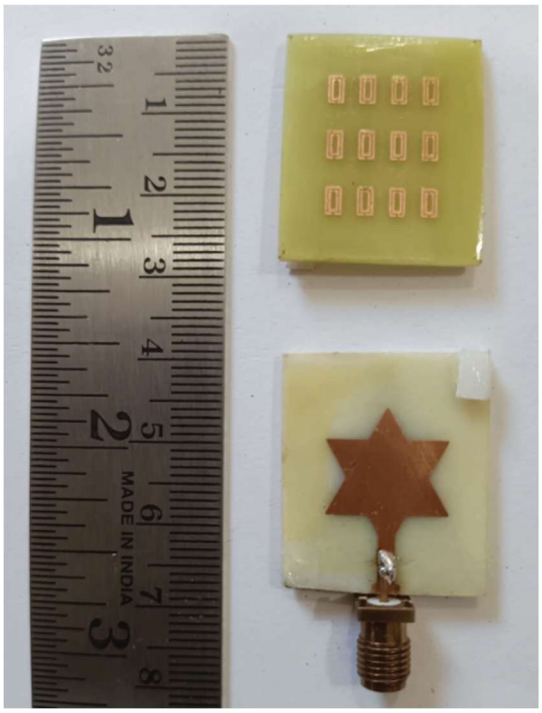


Figure 4.7. Fabricated star-shaped fractal patch with asymmetric notch and a metasurface.

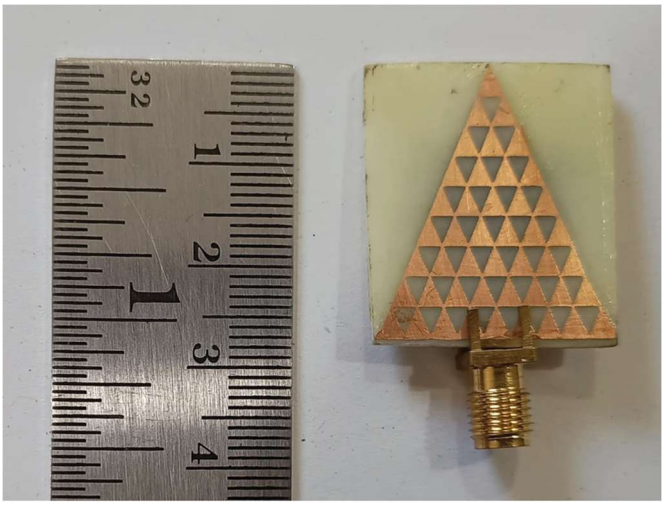


Figure 4.8 Bottom Group Layer of a fractal DGS with a Sierpinski triangle design

Table 4.1. Antenna component dimensions.

Description	Dimension (mm)
Substrate	FR4 (εr = 4.4)
Thickness	1.6
Loss Tangent	0.02λ
a	25
b	30
c	9.2
d	2.05
e	2
f	3.4
g	4.4
h	3
i	3.4
j	1.85
k	2.6
l	1.05
m	2.6
n	3.4
H	5.4

All components of the antenna are shown in Table 4.1, which includes the characteristics of the substrate, thickness of the substrate, loss tangent of the substrate and very important geometric parameters ("a" - "n"). The componential dimensioned information will impact antenna performance based on the operating frequency range of the antenna; i.e. the performance affects the performance is determined by the use of the appropriate componential dimensions for proper construction based on the antenna design to achieve the desired gain, bandwidth, and radiation pattern.

4.3. Results and Discussions

The main experimental results establish their origin from testing the prototype antenna that uses a star-shaped fractal radiating element together with a Sierpinski triangle design that serves as its fractal defective ground structure and an appropriate metasurface superstrate. The process of experimental validation operates as a vital component that supports the assessment of theoretical analyses together with simulation models while testing methods which enhance critical performance metrics including impedance bandwidth and gain and radiation efficiency and overall radiation characteristics. The researchers conducted complete measurements to evaluate how antennas perform under actual operating conditions. The results have been review systematically and compared to predicted values to demonstrate the effectiveness of the proposed design approach. A key emphasis has been placed on determining the impact of the fractal geometries and incorporation of the metasurface on antenna performance in the relevant frequency bands. These results shed light on how the interaction of fractal and metasurface features enhance performance efficiency, produce stable radiation characteristics and enhance electromagnetic performance capabilities for modern wireless communication systems.

4.3.1. Experimental Setup

The testing of the manufactured fractal antenna was done under precisely controlled experimental conditions for accurate characterization of its performance. In order to provide a complete assessment of the antenna's operation, return loss, impedance bandwidth, and radiation patterns were measured. A vector network analyzer (VNA) was used to measure reflection characteristics over the full operational frequency range in order to determine the impedance matching and bandwidth accurately. Radiation measurements were taken in an anechoic chamber, which is designed to reduce unwanted reflections and outside electrical interference so that the measurement conditions approach free space conditions as closely as

possible, as shown in Figure 4.9. Overall, the final arrangement of measurements for this experiment closely mimicked a practical operating environment thereby allowing the measurement of the performance of the fractal antenna to correlate with how it will perform in a real-world scenario when used in a wireless communications application.

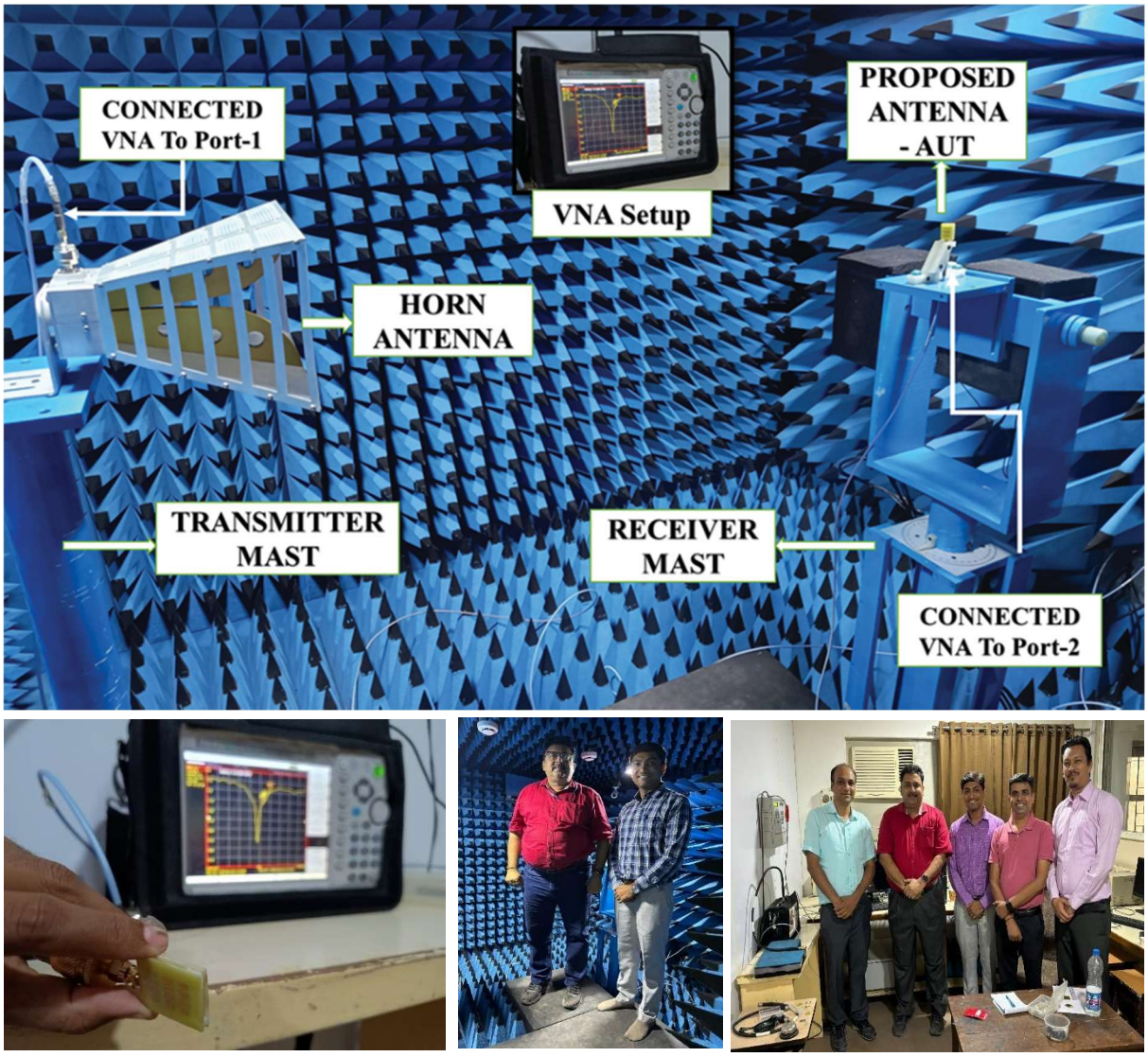


Figure 4.9. Proposed Star Fractal antenna with Metasurface in an anechoic chamber for measurement

4.3.2. Detailed Analysis of Return Loss Measurements

A close observation of the return loss value is required for assessing the impedance characteristics of the fractal antenna, as the return loss value has a direct effect on the radiation efficiency and overall performance of the antenna. The return loss values, as depicted in Figure 4.10, help in understanding the impedance matching between the fractal antenna and the transmission line, with lower values representing lower reflection of signals

and higher power transfer. The experimental analysis clearly reveals the significantly low return loss values at the critical operating frequencies, thus establishing the excellent impedance matching characteristics. The principal resonance frequencies of the fractal antenna are 5.22 GHz, 5.47 GHz, and 5.76 GHz, where the minimum return loss values of around 55.68 dB are obtained.

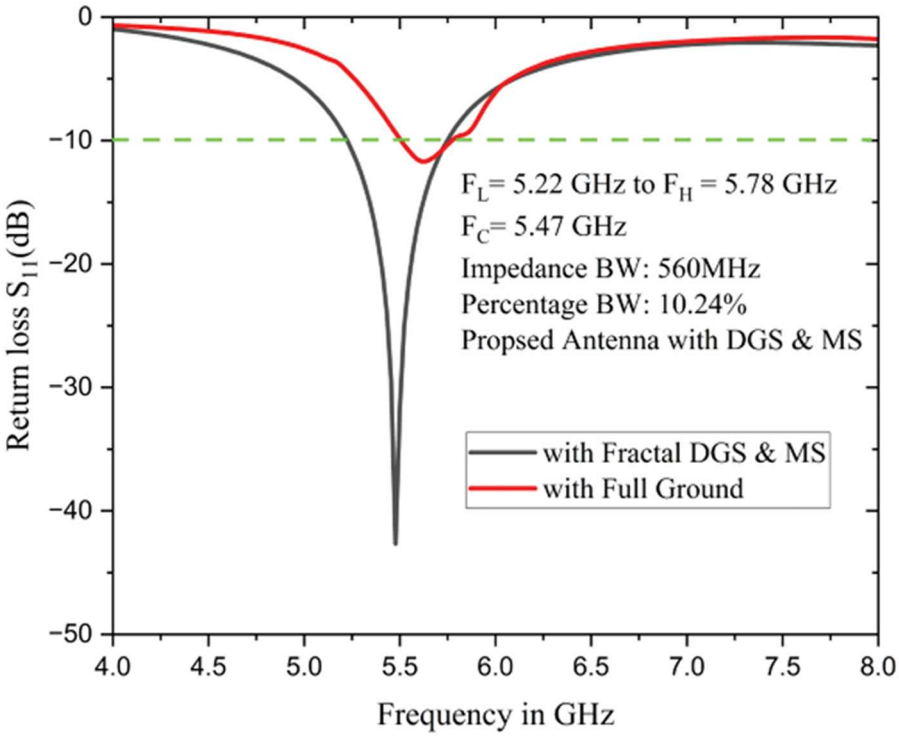


Figure 4.10. Return Loss Plot demonstrating impedance matching with full ground and with Fractal DGS and MS.

The antenna system was built for optimal performance, maintaining its impedance stability over the designated frequency range, as seen by the existence of such profound resonance nulls across the operating band. The system's resonant frequency behavior and current distribution demonstrate that fractal geometry design yields reliable outcomes. The characteristics of the system function as essential advantages for wireless communication systems that depend on their ability to control impedance and transmit signals effectively. The measured return loss results demonstrate that the antenna system effectively reduces energy losses while providing advanced communication capabilities, which require high-performance signal management.

4.3.3. Analysis of Voltage Standing Wave Ratio (VSWR)

The VSWR measurements provide a precise measurement of the antenna's ability to match impedance throughout the complete frequency range, which they investigated as shown in Figure 4.11. The VSWR curve shows optimal performance at the target operating frequencies with strongest results occurring at 5.47 GHz because the VSWR value approaches ideal conditions at approximately 1.0033. The extremely low VSWR value demonstrates that the antenna and feed line have achieved almost perfect impedance matching, which allows most input power to be radiated while only a tiny amount reflects back to the source.

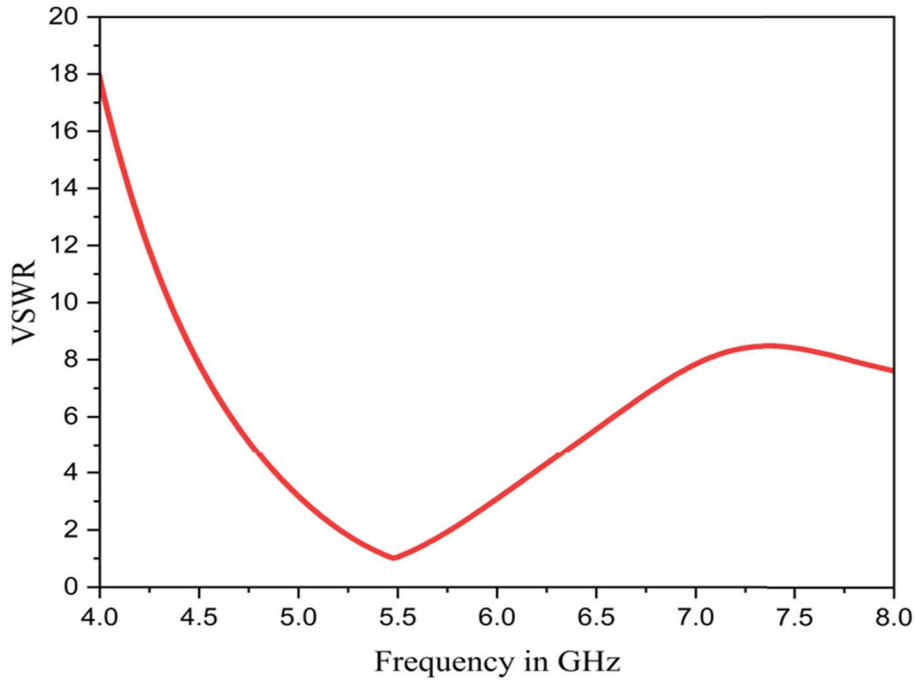


Figure 4.11. VSWR vs frequency plot.

The wireless communication system needs this particular feature to reach its maximum operational efficiency. The measured VSWR maintains its performance below the acceptable threshold of 2 throughout the entire frequency range which shows that the system maintains stable impedance matching across the antenna's operational bandwidth.

4.3.4. Interpretation of the Impedance plot

The impedance can show how well an antenna can send and receive signals at various frequencies. The measurements of the antenna at about 5.48 GHz show it has an impedance close to 1.0023 - 0.0024i Ohms (near zero), meaning there is very little reactive component compared to its real or resistive component; indicating that the antenna is matched perfectly

(i.e., not any energy lost due to mismatched impedances). The close proximity to an ideal resistive condition confirms this match and the overall quality of the antenna as an efficient radiator of electromagnetic energy (due primarily to its minimum reflections). It is also shown that there is very little phase lag present (about -46.5808°) confirming that there will be very little power loss by only being able to send the minimum amount of energy from the source into the antenna.

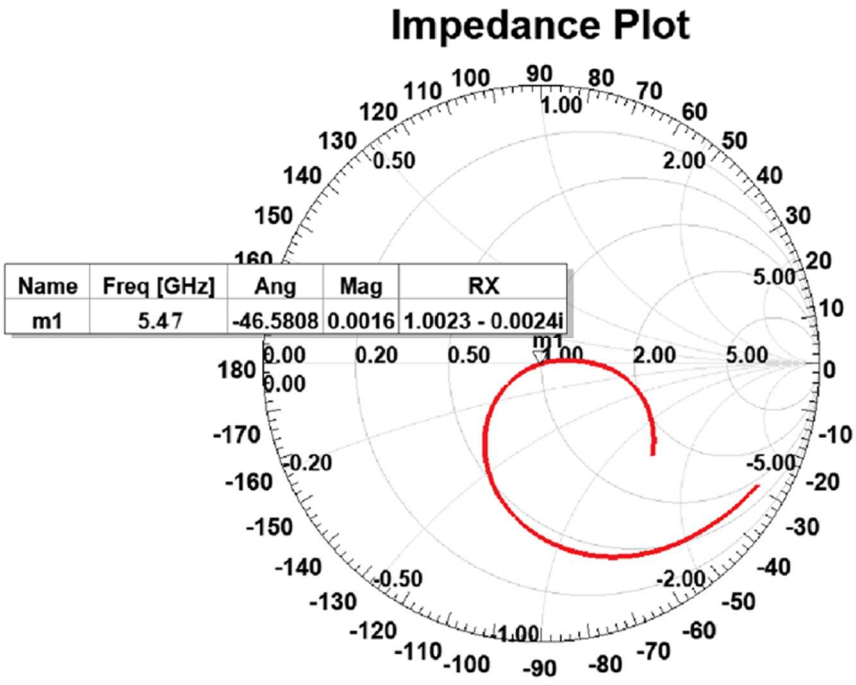


Figure 4.12. Impedance plot at the resonant frequency showing near-ideal antenna impedance with minimal reactive component and optimal resistive matching.

In RF systems, where dependable operation within the assigned frequency range and effective energy use are crucial criteria, such beneficial impedance behaviour is necessary to achieve optimal performance.

4.3.5. Analysis of Gain and Directivity Characteristics

As shown in Figure 4.13, the gain analysis provides crucial information on the fractal antenna's directional performance and radiation efficiency at different angles of incidence. By employing uniform scaling in the radiation pattern plots, a clearer comparative visualization across different planes is achieved. With a maximum value of 4.38 dB, the measured gain shows a significant range, suggesting that the antenna may effectively focus

electromagnetic energy in targeted directions. The antenna's directivity potential, which is essential for applications needing effective signal transmission and reception, is clearly highlighted by this peak gain.

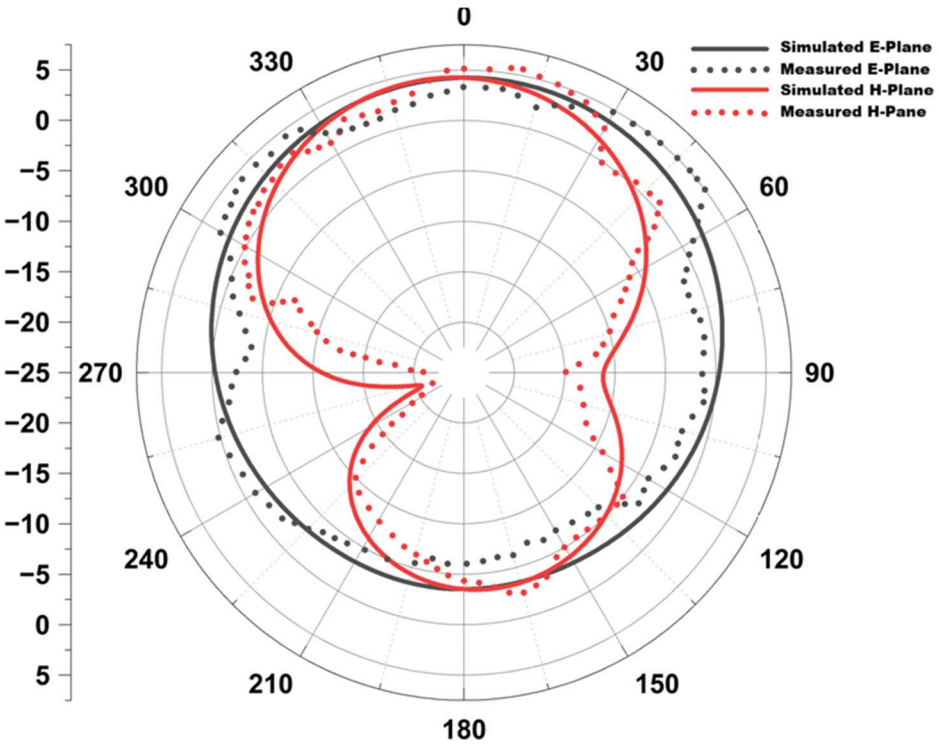


Figure 4.13. Simulated and measured radiation plots.

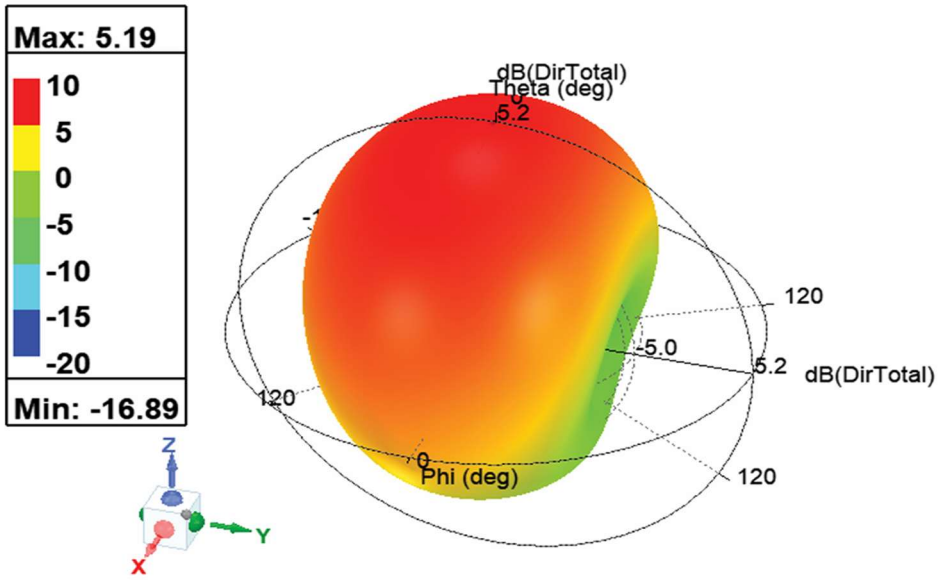


Figure 4.14. 3D directive plot indicating the fractal antenna's ability to focus energy, highlighting its peak and minimum directivity values across different angles.

Antenna behavior studies reveal that its high-gain areas function as proof of its energy focusing capability that extends its communication distance while enhancing signal reception. The gain plot displays multiple angular regions that measure negative values with a maximum drop to −17.71 dB, which indicates that the antenna emits less radiation power. The gain distribution visualization demonstrates its importance because it helps researchers comprehend how the antenna emits radiation while they determine ways to use it in real-world situations.

The Figure 4.14 directivity characteristics reveal that the antenna can direct its emitted power toward specific intended targets. The antenna demonstrates a maximum directivity value of 5.19 dBi that shows its capacity to boost power density when compared with an isotropic radiator. The design successfully achieves its intended purpose through beam steering at specific angles that produce peak results. The antenna demonstrates decreased performance in particular directions that are identified through regions that show low directivity to −16.89 dBi. Engineers need to understand all aspects of gain and directivity patterns to select the best antenna locations in complex spaces, which will help decrease interference while increasing communication efficiency.

4.3.6. Analysis of Radiation Efficiency

As seen in Figure 4.15, the fractal antenna's radiation efficiency measures the percentage of input power transformed into radiated electromagnetic energy when measured over the frequency range of 5.00–6.00 GHz.

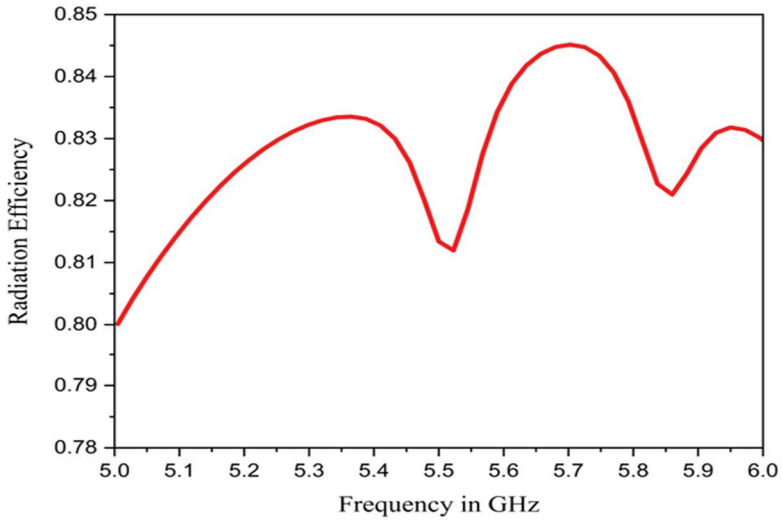


Figure 4.15 Radiation efficiency plot showing the proportion of input power effectively radiated across the frequency range

The findings show that a sizable amount of the given power is successfully radiated at 5.4775 GHz, with a maximum efficiency of roughly 82.88% (0.8288) at this frequency. Longer transmission lengths and more consistent signal quality are made possible by wireless communication systems' increased overall performance and decreased energy losses, which are made possible by such high radiation efficiency. At higher frequencies, efficiency gradually decreases, reaching lower levels close to 6.00 GHz. This could be a symptom of decreased performance or intrinsic design limitations in this frequency range. In Complete, the radiation efficiency profile verifies that the antenna functions efficiently within the designated spectrum and offers dependable power consumption for real-world uses.

4.3.7. Analysis of Radiation Efficiency

The radiation intensity profile which shows maximum radiation intensity (Max U) according to Figure 4.16 shows essential information about the fractal antenna's energy distribution and directional performance across the 5.00-6.00 GHz frequency range. The antenna emits the most power at 5.4775 GHz, as indicated by the plot's peak radiation intensity of 0.2181 at this frequency. The antenna demonstrates its ability to focus energy efficiently within this operational range through its initial rise to peak performance followed by its later decline.

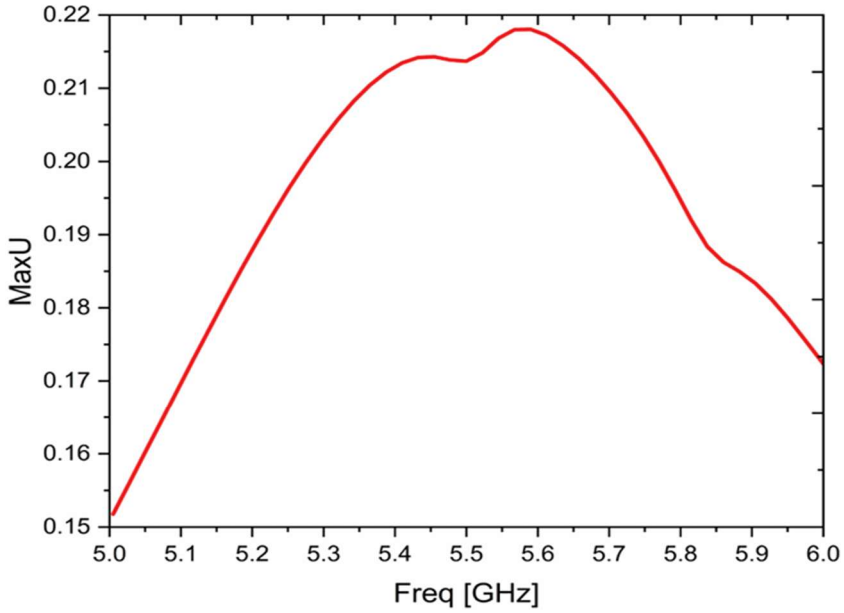


Figure 4.16. Radiation intensity plot showing the peak emission across the operational frequency range, highlighting the antenna's optimal operating frequency.

This behavior will be especially crucial for applications such as satellite communication systems and radar that need precise energy targeting or directional control. The reduction in radiation strength following the peak indicates the practical limits of the antenna's effective frequency range, showing that the antenna's capacity to efficiently direct radiated energy diminishes as frequency increases. The antenna's ability to concentrate electromagnetic power within the designated operating bandwidth is validated by this examination.

4.3.8. Comprehensive Discussion of Experimental Results

The experimental results from testing the fractal antenna that was developed to improve wireless network performance are presented in Table 4.2. The proposed antenna design methodology proves its effectiveness through the combination of measurement data and simulation results.

The return loss plots in Figure 4.17 compare VNA-measured data with simulation results. The dataset contains essential performance measurements that include gain, directivity, radiation intensity, efficiency, and power handling, which were thoroughly assessed throughout the 5.00 GHz to 6.00 GHz frequency range. These overlaid parameters consistently evaluate and verify that the antenna meets the strict requirements for high-frequency applications, including modern telecommunications and radar systems.

Table 4.2. Experimental assessment of antenna performance parameters.

Frequency (GHz)	Gain (dB)	Power (dBm)	Radiation Intensity	Efficiency (%)
5.00	4.50	28.90/28.10	0.1900	80.75
5.10	4.85	29.10/28.30	0.1950	81.00
5.20	5.10	29.30/28.50	0.2000	81.25
5.30	5.10	29.50/28.70	0.2050	81.50
5.40	5.15	29.70/28.90	0.2100	81.75
5.47	5.19	30.00/29.18	0.2181	82.88
5.50	5.10	29.85/29.05	0.2150	82.50
5.60	5.05	29.65/28.85	0.2100	82.25
5.70	4.00	29.45/28.65	0.2050	82.00
5.80	3.95	29.25/28.45	0.2000	81.75
5.90	3.15	29.05/28.25	0.1950	81.50
6.00	2.55	28.85/28.05	0.1900	81.25

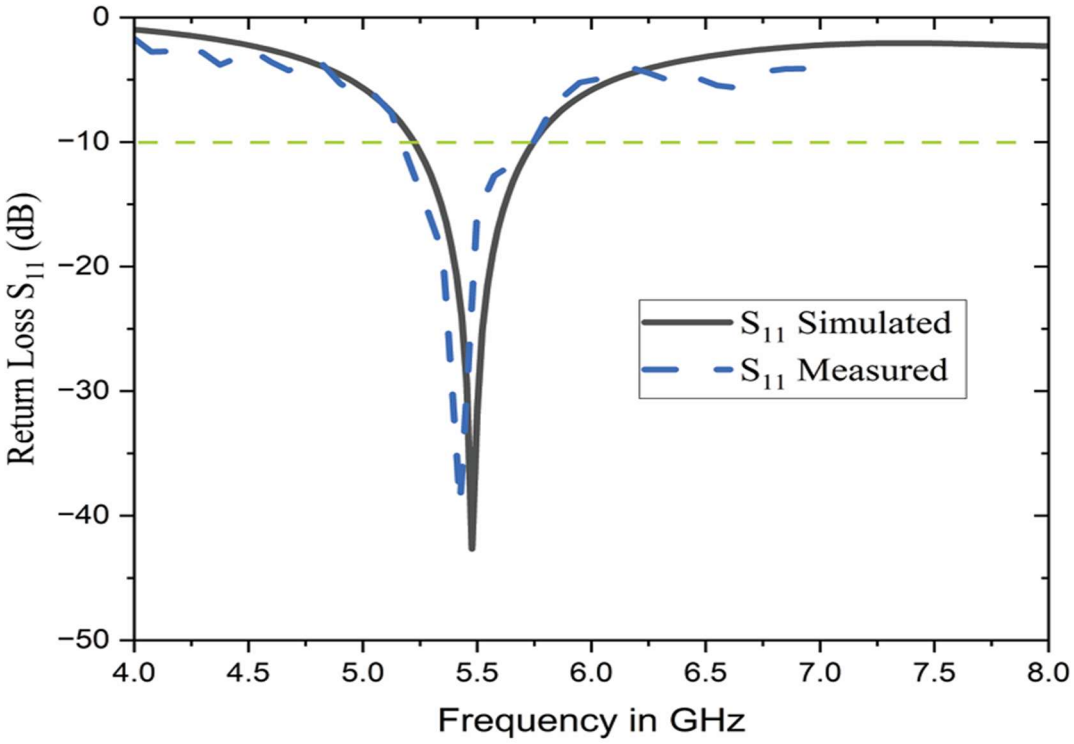


Figure 4.17. Return loss plots of simulated and measured in VNA

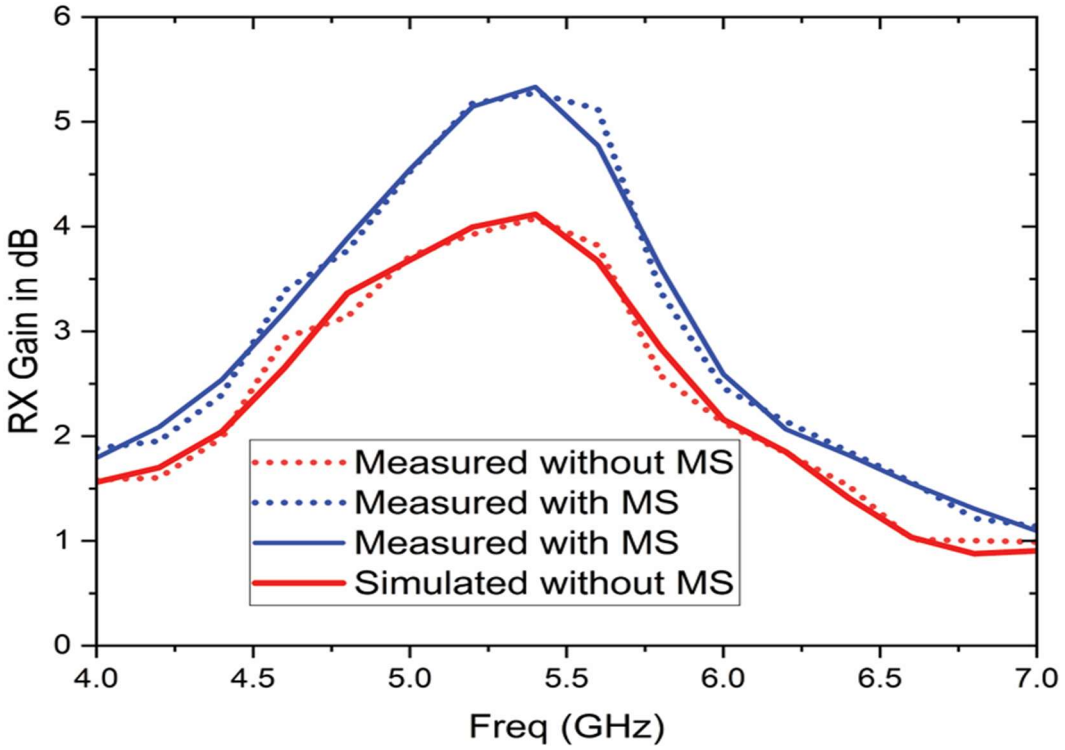


Figure 4.18. Simulated and measured gain plots with and without a metasurface

As indicated in Table 4.3, this antenna is very efficient when testing its performance. The best gain and directivity occur at 5.47 GHz with the maximum radiation intensity and efficiency. This shows the antenna has the capability to provide high levels of directional accuracy and transfer power effectively. As you go above this frequency, there is a progressive decrease in both gain and directivity as a result of the antenna's limited operational bandwidth; this is an important aspect for designers. Looking at the data in terms of just the performance characteristics will assist in optimizing the design of antennas while ensuring proper operation within the frequency bands. The findings further highlight how fractal antenna design is beneficial for modern wireless communication systems where high levels of efficiency and directional accuracy are critical. The data presented in this study have confirmed the concept of measured vs simulated performance, with only minor discrepancies due to real-world variables including substrate material properties, fabrication tolerances, and measurement uncertainties for instrument calibration and antenna alignment. The differences between the two sets of data fall below acceptable ranges, with a maximum estimate of ±0.2 dB for return loss and ±0.5 dB for gain. Therefore, none of these variables have a negative effect on the overall performance of the antenna. Further confirmation of the operational frequency range and the accuracy of the design can be seen in the strong correlations between the measured return loss and simulation return loss plots shown in Figure 4.17. The small frequency shifts result from the factory tolerances which affect both fractal geometry and DGS and from the minor changes in FR4 dielectric constant and from the impedance effects which result from SMA connector soldering.

The experimental research investigates how the metasurface affects the antenna gain. The experimental gain measurements demonstrate a clear enhancement when the metasurface is integrated with the fractal patch, as seen in Figure 4.18 The metasurface improves radiation characteristics without causing any negative effects on the antenna impedance bandwidth. The study demonstrates that using a fractal-based ground structure together with a metasurface produces a practical method which effectively improves antenna performance. The results of this study are contextualized through a performance comparison with recent fractal and metamaterial-inspired antenna designs which were published in existing literature, as shown in Figure 4.3.

Table 4.3. Performance comparison of the proposed metamaterial-inspired fractal antenna with existing literature.

Reference	Frequency Band	Bandwidth	Gain	Efficiency	Features
[93]	S, C, X band	100 MHz	6 dBi	Moderate	Wearable, DGS
[94]	C band	150 MHz	5 dBi	High	LAPO optimization
[95]	Multi-Band	100 MHz	4.37 dBi	High	Flexible, Minkowski structure
[96]	Multi-Band	120 MHz	7 dBi	High	Chrysanthemum-like structure
[97]	Satellite bands	80 MHz	3 dBi	Moderate	Triangular-shaped hexagonal
[98]	5G & Satellite bands	250 MHz	8 dBi	High	SRR-inspired, high-performance
[99]	Multi-Band	120 MHz	6.58 dBi	Moderate	Flower shaped with DGS, Compact
Proposed Antenna	C-band (5.22–5.78 GHz)	560 MHz	5.2 dBi	High	Compact, superior performance

Fractal antenna research continues to develop as an active research field because researchers have achieved major antenna performance enhancements through their work on geometric design and intelligent methods and miniaturization and metasurface technology and hybrid design approaches. The developments demonstrate how hybrid fractal metasurface systems function as essential components for upcoming wireless communication technology. The evaluation of the proposed antenna design requires assessment through fundamental design parameters which include operating frequency band and bandwidth and gain and efficiency. In summary, the evaluation of the star-shaped fractal antenna confirms its capacity for wireless C-band applications requiring compact antennas. The antenna has an excellent impedance bandwidth of 10.24%, a low return loss, near unity VSWR, moderate gain with greater directivity, and high radiation efficiency across the frequency range of 5.22–5.78 GHz. The metasurface superstrate will improve forward radiation performance by providing stable impedance matching with the star fractal patch and recursive Sierpinski DGS while substantially eliminating undesired surface currents; all

of these elements will combine to ensure reliable link performance and improved spectral flexibility for next-generation wireless and IoT systems. Agreement between simulated and measured data from this study indicates validation of the design methodology used and provides evidence for the practical applicability of this type of design approach. Although minor frequency shifts and minor variations in gain will occur, primarily resulting from the fixed superstrate and fabrication tolerances, the results demonstrate the feasibility of co-designing fractal geometries, customized DGS and metasurfaces with a simultaneous increase in gain, directivity, and matching. Future work should investigate the use of reconfigurable metasurfaces, expanded frequency scalability in the use of the antenna, and adaptive control of impedance to facilitate advancements in wireless antennas used in the next generation of wireless systems.

CHAPTER 5

CONCLUSION AND FUTURE WORK

5.1. Conclusion

Antenna architectures based on fractal and metamaterials provide excellent answers to meet the needs of future generations of wireless and IoT systems. Just as importantly, the results of the antenna designs validated experimentally together with recent literature (2022-2025) show that combining fractals and metasurfaces, metamaterials can increase performance in miniaturization, bandwidth, impedance matching, gain, and radiation efficiency compared to conventional microstrip patch antennas. The literature review presented (2022–2025) indicates that fractal–metamaterial antennas have consistently achieved compact sizes of 30% to 60% smaller than standard patch antennas, multiband and ultra-wideband characteristics (sub-6 GHz to the millimeter-wave bands), and improved gain of typically between 2 and 5 dB compared with standard patch antennas. All of these characteristics address the needs of IoT devices, which must be small, work with multiple standards, and conserve energy while operating. Based upon these findings, the proposed asymmetrical star shaped fractal antenna with integrated split-ring resonators (SRR) based metasurface demonstrates stable impedance matching, with a return loss of less than −10 dB measured across the frequency range from 4.5 to 10 GHz. A strong, well-defined resonance was obtained at 5.2 GHz, with directivity and radiation efficiency outperforming an equivalent conventional patch antenna on an FR4 substrate. The metasurface design achieves better radiation performance through its surface wave suppression and impedance matching enhancement techniques that maintain the original antenna dimensions. The performance-enhanced star fractal antenna reaches its maximum performance through the combination of its Sierpinski triangle fractal defective ground structure (DGS) and rectangular SRR (R-SRR) metasurface superstrate. The double-fractal system operates at a frequency range that extends from 5.22 GHz to 5.78 GHz which results in a 10.24% measured fractional bandwidth. The antenna shows significant improvements in gain and directivity performance throughout the C-band frequency range while its size remains small and its impedance matching stays effective. The proposed design method demonstrates dependable design

results because simulated results match anechoic chamber test measurements. The study demonstrates that fractal metamaterial antennas provide wideband performance, with return loss below -10 dB and increased gain, enabling their use in mid-band wireless communication, IoT devices, and advanced smart systems. However, it is vital to acknowledge specific experimental limitations, particularly the dielectric losses associated with the FR4 substrate at higher frequencies and the constraint that validation was limited to a controlled anechoic chamber environment. Despite these limitations, the research demonstrates that fractal metamaterial antenna technology offers an environmentally friendly approach to high-performance antenna design, significantly expanding design possibilities compared to traditional antenna structures.

5.2. Future Work

- Using active components like PIN diodes, varactor diodes, or RF MEMS switches, future research will concentrate on incorporating dynamic reconfiguration methods in metamaterial inspired fractal antennas. In order to support adaptive and multi standard wireless systems, this will allow for real time control of the operating frequency, radiation pattern, and polarization.
- Upcoming research will focus on expanding the fractal metamaterial antennas' operational bandwidth toward ultra wideband performance while preserving their small size, consistent radiation properties, and effective impedance matching throughout the whole frequency range.
- To create adjustable and selective frequency bands, research will investigate the creation of frequency-selective and multi-resonant metamaterial unit cells. This will increase spectrum efficiency by enabling antennas to dynamically activate or suppress particular bands according to application requirements.
- To concurrently accomplish bandwidth management, gain enhancement, and interference reduction, future research may entail the creation of innovative metasurface designs with tunable and multifunctional unit cells.
- To enable intelligent and context-aware antenna systems for next-generation wireless and Internet of Things applications, it may be possible to integrate intelligent control and optimization algorithms to automatically modify antenna settings.

REFERENCES

[1] Q. V. Khanh, N. V. Hoai, L. D. Manh, A. N. Le, and G. Jeon, “Wireless communication technologies for IoT in 5G: Vision, applications, and challenges,” Wireless Communications and Mobile Computing, vol. 2022, article no. 3229294, 2022, doi: 10.1155/2022/3229294.

[2] M. Z. Chowdhury, M. Shahjalal, M. K. Hasan, and Y. M. Jang, “The role of optical wireless communication technologies in 5G/6G and IoT solutions: Prospects, directions, and challenges,” *Applied Sciences*, vol. 9, no. 20, p. 4367, 2019, doi: 10.3390/app9204367.

[3] H. B. Celebi, A. Pitarokoilis, and M. Skoglund, “Wireless communication for the industrial IoT,” in Industrial IoT: Challenges, Design Principles, Applications, and Security, Cham, Switzerland: Springer International Publishing, 2020, pp. 57–94, doi: 10.1007/978-3-030-42500-5_2.

[4] B. Sapkota, R. Ghimire, P. Pujara, S. Ghimire, U. Shrestha, R. Ghimire, et al., “5G network deployment planning using metaheuristic approaches,” Telecom, vol. 5, no. 3, pp. 588–608, Jul. 2024, doi: 10.3390/telecom5030030.

[5] F. Rinaldi, A. Raschella, and S. Pizzi, “5G NR system design: A concise survey of key features and capabilities,” Wireless Networks, vol. 27, no. 8, pp. 5173–5188, 2021, doi: 10.1007/s11276-021-02811-y.

[6] A. I. Zreikat, Z. AlArnaout, A. Abadleh, E. Elbasi, and N. Mostafa, “The integration of the Internet of Things (IoT) applications into 5G networks: A review and analysis,” Computers, vol. 14, no. 7, p. 250, 2025, doi: 10.3390/computers14070250.

[7] S. Khan, T. Mazhar, T. Shahzad, A. Bibi, W. Ahmad, M. A. Khan, *et al*., “Antenna systems for IoT applications: a review,” *Discover Sustainability*, vol. 5, no. 1, p. 412, 2024, doi: 10.1007/s43621-024-00638-z.

[8] A. Hassan, N. Nizam-uddin, A. Quddus, S. R. Hassan, S. Bharany, A. U. Rehman, and S. Hussen, “Design strategies and performance of IoT antennas: A comprehensive review,” Discover Computing, vol. 28, no. 1, p. 39, 2025, doi: 10.1007/s10791-025-09536-y.

[9] S. Koziel, A. Pietrenko-Dabrowska, and U. Ullah, “Global miniaturization of broadband antennas by prescreening and machine learning,” Scientific Reports, vol. 14, no. 1, p. 29427, 2024, doi: 10.1038/s41598-024-80182-y.

[10] K. Aliqab, I. Nadeem, and S. R. Khan, “A comprehensive review of in-body biomedical antennas: Design, challenges and applications,” Micromachines, vol. 14, no. 7, p. 1472, 2023, doi: 10.3390/mi14071472.

[11] D. Gopinath and P. Marichamy, “On the design and analysis of multi-band micro-strip patch antenna for wireless body area network applications,” EURASIP Journal on Wireless Communications and Networking, vol. 2025, no. 1, p. 13, 2025, doi: 10.1186/s13638-025-02442-3.

[12] H. Mallani, A. Agrawal, and R. K. Saraswat, “Implementation of fractal metamaterial inspired antenna for multi-standard wireless applications,” Progress In Electromagnetics Research B, vol. 108, p. 2024, doi: 10.2528/PIERB24072905.

[13] Vijay, S., & Chauhan, B. (2021). Antenna miniaturization for IoT applications. Next-Generation Antennas: Advances and Challenges, 105-117. DOI:10.1002/9781119792765.ch6

[14] S. Malisuwan, “Challenges, opportunities, and future research in the integration of 5G/6G networks, LEO satellites, and IoT for environmental protection and sustainable development at ECSTAR,” Journal of Environmental Science and Engineering B, vol. 12, pp. 146–159, 2023, doi: 10.17265/2162-5263/2023.03.005.

[15] M. N. A. Siddiky, M. E. Rahman, and M. S. Uzzal, “Beyond 5G: A comprehensive exploration of 6G wireless communication technologies,” preprint, May 2024, doi: 10.20944/preprints202405.0715.v1.

[16] A. J. Alqaraghuli, J. V. Siles, and J. M. Jornet, “The road to high data rates in space: Terahertz versus optical wireless communication,” IEEE Aerospace and Electronic Systems Magazine, vol. 38, no. 6, pp. 4–13, 2023, doi: 10.1109/MAES.2023.3243584.

[17] H. Shah, “Millimeter-wave mobile communication for 5G,” International Journal of Transcontinental Discoveries, vol. 5, no. 1, pp. 68–74, Jul. 2018. Available: https://internationaljournals.org/index.php/ijtd/article/view/102

[18] D. H. Devi, K. Duraisamy, A. Armghan, M. Alsharari, K. Aliqab, V. Sorathiya, et al., “5G technology in healthcare and wearable devices: A review,” Sensors, vol. 23, no. 5, p. 2519, 2023, doi: 10.3390/s23052519.

[19] A. Al Ka'bi, "Proposed antenna design for IoT and 5G-WiFi applications," in 2022 IEEE World AI IoT Congress (AIIoT), Jun. 2022, pp. 786–790, doi: 10.1109/AIIoT54504.2022.9817261.

[20] N. Kishore and A. Senapati, "5G smart antenna for IoT application: A review," International Journal of Communication Systems, vol. 35, no. 13, p. e5241, 2022, doi: 10.1002/dac.5241.

[21] M. Alibakhshikenari, E. M. Ali, M. Soruri, M. Dalarsson, M. Naser-Moghadasi, B. S. Virdee, et al., "A comprehensive survey on antennas on-chip based on metamaterial, metasurface, and substrate integrated waveguide principles for millimeter-waves and terahertz integrated circuits and systems," IEEE Access, vol. 10, pp. 3668–3692, 2022, doi: 10.1109/ACCESS.2021.3140156.

[22] M. Alibakhshikenari, B. S. Virdee, A. A. Althuwayb, D. Mariyanayagam, and E. Limiti, "Compact and low-profile on-chip antenna using underside electromagnetic coupling mechanism for terahertz front-end transceivers," Electronics, vol. 10, no. 11, p. 1264, 2021, doi: 10.3390/electronics10111264.

[23] A. A. Althuwayb, "On-chip antenna design using the concepts of metamaterial and SIW principles applicable to terahertz integrated circuits operating over 0.6–0.622 THz," International Journal of Antennas and Propagation, vol. 2020, article no. 6653095, 2020, doi: 10.1155/2020/6653095.

[24] Y. S. Gurbet and S. Doğu, "Comprehensive review of Ku, K, and Ka band antenna designs: Applications in CubeSats," International Journal of Aeronautical and Space Sciences, pp. 1–50, 2025, doi: 10.1007/s42405-025-00989-5.

[25] Y. Huang, J. Zhang, X. Li, Z. Qi, F. Lu, H. Jiang, et al., "A low-profile dual-polarized high-gain low cross-polarization phased array for Ku-band satellite communications," Sensors, vol. 25, no. 13, p. 3986, 2025, doi: 10.3390/s25133986.

[26] Y. Wang, F. P. Sun, and X. Wang, "Defensive performance evaluation methods of the GNSS for satellite navigation countermeasures," IEEE Access, vol. 12, pp. 51719–51739, 2024, doi: 10.1109/ACCESS.2024.3373057.

[27] F. Mehmood and A. Mehmood, "Recent advancements in millimeter-wave antennas and arrays: From compact wearable designs to beam-steering technologies," Electronics, vol. 14, no. 13, p. 2705, 2025, doi: 10.3390/electronics14132705.

[28] W. Jiang, Q. Zhou, J. He, M. A. Habibi, S. Melnyk, M. El-Absi, et al., "Terahertz communications and sensing for 6G and beyond: A comprehensive review," IEEE

Communications Surveys & Tutorials, vol. 26, no. 4, pp. 2326–2381, 2024, doi: 10.1109/COMST.2024.3385908.

[29] V. Godase, "Graphene-Based Nano-Antennas for Terahertz Communication," International Journal of Digital Electronics and Microprocessor Technology, vol. 1, no. 2, pp. 1–14, 2025. Available: https://matjournals.net/engineering/index.php/IJDEMT/article/view/2268

[30] W. Li, D. Li, K. Zhou, Q. Fu, X. Yuan, and X. Zhu, "A survey of antenna miniaturization technology based on the new mechanism of acoustic excitation," IEEE Transactions on Antennas and Propagation, vol. 71, no. 1, pp. 263–274, 2023, doi: 10.1109/TAP.2022.3220663.

[31] D. S. Kumar and S. Suganthi, "Antenna array miniaturization using a defected ground structure," Trends in Sciences, vol. 19, no. 13, p. 4634, 2022, doi: 10.48048/tis.2022.4634.

[32] K. Ramahatla, M. Mosalaosi, A. Yahya, and B. Basutli, "Multiband reconfigurable antennas for 5G wireless and CubeSat applications: A review," IEEE Access, vol. 10, pp. 40910–40931, 2022, doi: 10.1109/ACCESS.2022.3166223.

[33] O. Benkhadda, M. Saih, A. Reha, S. Ahmad, K. Chaji, H. Singh, and A. J. A. Al-Gburi, "A miniaturized reconfigurable antenna for modern wireless applications with broadband and multi-band capabilities," Progress In Electromagnetics Research M, vol. 127, pp. 93–101, 2024, doi: 10.2528/PIERM24042801.

[34] D. Sarkar, T. Khan, F. A. Talukdar, and Y. M. Antar, "Computational intelligence paradigms for UWB antennas: A comprehensive review of analysis, synthesis and optimization," Artificial Intelligence Review, vol. 56, no. 1, pp. 655–684, 2023, doi: 10.1007/s10462-022-10181-w.

[35] L. Matta, B. Sharma, and M. Sharma, "A review on bandwidth enhancement techniques and band-notched characteristics of MIMO-ultra wide band antennas," Wireless Networks, vol. 30, no. 3, pp. 1339–1382, 2024, doi: 10.1007/s11276-023-03586-0.

[36] Y. Sun, B. Cai, L. Yang, L. Wu, Y. Cheng, H. Luo, et al., "High-gain dual-polarization microstrip antenna based on transmission focusing metasurface," Materials, vol. 17, no. 15, p. 3730, 2024, doi: 10.3390/ma17153730.

[37] H. Soh and N. Keljovic, "Development of highly reconfigurable antennas for control of operating frequency, polarization, and radiation characteristics for 5G and 6G

systems," National Journal of Antennas and Propagation, vol. 6, no. 1, pp. 31–39, 2024, doi: 10.31838/NJAP/06.01.05.

[38] T. Nivethitha, A. K. Kumar, and P. K. Poonguzhali, "Fractal antennas in medicine: A comprehensive review of design, performance, and medical applications," in Antennas for Industrial and Medical Applications with Optimization Techniques for Wireless Communication, pp. 70–95, 2024, doi: 10.1201/9781003560487-5.

[39] F. Venneri, S. Costanzo, and A. Borgia, "Fractal metasurfaces and antennas: An overview for advanced applications in wireless communications," Applied Sciences, vol. 14, no. 7, p. 2843, 2024, doi: 10.3390/app14072843.

[40] R. Amrutha and R. Gayathri, "Investigation on mathematical modeling of fractal geometry using IFS for microstrip antenna," in 2022 6th International Conference on Electronics, Communication and Aerospace Technology (ICECA), Dec. 2022, pp. 109–115, doi: 10.1109/ICECA55336.2022.10009507.

[41] J. Patiño Ortiz, M. Patiño Ortiz, M. Á. Martínez-Cruz, and A. S. Balankin, "A brief survey of paradigmatic fractals from a topological perspective," Fractal and Fractional, vol. 7, no. 8, p. 597, 2023, doi: 10.3390/fractalfract7080597.

[42] S. Mathew and V. S. Ponnapalli, "Fractal geometry based antennas and arrays: A review," International Journal of Student Project Reporting, vol. 1, no. 3, pp. 232–260, 2023, doi: 10.1504/IJSPR.2023.132516.

[43] O. Elalaouy, M. El Ghzaoui, and J. Foshi, "Enhancing antenna performance: A comprehensive review of metamaterial utilization," Materials Science and Engineering: B, vol. 304, p. 117382, 2024, doi: 10.1016/j.mseb.2024.117382.

[44] A. Manwar, T. Bhongade, P. Kulkarni, A. Satdive, S. Tayde, B. Toksha, et al., "Insights and applications of double positive medium metamaterials," in Electromagnetic Metamaterials: Properties and Applications, pp. 85–99, 2023, doi: 10.1002/9781394167074.ch4.

[45] K. Anusha, D. Mohanageetha, K. H. Priya, A. S. Harini, and M. Naveena, "Performance analysis of CSRR and SRR structure incorporated multiband slotted antenna," in 2022 3rd International Conference on Electronics and Sustainable Communication Systems (ICESC), Aug. 2022, pp. 278–283, doi: 10.1109/ICESC54411.2022.9885708.

[46] K. Yang, Y. Liang, H. C. Zhang, and G. Feng, "On-chip SRR and CSRR for millimeter-wave integrated systems: Review and applications," Microelectronics Journal, vol. 131, p. 105664, 2023, doi: 10.1016/j.mejo.2022.105664.

[47] A. Valipour, M. H. Kargozarfard, M. Rakhshi, A. Yaghootian, and H. M. Sedighi, "Metamaterials and their applications: An overview," Proceedings of the Institution of Mechanical Engineers, Part L: Journal of Materials: Design and Applications, vol. 236, no. 11, pp. 2171–2210, 2022, doi: 10.1177/146442072199585.

[48] W. Yang, J. Li, D. Chen, Y. Cao, Q. Xue, and W. Che, "Advanced metasurface-based antennas: A review," IEEE Open Journal of Antennas and Propagation, vol. 5, pp, 2024, doi: 10.1109/OJAP.2024.3465513.

[49] L. Shi, Z. Wu, H. Liu, and L. Li, "Analysis and applications of electromagnetic bandgap metasurfaces," in Electromagnetic Metamaterials and Metasurfaces: From Theory to Applications, Singapore: Springer Nature Singapore, 2024, pp. 111–150, doi: 10.1007/978-981-99-7914-1_4.

[50] F. E. Zerrad and M. Taouzari, "Frequency selective surfaces (FSSs) in metamaterials," in Advanced Metamaterials for Engineers, Bristol, UK: IOP Publishing, 2023, ch. 6, pp. 6-1, doi: 10.1088/978-0-7503-5754-8ch6.

[51] S. A. Soliman, E. M. El-Desouki, S. M. El-Nady, and A. S. Abd El-Hameed, "Broadband low RCS based on polarization-dependent artificial magnetic conductor metasurface," IEEE Access, vol. 11, pp. 53176–53184, 2023, doi: 10.1109/ACCESS.2023.3280126.

[52] A. Ezhumalai, N. Ganesan, and S. Balasubramaniyan, "An extensive survey on fractal structures using iterated function system in patch antennas," International Journal of Communication Systems, vol. 34, no. 15, p. e4932, 2021, doi: 10.1002/dac.4932.

[53] A. Chinnamuthu, N. Iruthayanathan, S. Ramprabhu, R. V. Arjunan, and T. Shailesh, "Fractal-based compact quad-port THz MIMO antenna with ultra-wideband and high isolation for 6G and TWPAN applications," Scientific Reports, vol. 15, no. 1, p. 35670, 2025, doi: 10.1038/s41598-025-19595-2.

[54] S. H. Ghadeer, S. K. A. Rahim, M. Alibakhshikenari, B. S. Virdee, T. A. Elwi, A. Iqbal, and M. Al-Hasan, "An innovative fractal monopole MIMO antenna for modern 5G applications," AEU - International Journal of Electronics and Communications, vol. 159, p. 154480, 2023, doi: 10.1016/j.aeue.2022.154480.

[55] M. Kaur and J. S. Sivia, "ANN and FA based design of hybrid fractal antenna for ISM band applications," Progress in Electromagnetics Research C, vol. 98, pp. 127–140, 2020, doi: 10.2528/PIERC19110901.

[56] A. I. Imran, T. A. Elwi, and A. J. Salim, "On the distortionless of UWB wearable Hilbert-shaped metamaterial antenna for low energy applications," Progress In

Electromagnetics Research M, vol. 101, pp. 219–239, 2021, doi: 10.2528/PIERM20113008.

[57] A. Mohanty and S. Sahu, “Compact wideband hybrid fractal antenna loaded on AMC reflector with enhanced gain for hybrid wireless cellular networks,” AEU-International Journal of Electronics and Communications, vol. 138, p. 153837, 2021, doi: 10.1016/j.aeue.2021.153837.

[58] M. Naderi, F. B. Zarrabi, F. S. Jafari, and S. Ebrahimi, “Fractal EBG structure for shielding and reducing the mutual coupling in microstrip patch antenna array,” AEU-International Journal of Electronics and Communications, vol. 93, pp. 261–267, 2018, doi: 10.1016/j.aeue.2018.06.028.

[59] H. Rajabloo, V. A. Kooshki, and H. Oraizi, “Compact microstrip fractal Koch slot antenna with ELC coupling load for triple band application,” AEU-International Journal of Electronics and Communications, vol. 73, pp. 144–149, 2017, doi: 10.1016/j.aeue.2016.12.027.

[60] N. Kaur, J. S. Sivia, and M. Kumar, “SRR and rectangular stubs loaded novel fractal antenna realization for multiband wireless applications,” Wireless Personal Communications, vol. 120, no. 1, pp. 515–533, 2021, doi: 10.1007/s11277-021-08472-6.

[61] H. Hussein, F. Atasoy, and T. A. Elwi, “Miniaturized antenna array-based novel metamaterial technology for reconfigurable MIMO systems,” Sensors, vol. 23, no. 13, p. 5871, 2023, doi: 10.3390/s23135871.

[62] M. Ameen and R. Chaudhary, “Metamaterial circularly polarized antennas: Integrating an epsilon negative transmission line and single split ring-type resonator,” IEEE Antennas and Propagation Magazine, vol. 63, no. 4, pp. 60–77, 2020, doi: 10.1109/MAP.2019.2950920.

[63] N. Sharma and S. S. Bhatia, “Split ring resonator based multiband hybrid fractal antennas for wireless applications,” AEU-International Journal of Electronics and Communications, vol. 93, pp. 39–52, 2018, doi: 10.1016/j.aeue.2018.05.035.

[64] S. S. Al-Bawri, H. Hwang Goh, M. S. Islam, H. Y. Wong, M. F. Jamlos, A. Narbudowicz, et al., “Compact ultra-wideband monopole antenna loaded with metamaterial,” Sensors, vol. 20, no. 3, p. 796, 2020, doi: 10.3390/s20030796.

[65] S. Douhi, Y. Houssaini, S. Das, V. Subramanian, B. T. P. Madhav, M.’hammed Mazroui, and A. Eddiai, “Metamaterial-integrated wearable UWB antenna with SAR reduction and gain enhancement for Wireless Body Area Sensor Networks

(WBASNs): Design and experimental verification," Sensors and Actuators A: Physical, vol. 388, p. 116499, 2025, doi: 10.1016/j.sna.2025.116499.

[66] F. Ez-Zaki, H. Belahrach, A. Ghammaz, S. Ahmad, A. Khabba, K. Ait Belaid, et al., "Double negative (DNG) metamaterial-based Koch fractal MIMO antenna design for sub-6-GHz V2X communication," IEEE Access, vol. 11, pp. 77620–77635, 2023, doi: 10.1109/ACCESS.2023.3296599.

[67] M. Alibakhshikenari, M. Khalily, B. S. Virdee, C. H. See, R. A. Abd-Alhameed, and E. Limiti, "Mutual coupling suppression between two closely placed microstrip patches using EM-bandgap metamaterial fractal loading," IEEE Access, vol. 7, pp. 23606–23614, 2019, doi: 10.1109/ACCESS.2019.2899326.

[68] I. Aggarwal, S. Pandey, and M. R. Tripathy, "A high gain super wideband metamaterial based antenna," Journal of Microwaves, Optoelectronics and Electromagnetic Applications, vol. 20, pp. 248–273, 2021, doi: 10.1590/2179-10742021v20i21147.

[69] V. V. Reddy, "Metamaterial loaded circularly polarized fractal antenna for 2.4 GHz frequency applications," IETE Journal of Research, vol. 69, no. 6, pp. 3573–3582, 2023, doi: 10.1080/03772063.2021.1920851.

[70] M. H. Reddy, D. Sheela, V. K. Parbot, and A. Sharma, "A compact metamaterial inspired UWB-MIMO fractal antenna with reduced mutual coupling," Microsystem Technologies, vol. 27, no. 5, pp. 1971–1983, 2021, doi: 10.1007/s00542-020-05024-z.

[71] S. Tariq, A. A. Rahim, W. T. Sethi, F. Faisal, and T. Djerafi, "Metasurface based antenna array with improved performance for millimeter wave applications," AEU-International Journal of Electronics and Communications, vol. 177, p. 155195, 2024, doi: 10.1016/j.aeue.2024.155195.

[72] M. G. Rangula, P. Paul, B. Majumder, and K. Kandasamy, "An ultra-broadband polarization conversion metasurface for enhanced stealth and RCS mitigation in MIMO configurations," AEU-International Journal of Electronics and Communications, vol. 196, p. 155793, 2025, doi: 10.1016/j.aeue.2025.155793.

[73] A. Sabban, "Novel meta-fractal wearable sensors and antennas for medical, communication, 5G, and IoT applications," Fractal and Fractional, vol. 8, no. 2, p. 100, 2024, doi: 10.3390/fractalfract8020100.

[74] R. K. Saraswat, “A hybrid fractal metamaterial inspired multiband antenna for wireless applications,” Wireless Personal Communications, vol. 124, no. 3, pp. 2593–2612, 2022, doi: 10.1007/s11277-022-09480-w.

[75] M. Elhabchi, M. N. Srifi, and R. Touahni, “A fractal metamaterial antenna for Bluetooth, WLAN, WiMAX and X-band applications,” in 2020 International Conference on Intelligent Systems and Computer Vision (ISCV), Jun. 2020, pp. 1–5, doi: 10.1109/ISCV49265.2020.9204208.

[76] N. F. Habib, A. G. Wadday, and F. M. Ali, “Circular fractal slot antenna with metasurface for satellite communication,” in AIP Conference Proceedings, vol. 2290, no. 1, p. 050046, Dec. 2020, doi: 10.1063/5.0027412.

[77] H. Sudarsan, R. Gayathri, and K. Mahendran, “A novel square fractal dual port MIMO antenna with tri-band rejection capabilities,” Journal of Ambient Intelligence and Humanized Computing, pp. 1–18, 2021, doi: 10.1007/s12652-021-03035-w.

[78] A. N. Bespalov, A. L. Buzov, D. S. Klyuev, and A. M. Neshcheret, “Research of antenna complexes using chiral metamaterials and fractal geometry of radiators for MIMO systems,” Физика волновых процессов и радиотехнические системы, vol. 23, no. 4, pp. 97–110, 2020, doi: 10.18469/1810-3189.2020.23.4.97-110.

[79] S. Costanzo and F. Venneri, “Polarization-insensitive fractal metamaterial surface for energy harvesting in IoT applications,” Electronics, vol. 9, no. 6, p. 959, 2020, doi: 10.3390/electronics9060959.

[80] F. Venneri, S. Costanzo, A. Borgia, and G. Buonanno, “Fractal metamaterial surfaces for UHF sensing applications,” IEEE Access, vol. 12, pp. 65810–65824, 2024, doi: 10.1109/ACCESS.2024.3398537.

[81] S. Manoharan, P. Ramasamy, and R. Singaravelu, “A quad-band fractal antenna with metamaterial resonator-backed ground for sub-6 GHz, C and X band applications,” Applied Physics A, vol. 127, no. 9, p. 703, 2021, doi: 10.1007/s00339-021-04862-6.

[82] P. Iyampalam and I. Ganesan, “Metamaterial inspired penta-band decagon fractal antenna for wireless applications,” e-Prime-Advances in Electrical Engineering, Electronics and Energy, vol. 6, p. 100358, 2023, doi: 10.1016/j.prime.2023.100358.

[83] P. Wang, G. Xu, B. Yin, and W. Wang, “Dual-Band Dual-Circularly Polarized Tensor Holographic Metasurface Antenna for IoV Sensing and Communications,” IEEE Internet Things J., vol. 12, no. 10, pp. 14447-14455, 2025, doi: 10.1109/jiot.2024.3525176.

[84] S. Rajpoot, S. Ghosh, and M. V. Swati, ”A Low-Profile, Aperture-Coupled, Diagonal Square Fractal Antenna for Dual-Band Vehic ular Communication,” International Journal of Communication Systems, vol. 38, no. 1, Jan. 2025, doi: 10.1002/dac.70003.

[85] S. K. Budarapuand M. S. Sunder, “A Wide Band Circularly Polarized Antenna Using Meta Surface for Wi-Fi Applications,” Physica Scripta, vol. 100, no. 3, Jan. 2025, doi: 10.1088/1402-4896/adae40.

[86] S. V. Pande, D. Patil, A. Kumar, A. Tyavlovsky, and A. Muthanna, “Design of a Metasurface Loaded with RF Varactor and PIN Diode Integration Dual-Band Reconfigurable Antenna,” Physica Scripta, vol. 100, no. 2, Jan. 2025, doi: 10.1088/1402-4896/adac15.

[87] A. M. Silaghi, F. Mir, A. De Sabata, and L. Matekovits, “Design and experimental validation of a switchable frequency selective surface with incorporated control network,” Sensors, vol. 23, no. 9, p. 4561, 2023, doi: 10.3390/s23094561.

[88] M. K. Emara, D. Kundu, K. Macdonell, L. M. Rufail, and S. Gupta, “Coupled resonator-based metasurface reflector with enhanced magnitude and phase coverage,” IEEE Transactions on Antennas and Propagation, vol. 72, no. 1, pp. 901–914, 2024, doi: 10.1109/TAP.2023.3332436.

[89] K. Pitra, Z. Raida, and J. Lacik, “Low-profile circularly polarized antenna exploiting Fabry-Perot resonator principle,” Radioengineering, vol. 24, no. 4, pp. 898, 2015, doi: 10.13164/re.2015.0898.

[90] H. Umair, T. B. A. Latef, Y. Yamada, T. Hassan, W. N. L. B. W. Mahadi, M. Othman, et al., “Quarter wavelength Fabry–Perot cavity antenna with wideband low monostatic radar cross section and off-broadside peak radiation,” Applied Sciences, vol. 11, no. 3, p. 1053, 2021, doi: 10.3390/app11031053.

[91] C. Ni, C. Liu, Z. Zhang, M. Chen, L. Zhang, and X. Wu, “Design of broadband high gain polarization reconfigurable Fabry-Perot cavity antenna using metasurface,” Frontiers in Physics, vol. 8, p. 316, 2020, doi: 10.3389/fphy.2020.00316.

[92] X. Sheng, X. Lu, N. Liu, and Y. Liu, “Design of broadband high-gain Fabry–Pérot antenna using frequency-selective surface,” Sensors, vol. 22, no. 24, p. 9698, 2022, doi: 10.3390/s22249698.

[93] S. S. Sran and J. S. Sivia, “ANN and IFS based wearable hybrid fractal antenna with DGS for S, C and X band application,” AEU - International Journal of Electronics and Communications, vol. 127, p. 153425, 2020, doi: https://doi.org/10.1016/j.aeue.2020.153425.

[94] R. Anand and P. Chawla, “Optimization of inscribed hexagonal fractal slotted microstrip antenna using modified lightning attachment procedure optimization,” Int. J. Microw. Wirel. Technol., vol. 12, no. 6, pp. 519–530, 2020, doi: DOI: 10.1017/S1759078720000148.

[95] K. Liu, D. Sun, T. Su, X. Zheng, and C. Li, “Design of Flexible Multi-Band Miniature Antenna Based on Minkowski Fractal Structure and Folding Technique for Miniature Wireless Transmission System,” Electronics (Switzerland), vol. 12, no. 14, Jul. 2023, doi: 10.3390/electronics12143059.

[96] Z. Yu, Z. Lin, G. Zhang, Y. Li, and X. Ran, “A Novel Chrysanthemum-Like Fractal Structure Multi-Band Antenna for Mobile Terminals,” International Journal of RF and Microwave Computer-Aided Engineering, vol. 2023, 2023, doi: 10.1155/2023/1102668.

[97] B. Agrawal, R. Sharma, and R. K. Khanna, “A novel design of triangular-shaped hexagonal fractal antenna for satellite communication,” International Journal of Advanced Technology and Engineering Exploration, vol. 10, no. 99, pp. 233–244, Feb. 2023, doi: 10.19101/IJATEE.2021.875390.

[98] U. Patel et al., “Split ring resonator geometry inspired crossed flower shaped fractal antenna for satellite and 5G communication applications,” Results in Engineering, vol. 22, p. 102110, 2024, doi: https://doi.org/10.1016/j.rineng.2024.102110.

[99] S. Attioui, A. Khabba, S. Ibnyaich, A. Zeroual, Z. Zakaria, and A. J. A. Al-Gburi, “Design of a Miniaturized Circular Flower-Shaped Fractal Antenna with a Defected Ground Structure for Multiband Applications,” Progress in Electromagnetics Research C, vol. 155, pp. 203–211, 2025, doi: 10.2528/PIERC25022001.

LIST OF PUBLICATIONS

[1] P. Dalsania and J. M. Rathod, "Fractal Metamaterial Antennas for Next-Generation IoT Devices: A Comprehensive Review," *Journal of Advanced Research in Electronics Engineering and Technology*, vol. 12, no. 3 & 4, pp. 1-9, Aug. 2025, doi: 10.24321/2456.1428.202502.

[ISSN: 2456-1428 Peer-Reviewed Journal]

[2] P. Dalsania and J. M. Rathod, "Design and analysis of an asymmetrical star-shaped fractal antenna with meta-surface integration at 5.2 GHz," *Bulletin of Electrical Engineering and Informatics*, vol. 14, no. 6, pp. 4420–4432, Dec. 2025, doi: 10.11591/eei.v14i6.10163.

[ISSN No. 2302-9285 SCOPUS Indexed Journal]

[3] P. Dalsania and J. M. Rathod, "Performance Enhanced Star Fractal Antenna with Fractal DGS and Metasurface Integration," *Progress in Electromagnetics Research C*, vol. 161, 2025, doi: 10.2528/PIERC25082001**.**

[ISSN No. 1937-8718 SCOPUS Indexed Journal]

Patent Published

[1] "Rectangular Printed Antenna for Wireless Applications" P. Dalsania and J. M. Rathod, Trushit Upadhyay, Tushar Dave, Design No. 456492-001 Date: 24/04/2025, The patent Office, Government of India (INDIA Patent No. 202321046695 A). The Patent Office Journal No. 32/2023 Dated 11/08/2023.

[Design Patent Grant]